Dissertation on

INVESTIGATION OF THE ANISOTROPY OF GALACTIC COSMIC RAYS WITH SCINTILLATION TELESCOPES

Presented

by

LALJI V. KARGATHRA

for the Degree of

DOCTOR OF PHILOSOPHY

of the

Gujarat University

July 1972

Physical Research Laboratory

Ahmedabad.

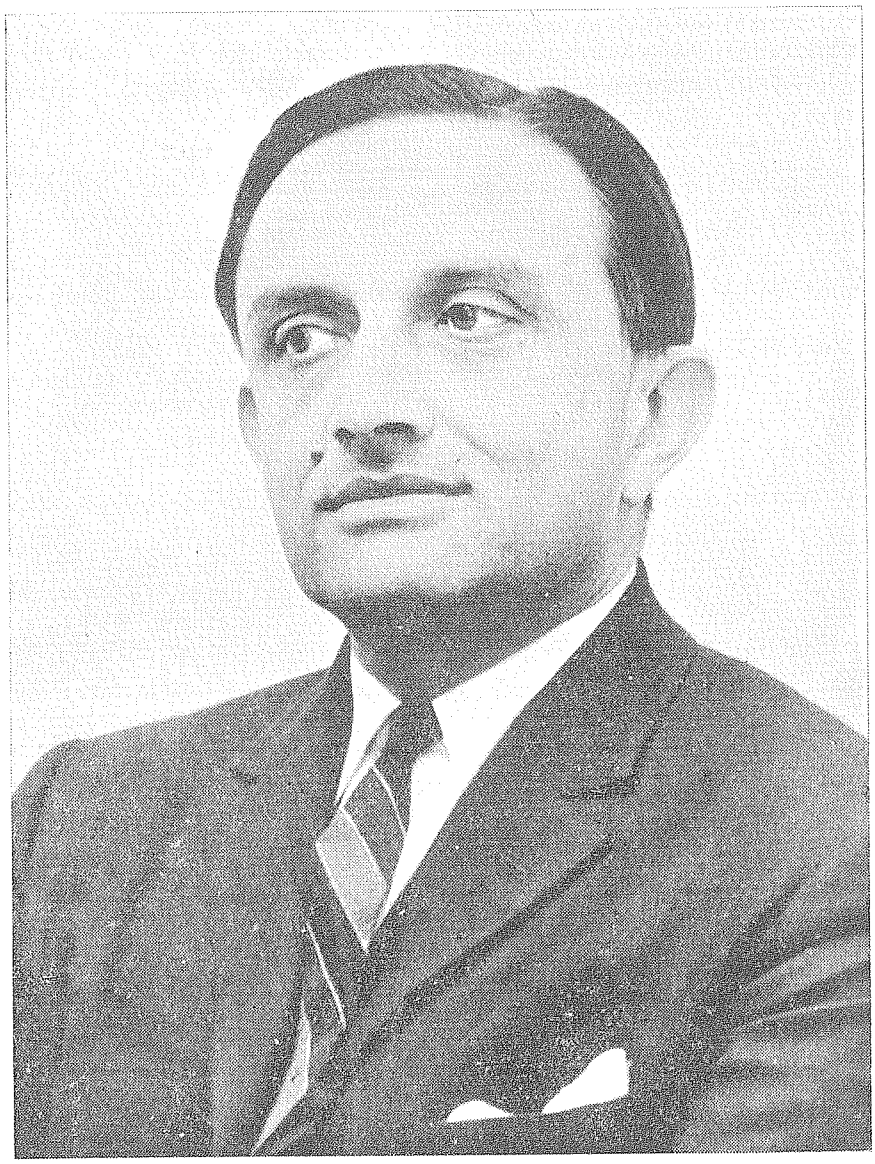

DEDICATED TO

LATE PROF. VIKRAM A. SARABHAI

S T A T E M E N T

The subject of cosmic ray time variations has been studied by a large number of workers in the past. The study has included both short term and long term variations. Some of these variations, like the solar diurnal and semi-diurnal variations, are quite small ($<1\%$) and consequently their study demands very high counting rate instruments with good stability. Till about 1960, the study of cosmic ray time variations has been conducted primarily by ground based observations and that too with low counting rate instruments. It is only in the last decade a large number of space observations at low energies have become available giving a new insight into the cosmic ray particle propagation in the interplanetary medium. In addition, the establishment of very high counting rate ground based instruments like the super neutron monitors for studying cosmic ray time variations with low amplitude has also added considerably to our understanding of the electromagnetic state of the interplanetary medium.

Most of the ground based observations have been accomplished with the neutron and meson monitors. Whereas, the data from the super neutron monitors can be unambiguously interpreted in terms of primary anisotropy, the interpretation of meson data is rendered difficult due to our inability to adequately correct it for the variations in the atmospheric temperature. However, the advantage of having both meson and neutron monitor data has been recognised, particularly in

understanding the energy dependence of the cosmic ray time variations. The difficulty in applying correction for atmospheric temperature variations can be cleverly overcome by utilising the data from directional telescopes inclined at the same zenith angle but in different azimuths. The earlier efforts by Elliot & Dolbear (1951), Elliot & Rothwell(1956), Parsons(1957), Rao & Sarabhai (1961) provided some insight into the cosmic ray time variations at high energies inspite of the low counting rates.

Having realised the importance of establishing high counting rate inclined telescopes, the author took the complete responsibility of setting up large area scintillation telescopes at Ahmedabad in vertical as well as in inclined directions (inclined at 51^{o} to the zenith along the East, West, North and South directions). The author was intimately involved in the fabrication of the scintillators, their reannealing and polishing, fabrication of the detector optics as well as the development of the entire electronics circuitry associated with the set-up. The scintillation telescopes at Ahmedabad have been in operation since June 1968 and the data from these telescopes have been analysed and intercompared with neutron observations to derive the properties of the cosmic ray daily variation.

The author calculated the variational coefficients applicable to each of the inclined as well as the vertical meson telescopes at Ahmedabad. Realising that the difference in the variations observed by two different inclined telescopes inclined at the same zenith angle but in different azimuths, is free from

the meteorological variations, the author developed the method to relate these difference-variations to the primary anisotropy using the appropriate variational coefficients.

The thesis is divided into five chapters. The first chapter briefly reviews the subject of time variations of cosmic ray intensity in particular the present understanding of the daily variation. The second chapter describes in detail the experimental set-up of the large area scintillation telescopes at Ahmedabad. The analytical methods employed in processing the data are described in third chapter. The results from the meson observations carried out at Ahmedabad during 1968 to 1970 are presented in the fourth chapter. These results are compared with the results obtained from the neutron monitor data during 1968 and 1969. Chapter five summarises the conclusions drawn from the present investigations.

Some of the important results that have emerged from the present investigation are listed below.

1) The yearly average diurnal variation observed by various difference-telescopes are consistent with the concept of the cosmic ray particles undergoing corotation with the sun. The corotation extends upto an upper limiting energy E_{max} of about 85 ± 10 GeV during the period 1968 to 1970. The average diurnal anisotropy obtained using neutron data and Ahmedabad difference-telescope data has an amplitude of 0.42% and a time of maximum

along 1800 hours direction and is further found to be invariant during the period of this study.

2) The average semi-diurnal anisotropy derived from the data has an amplitude which depends on the energy as $\sim 0.0025\ E^{+1}$ and a time of maximum along $\sim$ 0300 hour direction which is roughly perpendicular to the interplanetary magnetic field direction. The amplitude of the semi-diurnal anisotropy shows a slight decrease from 1968 to 1970, however its time of maximum is practically invariant.

3) The spectral exponent 'β' for both diurnal and semi-diurnal anisotropy is highly variable on a day-to-day basis. However, on an average basis the diurnal anisotropy seems to be energy independent and the semi-diurnal anisotropy varies as E^{+1}, both consistent with the theoretical prediction.

4) The average diurnal variation during days on which the interplanetary magnetic field is directed away from the sun (positive) is compared with days on which the field is directed towards the sun (negative) for both the years 1968 and 1969 separately. During 1968 the average diurnal variation for positive polarity group shows a larger amplitude and an earlier time of maximum as compared to the average diurnal variation obtained for the negative polarity group. During 1969, however, the observation shows completely opposite results. Even though, the results obtained for 1968 are consistent with similar observations by other workers, the reversal observed in 1969

is reported here for the first time. An attempt is made to explain the reversal in 1969 as due to a reversal of the B_z component of the interplanetary magnetic field in positive and negative polarity group compared to that in 1968.

5) The anisotropy resulting due to the cosmic ray density gradients and the interplanetary magnetic field direction shows a positive exponent for the energy spectrum of variation.

6) A sidereal anisotropy arising due to the azimuthal components of the interplanetary magnetic field and the radial cosmic ray density gradient is found with meson data for the year 1969. The amplitude of the anisotropy is 0.0049% at 1 GeV primary energy and the time of maximum is along $\sim$ 0700 hours.

When interplanetary magnetic field data for 1969 to 1971 becomes available it is hoped that some of the conclusions drawn in this thesis, particularly about the anisotropy related to the interplanetary magnetic field, will be verified.

(U. R. RAO) (L.V. KARGATHRA)

ACKNOWLEDGEMENT

I wish to acknowledge with gratitude my indebtedness to Professor Vikram A.Sarabhai for his constant encouragement, supervision and guidance till his sudden sad demise. Prof. U.R.Rao kindly took over the responsibility of guiding me for my Ph.D.work immediately after the death of Prof.Sarabhai. I express my heartiest gratitude to Prof.U.R.Rao for his encouragement, suggestions, generous support and guidance which led me to finish this work. I also wish to express my sincere appreciation to Dr.G.Subramanian for his help, suggestions and discussions.

I express my sincere thanks to Dr.N.W.Nerurkar with whom I was closely associated in the initial stages. I am also thankful to Dr.P.N.Pathak, Dr.Dinesh Patel, Dr.K.N.Nair and Mr.Y.Sunderarajan for useful discussions and to Mr.S.R.Thakore, Chief of the Computing Centre, Physical Research Laboratory, for providing the computer facility.

I gratefully acknowledge the technical assistance rendered by Mr.B.B.Lal and Mr.T.M.Raval. I am very thankful to Mr.D.K.Patel for his help in processing the data. Computational help of Miss Chhaya Shah is also acknowledged. Thanks are also due to Miss Meena Shah for typing the draft. Mr.Ramesh Nair receives special thanks for the painstaking and excellent job of typing the thesis.

Thanks are also due to:

i) the staff of the P.R.L.Workshop and Carpentry Section for their timely help whenever required in carrying out the project work successfully;

ii) the Maintenance group for rendering necessary help in maintaining the air-conditioning plant well;

iii) the Computing Centre for the help in punching the data cards, running programmes and their kind cooperation; and

iv) the Draughting and Photography Section of the Laboratory for their cooperative help.

I am grateful to Dr.C.P.Sonett for making available to us the unpublished interplanetary magnetic field data (1967 and 1968) from Satellite Explorer-33.

I greatly appreciate the cooperation and the moral support from my wife Hansa throughout the work.

Finally I am deeply indebted to my parents for their continued interest and encouragement.

The financial support received from the Department of Atomic Energy, Government of India is gratefully acknowledged.

(L.V. Kargathra)

C O N T E N T S

CHAPTER - I

INTRODUCTION

1.1 Time Variation of Cosmic Ray Intensity

The study of time variation of cosmic ray intensity in the past two decades has been of significant help, in understanding the electromagnetic processes in the interplanetary space. Even though galactic cosmic radiation is grossly isotropic outside the solar system, these particles, as they pass through the interplanetary medium, undergo considerable modulation. Superimposed upon the cosmic ray particles of galactic origin very often relativistic particles of solar origin are also present in the interplanetary medium. Historically in the past, it is by studying the time profile and anisotropy characteristics of solar particles, the gross interplanetary field configuration was first inferred. Intensive studies in the recent past have clearly demonstrated the usefulness of time variation studies of both galactic and solar cosmic rays as probes for studying the electromagnetic conditions of interplanetary space.

Unlike the in situ measurements of interplanetary parameters the cosmic ray time variation studies yield a complete profile of electromagnetic conditions of the entire interplanetary medium between the sun and the earth. Therefore, in spite of the availability of direct means of probing with satellites

and deep space probes, the cosmic ray time variation studies will continue to be of great importance and will provide inputs which will be complementary to the direct in situ measurements.

A comprehensive survey of the results obtained so far and their theoretical interpretation have been discussed at length by various authors such as, Dorman, (1963, 1969); Parker, (1966, 1969); Forbush, (1966); Quenby, (1967); Webber, (1968); Jokipii, (1971); McCracken & Rao, (1970); Pomerantz & Duggal, (1971) and Rao, (1972). Even though a fairly accurate picture of the gross features of the average cosmic ray variations has emerged from the past studies, a clear understanding of the day to day variability of cosmic ray flux is still lacking. It is, therefore, essential that the future work should be directed to achieve a further understanding of the detailed characteristics of cosmic ray anisotropy.

Most of the cosmic ray time variation studies, particularly at high energies ($\geq$1 GeV), have been mainly carried out using ground based cosmic ray observations. Continuous registration of ground level cosmic ray intensity has been systematically done since 1936. Even though early measurements were made with ionization chambers, the emphasis of late has shifted to the use of high counting rate neutron monitors and meson telescopes. However, before being able to interpret the observed secondary cosmic ray variations on ground in terms of primary anisotropy,

it is essential to understand and correct the data for the geomagnetic effects and the atmospheric transition effects.

Several distinct types of time variations of primary cosmic ray intensity with time scales ranging from several years to a few hours have been investigated. More recently, time variations having a periodicity of a few minutes have also been discovered (Dhanju and Sarabhai, 1967). In general, the observed time variations can be broadly classified into two groups viz. periodic (regular) and aperiodic (irregular) variations. Amongst the periodic variations are (1) 11-year variations which are inversely correlated with the 11-year solar activity; (2) 27-day recurrent variations, associated with the synodic rotation of the sun and (3) diurnal and semi-diurnal variations, which are connected with the rotation of the earth and the anisotropy of cosmic ray intensity in interplanetary space. The aperiodic variations include (1) sudden increases in cosmic ray intensity due to production of relativistic cosmic ray particles in solar flares and (2) sudden decreases in cosmic ray intensity called "Forbush decreases" usually observed in association with geomagnetic storms.

1.2 Geomagnetic and Atmospheric effects

1.2.1 Geomagnetic effects

It is well known that the primary cosmic rays are deflected by the geomagnetic field. At any given place on the

earth and for a given direction, cosmic rays below a certain rigidity are excluded by the geomagnetic field. The cut-off rigidities for different directions below which particles can not arrive at the given location have been investigated by a number of workers starting with Stormer, (1936) and Lemaitre and Vallarta, (1936 a,b) using the dipole approximation to the geomagnetic field. Following Alpher (1950) the cut-off rigidity in such a field can be calculated by the formula

$$P_c = \frac{300 \times M \ \cos^4\lambda}{a^2\left\{1 + \sqrt{1 - \sin^2\theta \cos\phi \cos^2\lambda}\right\}^2} \qquad \ldots\ldots 1.01$$

where 'a' is the radius of the earth, θ is the zenith angle, ϕ is the azimuth, λ is the geomagnetic latitude of the station and 'M' is the magnetic moment of the earth. Even though the results obtained using the above formula are correct to a first degree of approximation, for accurate calculation of the directional response characteristics of cosmic ray telescopes it is necessary to obtain more accurate cut-off rigidities based on realistic models of the geomagnetic field. Such calculations have also been done by Quenby and Webber (1959) and by Quenby and Wenk (1962) using certain approximations to include non dipole terms for the geomagnetic field. Shea et al.(1965) have calculated the cut-off rigidity very accurately by taking into account all the non dipole terms by a sixth degree simulation of the geomagnetic field (Finch and Leaton, 1957).

1.2.1.1 Asymptotic directions and Asymptotic cones of acceptance of a detector

The asymptotic direction of approach has been defined as the direction of a cosmic ray particle prior to its entry into the geomagnetic field. The asymptotic direction of approach of cosmic ray particles which arrive at a particular station on the earth from the zenith angle θ and azimuth ϕ is shown in Figure 1.01. For a given station and a given direction of incidence (say θ and ϕ) the set of allowed asymptotic directions for different rigidities form a curve in the λ ψ plane, where λ is the asymptotic latitude and ψ the asymptotic longitude measured east of the station. Calculations of asymptotic directions of approach have been done both by using numerical methods and by performing scale model experiments. For example Schluter, (1951); Firor, (1954); Lust et al., (1955); Jory, (1956) and Gall and Lifshitz, (1958) have computed the individual orbits of primary particles of energies extending up to 10 GeV. Malmfors (1945) and Brunberg and Dattner (1953), on the other hand, evaluated the asymptotic directions through model (terrella) experiments. With the advent of fast electronic computers more accurate determinations of trajectories have been possible using a realistic approximation to the geomagnetic field (McCracken et al.1962). Very recently, the effect of the deformation of the geomagnetic field by the solar wind has also been considered for calculating the cut-off rigidity and

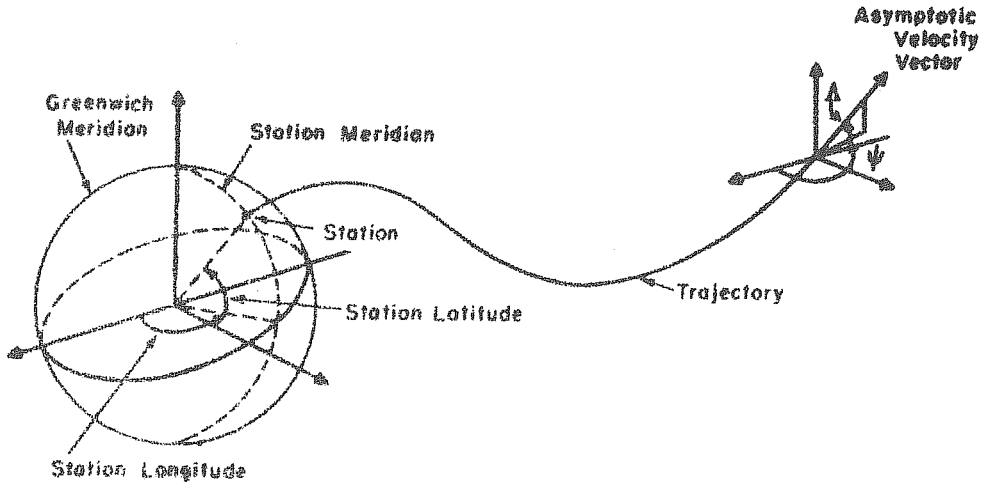

Fig.1.01 The trajectory of a charged particle through geomagnetic field.

particle trajectories. Using Mead's (1964) magnetospheric model Ahluwalia and McCracken (1965) and Makino and Kondo (1965) have tried to estimate the effect of the deformed geomagnetic field. Gall (1968) and Gall et al.(1968, 1969) used Williams and Mead's (1965) model and took into account the currents, both in the magnetopause and in the neutral sheet of the magnetospheric tail. We, however, wish to emphasize that the magnetospheric models used so far are at best crude and hence these calculations need to be refined with better models of the magnetosphere. Nevertheless the theories indicate that the effect of the deformation of the magnetic field is not very significant at energies above 10 GeV.

Knowing the trajectory information, it is possible to define the asymptotic cones of acceptance of a detector as the solid angle containing the asymptotic directions of approach which make a significant contribution to the counting rate of the detector (Rao et al., 1963). The concept of the asymptotic cones of acceptance is very useful and greatly facilitates the task of relating the observed variations to the primary anisotropy.

1.2.2 Atmospheric effects

Primary cosmic rays while passing through the atmosphere collide with air nuclei and produce various types of mesons and nucleons following the well-known cascade processes. The μ mesons which form the main part of the penetrating component

at sea-level has a very low probability of interaction. The μ mesons are also unstable and decay with a mean life-time of $\simeq 2.15 \times 10^{-6}$ sec. The observed secondary cosmic rays at sea level are subjected to absorption and decay processes in the atmosphere, all the way from the production level down to the recording level. In other words the secondary cosmic ray intensity observed at the ground is influenced by the variable atmospheric conditions above the recording instruments. The atmospheric effects are primarily due to (a) barometric pressure effect related to the absorption due to overlying atmosphere and (b) temperature effect which causes a change in the atmospheric character resulting in a change in the height of mean meson production level.

1.2.2.1 Barometric pressure effect

The dependence of cosmic ray intensity on atmospheric pressure can be described by an exponential law.

$$I = I_{Corr.} \exp(\beta \delta h) \qquad \ldots\ldots\ldots 1.02$$

where δh is the change in pressure at the observation level. Since the barometric coefficient 'β' for neutrons is considerably high ($\simeq -0.75\%$/mb) the computation of pressure correction uses the exponential formula. For the meson component, however, the pressure coefficient is low ($\simeq -0.13\%$/mb) and therefore the series expansion of equation (1.02) as

$$I = I_{Corr.} (1 + \beta \delta h) \qquad \ldots\ldots\ldots 1.03$$

is generally sufficient. The pressure coefficient is usually determined by a linear regression analysis.

The barometric coefficient varies with altitude, latitude and solar cycle. Systematic measurements of barometric coefficient for neutron monitors have been carried out by Bachelet et al.(1964, 1965 a) in 1963-64 and by Carmichael et al. (1965, 1968) in 1965-66. Bachelet et al.(1965 b) have suggested that the decrease of β in the lower atmosphere is due to the contribution of muons to the counting rate of the neutron monitor. Similarly a 6% change in the barometric coefficient has been reported by Griffiths et al.(1966) during the last solar cycle. From a careful analysis of β during Forbush decreases, McCracken and Johns (1959) have been able to show that change in 'β' is spectrum dependent. However, since the pressure coefficient applicable to mesons is quite small compared to that of neutrons, such changes are not very important in the case of meson monitors.

1.2.2.2 Temperature effect

The temperature variation in the atmosphere mainly affects the meson component due to its short decay time. Increase in the atmospheric temperature without any accompanying change in pressure, will increase the height of the mean meson production layer resulting in an increase in the path length of the mesons reaching the detector. Increased path length means

a greater probability of μ meson decay which will cause a decrease in the intensity of the registered meson component at the ground. In addition to the predominant negative temperature effect there is also a small positive temperature effect which arises from the competitive processes of $\pi - \mu$ decay and nuclear capture of π mesons near the meson production level ($\simeq$ 100 to 200 mb). With the increase in temperature at this height, the density decreases and the interaction distance increases. With the result more π mesons decay and fewer interact. Thus an increase in temperature at this level, will cause an increase in the production of μ mesons. The positive temperature effect is relatively small for a sea level meson monitor. It increases linearly with pion energy and therefore becomes progressively important for underground monitors. Even though the neutron monitors, by virtue of their dependence mainly on local production are more or less free from the atmospheric temperature effect, a small residual temperature effect does exist due to the neutron production through capture of μ mesons.

Unlike the evaluation of barometric correction, quantitative evaluation of temperature effect for μ mesons is quite complicated since it involves a knowledge of the temperature distribution throughout the atmosphere. A number of workers such as Maeda and Wada, (1954) and Dorman and Feinberg, (1955) have worked out a comprehensive theory of meteorological

effects. Following Dorman (1957) we can express the change in intensity as

$$\frac{\delta I}{I} = \beta \delta p + \int_0^{h_o} W_T(h) \, \delta T(h) \, \delta h \qquad \ldots\ldots\ldots 1.04$$

where δp is the change in pressure, β is the pressure coefficient, $\delta T(h)$ is the change in temperature of isobaric level of pressure h, and $W_T(h)$ is the density of the temperature coefficient.

From a detailed theoretical treatment of muon production and propagation in the atmosphere, Dorman (1957) has derived $W_T(h)$ for meson monitors at sea-level and at 25 and 55 m.w.e. For a sea-level telescope, $W_T(h)$ is approximately constant throughout the atmosphere from about 50 mb down to the ground level as proposed by Wada (1961) and has a mean value of $\simeq 0.3\%$/deg.atm. Maeda (1960) extended the calculations for $W_T(h)$, to include obliquely incident muons and the effect of the curvature of the isobaric levels. Even though one needs to consider the atmospheric temperature variations at all levels, for practical purposes Dorman found that it is adequate if the atmosphere is divided into 11 isobaric levels in which case the integral of equation (1.04) can be replaced by a summation as follows

$$\frac{\delta I}{I} = \beta \delta p + \sum_{i=1}^{11} K_i \, \delta T_i \qquad \ldots\ldots\ldots 1.05$$

where K_i is the partial temperature coefficient for the i'th

layer. Comparisons of various methods of temperature corrections have been published by Bachelet and Conforto, (1956); Mathews, (1959); Wada, (1961); Lindgren and Lindholm, (1961) and Carmichael et al.,(1967 a) and a comprehensive review of the atmospheric effects on meson and nucleonic components of cosmic rays is given by Bercovitch (1968).

Though, theoretically, the atmospheric effect on meson intensity near sea-level is fairly well understood, in practice, a simple and satisfactory method of applying the corrections for temperature variations on meson intensity has not yet been achieved. The major difficulty encountered is the non-availability of radio-sonde temperature data for different levels and at different times of the day. Besides, due to the large uncertainty in the radio-sonde data, resulting from insolation and lag errors, the available data is not sufficiently accurate for our purpose which poses a serious problem in the wider usage of meson data for time variation studies.

To overcome this difficulty pairs of directional telescopes inclined at the same angle to the zenith but pointing to different azimuths, have been used by several workers (Malmfors, 1949; Elliot and Dolbear, 1951; Rao and Sarabhai, 1962; Sandstrom, 1965; Sandstrom et al., 1968; Dorman, 1963; Fujii et al., 1969). Since the cosmic ray particles which are

registered by the two telescopes traverse an equal amount of the atmosphere in both the directions, the meteorological corrections applicable to both telescopes should be identical if the geomagnetic cut-off rigidity for the two directions are same. Even when the cut-off rigidities in the two directions differ slightly, we may consider that the atmospheric effect observed by both telescopes would be same to a first degree of approximation. Thus the difference in intensity recorded by the two telescopes would be free from the meteorological effects and therefore can be directly related to the primary anisotropy in space.

1.2.3 Relationship of Secondary variations to the Primary variations

Since the ground stations record only secondary cosmic rays, it is necessary to find how the secondary component is related to the primary cosmic ray particles. The function which generally describes the relation between the secondary component and the primary component has been called as the 'Multiplicity function', 'Generating function or Yield function' by various workers (Treiman, 1952; Fonger, 1953; Nagashima, 1953; Simpson et al., 1953; Dorman, 1957). In principle 'Multiplicity function' can be theoretically calculated from a knowledge of various interaction processes occurring in the atmosphere. Such calculations, however, are quite cumbersome and not reliable due to the number of uncertainties that exist

in our knowledge of high energy interactions. Most of the workers (Neher, 1952; Treiman, 1952; Simpson et al., 1953; Dorman, 1957) have, therefore, resorted to an experimental approach by making use of the observed latitude effect. Dorman's work in this field is the most comprehensive and we will take it as representative of such an attempt.

Following Dorman, the observed intensity $N_{\lambda}^{i}(h)$ of a secondary component of type i at a latitude λ and at an atmospheric height of 'h' can be represented as

$$N_{\lambda}^{i}(h) = \int_{E_{\lambda c}}^{\infty} D(E),\ M^{i}(E, h)\, dE \qquad \ldots\ldots 1.06$$

where $D(E)$ is the differential energy spectrum of primary particles and $M^{i}(E,h)$ is the multiplicity function that gives the number of secondary particles of type i produced at an atmospheric depth h, by a single primary particle of energy E and $E_{\lambda c}$, is the geomagnetic cut-off energy at the station latitude.

Variations in $N_{\lambda}^{i}(h)$ can result from variations in $D(E)$, $M^{i}(E,h)$ or in $E_{\lambda c}$. Differentiating equation (1.06) with respect to all these parameters and dividing by $N_{\lambda}^{i}(h)$ we obtain the expression for the change in intensity as

$$\frac{\delta N_{\lambda}^{i}(h)}{N_{\lambda}^{i}(h)} = -\delta E_{\lambda c} W_{\lambda}^{i}(E,h) + \int_{E_{\lambda c}}^{\infty} \frac{\delta D(E) W_{\lambda}^{i}(E,h)}{D(E)}\, dE + \int_{E_{\lambda c}}^{\infty} \frac{\delta M^{i}(E,h) W_{\lambda}^{i}(E,h)}{M^{i}(E,h)}\, dE \qquad \ldots\ldots 1.07$$

where $W^{i}_{\lambda}(E,h) = \frac{D(E)\, M^{i}(E,h)}{N^{i}_{\lambda}(h)}$ 1.08

is called the 'coupling coefficient' between the primary and secondary variation. It gives the percentage contribution of primaries of energy 'E' to the secondary component of type i at an atmospheric depth 'h' and at a latitude λ.

First term on the right hand side of equation (1.07) represents variation due to change in the geomagnetic cut-off energy which is not significant for all ground based observations even for large geomagnetic disturbances. Third term in equation (1.07) can be accounted for by appropriate meteorological corrections. Neglecting the change in cut-off energy, the variations in observed intensity $N^{i}_{\lambda}(h)$ after appropriate meteorological corrections can be expressed as

$$\frac{\delta N^{i}_{\lambda}(h)}{N^{i}_{\lambda}(h)} = \int_{E_{\lambda c}}^{\infty} \frac{\delta D(E)}{D(E)}\, W^{i}_{\lambda}(E,h)\, dE \qquad \ldots\ldots 1.09$$

Knowing the coupling coefficients we can relate the observed variations in the secondary cosmic ray intensity to $\frac{\delta D(E)}{D(E)}$ which is called the energy spectrum of the variational part of the primary cosmic rays.

From a study of the latitude effect, Dorman, (1957); and Quenby and Webber, (1959) have evaluated coupling coefficients for vertically incident nucleons and mesons upto 15 GeV. Beyond this energy the coupling coefficients have

been estimated by using extrapolation formulae of the type $W(E) = \frac{aE^{-a} + b(\bar{E}/E)}{\bar{E}}$. Constants A, 'a' and 'b' are fixed by tying in with the experimental values at E = 15 GeV.

Using primary cosmic ray energy spectrum of the type $KE^{-2.5}$, and the multiplicity, calculated by considering the Pal and Peters (1963) model of the elementary interaction of excited nucleons, Krimsky et al.(1966) have calculated the coupling coefficients for mesons incident from different zenith angles. The estimated response functions for the meson component incident at zenith angles 0°, 8°, 24°.....64° are shown in Fig.(1.02).

1.3 Relevant Experimental results on Daily Variation of Cosmic Ray intensity

Since the present work is mainly concerned with the daily variation of cosmic ray intensity, we shall discuss here only the relevant experimental observations. In the following sections we shall attempt to discuss these results in the frame work of the presently known properties of the interplanetary medium and the available theoretical formulations. Extensive analysis of the data obtained from the ionization chambers, neutron and meson monitors have now firmly established the existence of diurnal and semi-diurnal components in the daily variation of cosmic ray intensity. The average properties of these variations which are now reasonably well established are discussed in the next section.

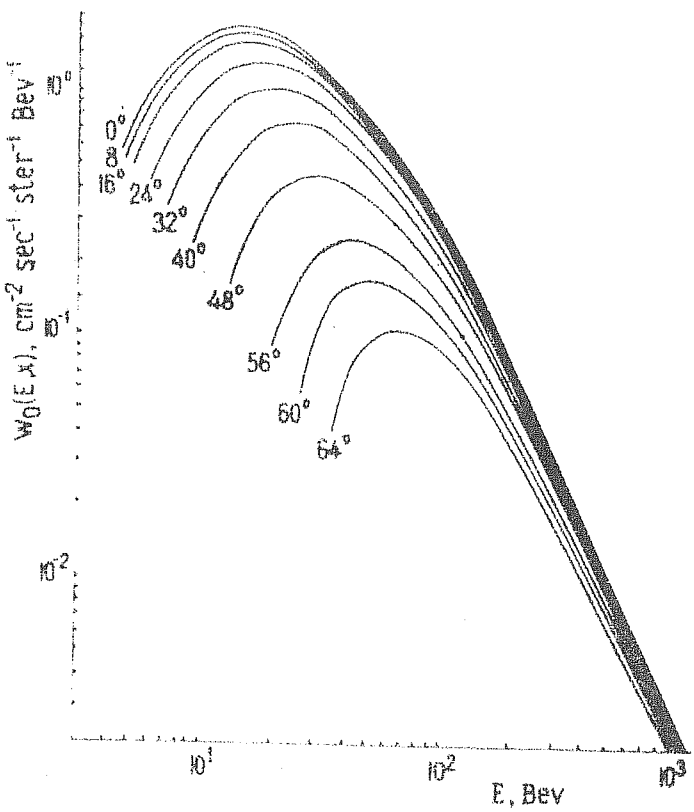

Fig.1.02 Coupling coefficients for the meson component at sea level for various zenith angles.

1.3.1 Average properties of Diurnal Variation

The observed yearly average cosmic ray diurnal variation in space obtained after correcting for the width of the asymptotic cones of acceptance of the detector and the geomagnetic bending have an amplitude $\simeq$ 0.4% (McCracken and Rao, 1965) and a time of maximum around 1800 hours in space (Rao et al., 1963; Bercovitch, 1963; McCracken and Rao, 1965; Faller and Marsden, 1966). The diurnal anisotropy is found to be energy independent in the energy range 2 GeV to E_{max}. The upper limit of energy, E_{max}, which is about 55 GeV. during 1965 seems to show a solar cycle variation (Jacklyn and Humble, 1965; Ahluwalia and Ericksen, 1969). The anisotropy is also found to vary as the cosine of the declination (Sandstrom et al., 1962; McCracken and Rao, 1965).

1.3.1.1 Long term changes of average diurnal variations

Long term variations, both in the amplitude and in the phase of the diurnal anisotropy with a period of one and two solar cycles, have been reported by many investigators (Sarabhai and Kane, 1953; Thambyahpillai and Elliot, 1953; Sarabhai et al., 1954; Steinmaurer and Gheri, 1955; Dorman, 1957; Forbush and Venkatesan, 1960; Forbush, 1967, 1969; Wada and Kudo, 1968; Duggal et al., 1970 a,b). The amplitude of the diurnal anisotropy seems to be lower during the minimum of solar activity. From an analysis of ionization chamber data recorded

over a period of more than 30 years at Cheltenham, Christchurch and Huancayo, Forbush, (1967, 1969) concluded that the average annual diurnal variation results from two distinct components W and V. The W component has its maximum (or minimum) in the direction 128° east of the sun-earth line. It varies sinusoidally about zero mean with a period of 20 years in the interval 1937-1966. The second component V has its maximum along 90° east of the sun-earth line and is subjected to larger variations, well correlated with the geomagnetic activity. It contains a wave with a periodicity corresponding to a single solar cycle having an amplitude of about 60% of that of W. The W component is directed along the Archimedean spiral. Duggal et al., (1970 a,b) have reported that the energy spectrum of diurnal variation for both the components (V and W) is same within the experimental uncertainties. It is important to realise that in all the above results, the meson observations have been used substantially.

However, study of the average diurnal variation as observed by neutron monitors over the period 1957-1965 by McCracken and Rao (1965) as well as by Duggal et al., (1967) have shown that it has been remarkably constant over these years, except for a decrease in the amplitude of about 30% in 1965. The time of maximum of the diurnal variation derived from neutron data, however, has remained practically constant over the entire solar cycle (McCracken and Rao, 1965).

over a period of more than 30 years at Cheltenham, Christchurch and Huancayo, Forbush, (1967, 1969) concluded that the average annual diurnal variation results from two distinct components W and V. The W component has its maximum (or minimum) in the direction 128° east of the sun-earth line. It varies sinusoidally about zero mean with a period of 20 years in the interval 1937-1966. The second component V has its maximum along 90° east of the sun-earth line and is subjected to larger variations, well correlated with the geomagnetic activity. It contains a wave with a periodicity corresponding to a single solar cycle having an amplitude of about 60% of that of W. The W component is directed along the Archimedean spiral. Duggal et al., (1970 a,b) have reported that the energy spectrum of diurnal variation for both the components (V and W) is same within the experimental uncertainties. It is important to realise that in all the above results, the meson observations have been used substantially.

However, study of the average diurnal variation as observed by neutron monitors over the period 1957-1965 by McCracken and Rao (1965) as well as by Duggal et al., (1967) have shown that it has been remarkably constant over these years, except for a decrease in the amplitude of about 30% in 1965. The time of maximum of the diurnal variation derived from neutron data, however, has remained practically constant over the entire solar cycle (McCracken and Rao, 1965).

Year to year changes of amplitude and phase in the diurnal variations registered by instrumentation having higher mean rigidities of response (sea-level and underground meson monitors) have always been found to be greater than the corresponding observations by instruments having low energy response. Some of the long term changes observed, particularly in amplitude, are attributable to changes in the upper limit of energy E_{max}. It is evident that changes in E_{max} will affect the higher energy response detectors substantially more than the lower energy ones. Using extensive data from neutron and underground meson monitors, Jacklyn et al., (1969, 1970) have concluded that the observed long term changes in diurnal anisotropy is understandable in terms of the changes in E_{max}, E_{max} varying from 55 GeV during sunspot minimum to about 100 GeV during sunspot maximum. Observations by Peacock et al.(1968); Hashim et al.(1968) and Ahluwalia and Ericksen (1969) are also in substantial agreement with the above conclusions. The changes of E_{max} derived from a comparison of Deep River neutron and Deep River meson data corrected with appropriate temperature coefficients by Agrawal et al.(1971) are also in agreement with the above observations. It is found that the cosmic ray data, particularly the neutron monitor data after 1957, do not indicate a solar cycle change except for a small decrease in amplitude observed in 1965, which can be attributed to a change in E_{max}. Recent meson monitor observations including underground

observations also indicate (Jacklyn et al.1970) only a change in amplitude which is explainable as due to change in E_{max}. These do not show any conclusive evidence for a systematic change in phase between 1958-1966. However the ion-chamber observations have always indicated a change in both amplitude and phase particularly during years of solar minimum around 1954, which is not completely understood in view of other evidences.

1.3.2 Semi-diurnal variation

It is only recently with the availability of high counting super neutron monitors and large area meson telescopes, the existence of a significant semi-diurnal component has been firmly established. The use of sophisticated analytical techniques including power spectrum analysis and complex demodulation has also considerably helped in this investigation (Ables et al.1966).

Average properties

The observed semi-diurnal anisotropy has an average amplitude of $\simeq 0.1\%$, with a time of maximum, in space $\sim$ 0300 hours, which is roughly perpendicular to the interplanetary magnetic field direction. The anisotropy is found to be energy dependent varying as the first power of rigidity (Ables et al.1966; Patel et al.1968; Lietti and Quenby, 1968; Quenby and Lietti, 1968; Rao and Agrawal, 1970; Fujii et al., 1970 and Subramanian, 1971b). The anisotropy is further found to vary as $\mathrm{Cos}^2\lambda$,

where λ is the mean asymptotic latitude of the station. Thus it is found that the observed semi-diurnal component is higher for low latitude station and for detectors having higher mean energy of response.

Examination of the yearly average semi-diurnal variation from a number of neutron monitor stations (Rao and Agrawal, 1970) has shown that the semi-diurnal anisotropy is time invarient between 1958 to 1968. The amplitude and the time of maximum do not seem to exhibit any significant changes with solar cycle during this period.

1.3.3 Short term changes in daily variation

Even though the average characteristics of the daily variation are fairly well understood, the day to day variations are found to be very complex. Study of daily variation on a day to day basis by a number of authors (Rao and Sarabhai, 1964; Subramanian, 1964; Sarabhai and Subramanian, 1965 and Patel et al. 1968) has conclusively shown that both the amplitude and the time of maximum of the diurnal as well as the semi-diurnal component, vary considerably on a day to day basis. Sarabhai et al.(1965) have reported that on a majority of days there exists a virtual sink of galactic cosmic rays along the garden hose direction. From an analysis of neutron and meson data from several stations, Sarabhai and Subramanian (1965) have shown that the spectral exponent 'β' for diurnal anisotropy

fluctuates over a wide range on individual days. Similar analysis by Patel et al. (1968) has shown that the semi-diurnal variation also exhibits similar spectral changes on a day to day basis. From a detailed analysis of the characteristics of the diurnal anisotropy these authors further conclude that a number of different mechanisms (processes) must be operative in the intensity variation on a day to day basis, to account for the large variability observed. Amongst these processes are (1) the azimuthal streaming (Parker, 1964; Axford, 1965 and Krimsky, 1964); (2) streaming due to non-uniform diffusion in a longitudinal sector structure of the interplanetary magnetic field (Parker, 1964); (3) scattering at irregularities along the interplanetary magnetic field, short circuiting latitudinal gradients (Sarabhai and Subramanian, 1966) and (4) latitudinal gradients in a relatively smooth magnetic field (Subramanian and Sarabhai, 1967 and Lietti and Quenby, 1968) may be mentioned.

Although the diurnal variation is altered during cosmic ray storms, no general relationships between the two have been established so far. There have been some reports that the amplitude of the diurnal variation increases and the phase advances to earlier hours when disturbances occur (Sekido and Yoshida, 1950; Yoshida, 1955; Dorman, 1957; Tanskanen, 1968; Ostman and Awadalla, 1970). However, these conclusions have not been supported by others (Crowden and Marsden, 1962; Kane, 1962).

The existence of trains of consecutive days having both abnormally large amplitudes ($> 1\%$, enhanced diurnal variations) and negligible diurnal variations have been pointed out by Mathews et al. (1969) and Hashim and Thambyahpillai, (1969). Enhanced diurnal variation occasionally occurs even when there are no accompanying geomagnetic disturbances or Forbush decreases. Mathews et al. (1969) and Hashim and Thambyahpillai (1969) have independently concluded that during many days exhibiting large amplitude waves, the anisotropy was predominantly caused by a large decrease along the garden-hose direction. Often during disturbed periods, the time of maximum of enhanced diurnal variation is found to shift to later hours (Mathews et al. 1969; Hashim and Thambyahpillai, 1969 and Rao et al., 1972). However, a few occasions have also been reported when the time of maximum shifts to morning (9-12) hours, associated with the recovery of Forbush decreases (Lindgren, 1970, and Razdan and Bemalkhedkar, 1971).

Using the available interplanetary magnetic field data in conjunction with the observed enhanced diurnal variation at Deep River Hashim et al. (1972) have shown that the diurnal anisotropy consists of two vectors one corresponding to radial convection and the other diffusion along the interplanetary magnetic field line. Rao et al.(1972) have shown that the enhanced diurnal variation which shows a maximum around 2000 hours is caused by the superposition of normal convection and

enhanced field aligned diffusion due to an enhanced positive density gradient. They also show that the diurnal variation during both quiet and disturbed periods can be understood in terms of convection and field aligned diffusion. Superimposed on the diurnal variations caused by radial gradients, it is also possible to have some contributions from latitudinal gradients.

Subramanian and Sarabhai (1965, 1967) suggested that the diurnal anisotropy caused by such latitudinal gradients should reverse as the magnetic field or the gradient reverses. Patel et al.(1968) have shown that during IMP-1 period when the interplanetary magnetic field was directed away from the sun the amplitude of the diurnal anisotropy was larger compared to the observed amplitude when the field was directed towards the sun. Venkatesan and Mathews (1968) have indicated that during IMP-1 period the days of enhanced diurnal variation were observed corresponding to the sectors having positive polarity. Using a wide band filter to the Deep River neutron intensity, Ryder and Hatton (1968) have also arrived at the same conclusion. These changes have been qualitatively attributed to the north-south gradient of cosmic ray density.

With underground meson monitor data obtained from Bolivia and Embudo stations, Swinson (1971) has shown that the diurnal amplitude was larger during days when the inter-planetary magnetic field(ipmf) direction was positive than

enhanced field aligned diffusion due to an enhanced positive density gradient. They also show that the diurnal variation during both quiet and disturbed periods can be understood in terms of convection and field aligned diffusion. Superimposed on the diurnal variations caused by radial gradients, it is also possible to have some contributions from latitudinal gradients.

Subramanian and Sarabhai (1965, 1967) suggested that the diurnal anisotropy caused by such latitudinal gradients should reverse as the magnetic field or the gradient reverses. Patel et al.(1968) have shown that during IMP-1 period when the interplanetary magnetic field was directed away from the sun the amplitude of the diurnal anisotropy was larger compared to the observed amplitude when the field was directed towards the sun. Venkatesan and Mathews (1968) have indicated that during IMP-1 period the days of enhanced diurnal variation were observed corresponding to the sectors having positive polarity. Using a wide band filter to the Deep River neutron intensity, Ryder and Hatton (1968) have also arrived at the same conclusion. These changes have been qualitatively attributed to the north-south gradient of cosmic ray density.

With underground meson monitor data obtained from Bolivia and Embudo stations, Swinson (1971) has shown that the diurnal amplitude was larger during days when the inter-planetary magnetic field(ipmf) direction was positive than

during days when the ipmf. direction was negative. On days having ipmf. direction positive the diurnal anisotropy occured earlier than the average direction of the anisotropy and it was later than the average value for days having negative ipmf. From the analysis Swinson, showed that the cosmic ray density was increasing with depth below the ecliptic plane during 1967 and 1968.

Using data from a number of neutron monitors during 1965-66 Hatton and Barker (1971) have also reported such changes in the amplitude and directions of the diurnal anisotropy during positive and negative magnetic field sectors. Hashim and Bercovitch (1971), used more stringent criterion in the selection of interplanetary magnetic field direction and obtained larger separation between the diurnal amplitudes during positive and negative field days. They restricted their analysis to days when the interplanetary magnetic field direction in the ecliptic was confined to $135^{\circ} \pm 30^{\circ}$ (positive) and $315^{\circ} \pm 30^{\circ}$ (negative) from sun-earth line. They also excluded the days when the interplanetary magnetic field had a large component out of the ecliptic plane ($> 2.5\ \gamma$) and days when the magnetic field had magnitude less than 2γ. Their results showed that the magnetic field related diurnal anisotropy was in a direction perpendicular to the average interplanetary magnetic field. The magnetic field related anisotropy could be expressed as a power law form i.e. $\frac{\delta I}{I}\% = 0.0275\ R^{0.4} \cos\lambda$, upto an upper limiting

rigidity of $\lesssim$ 100 GV. Assuming an interplanetary magnetic field of 4.5 γ, the gradient calculated from the anisotropy was of about 5.5. $R^{-0.6}$%/A.U.

These results will be further critically examined in Chapter IV and discussed along with the present results obtained by the author for the years 1968 and 1969, using data from a number of neutron monitors and data from Ahmedabad meson monitors.

1.4 Interplanetary Space

The study of solar modulation of galactic cosmic radiation can be essentially reduced to the study of the motion of cosmic ray particles in the disordered interplanetary magnetic field. It is therefore of interest to clearly understand the electromagnetic properties of the interplanetary medium before we discuss the theoretical formulation of the modulation mechanisms. In this section we describe briefly the properties of the solar wind and of the interplanetary magnetic field which are relevant to the cosmic ray time variation studies.

1.4.1 Solar Wind

The idea that solar corpuscular emission is responsible for geomagnetic storms and aurorae has been known for a long time. However, the concept of a continuous emission of corpuscular matter from the sun was first put forward by Biermann (1951, 1957), in order to explain the observed acceleration of gaseous comet tails. Based on theoretical

considerations, Parker (1958) showed that since the inner part of the solar corona has a temperature of the order of 10^6 ^oK, the solar corona should expand hydrodynamically against the solar gravitational force, resulting in a continuous emission of corpuscular matter which he termed as 'solar wind'.

The initial velocity of the solar wind at the photosphere is few km/sec. It becomes supersonic with a bulk velocity of several hundred km/sec., beyond a distance of about 10-20 $R_\odot$ (solar radius). The first direct observations of the solar wind were reported by Gringauz et al. (1960 a) and Shklovsky et al. (1961) from the space probe Lunik-II. Subsequent measurements by Gringauz, (1961) & Gringauz et al., (1962) on Lunik-III and Venus I, Bonetti et al. (1963 a, b) on Explorer 10 and Neugebauer and Snyder (1962) on Mariner-II confirmed the initial results. Since then a large number of direct observations have been accumulated over the last few years. A number of comprehensive reviews dealing with the observational properties of the solar wind and their theoretical implications are available in literature (Dessler, 1967; Lust, 1967; Ness, 1967; Axford, 1968; Hundhausen, 1968, 1970; Wilcox, 1968; Parker, 1967, 1969 and Holzer and Axford, 1970).

All the observations show that the density, velocity, temperature and relative chemical composition of solar wind are all highly variable. The solar wind density falls off at

the rate of $1/R^2$. From Vela Satellite results, the direction of plasma flow at the earth's orbit appears to be on an average from $\approx 1.6^{\circ}$ east of the sun (Strong et al., 1967; Hundhausen et al., 1967). The bulk velocity of the solar wind generally varies between 300-600 km/sec. and plasma temperature fluctuates between 10^4 °K to 10^6 °K. Table 1.01 lists the average properties of the solar wind.

Table 1.01

Bulk velocity	350 km/sec.
Proton or Electron density	8 cm^{-3}
Proton temperature	5×10^4 °K
Electron temperature	1.5×10^5 °K
Kinetic energy density	8×10^{-9} erg.cm^{-3}
Magnetic field	5 γ

One of the most puzzling aspects of the presently available observations concerns the long term variation of solar wind properties. During short periods, the 27-day recurrence tendency and an excellent correlation between solar wind velocity and geomagnetic activity have been very convincingly demonstrated by Snyder et al.(1963 a,b) and recently by Pai et al.(1967); & Bame et al.(1967). However, on a long term basis, when one examines the variations of solar wind properties over a solar cycle by comparing the data from

different space-crafts one observes that the average density, velocity and temperature of the solar wind are relatively constant over the solar cycle (Gosling et al., 1971; Mathews et al., 1971). The implications of the observed lack of variability of solar wind flux over a solar cycle on cosmic ray modulation will be discussed in the next section.

1.4.2 Interplanetary magnetic field

Alfven (1950) pointed out that a magnetic field embedded in a highly conducting plasma tends to behave as if it is 'frozen in' the plasma. Using the 'frozen in field' concept, Parker (1958) showed that the radially blowing solar wind together with the angular rotation of the sun, will stretch the magnetic field lines into a classical Archimedes spiral. For distances beyond 0.1 A.U. the radius of the sun may be neglected and the form of the spiral is given by

$$r = \frac{V(\phi - \phi_0)}{\Omega} \qquad \ldots\ldots\ldots 1.10$$

where 'r' is the radial distance, V is the solar wind velocity, ϕ is the heliocentric longitude measured from the reference longitude ϕ_0. Figure (1.03) shows the Archimedes spiral structure of the interplanetary magnetic field, in the equatorial plane of the sun, for a symmetrical solar wind velocity of 300 km/sec. The spiral angle θ often referred to as the 'garden hose angle' is defined as the angle between the interplanetary magnetic field direction and the radius vector as

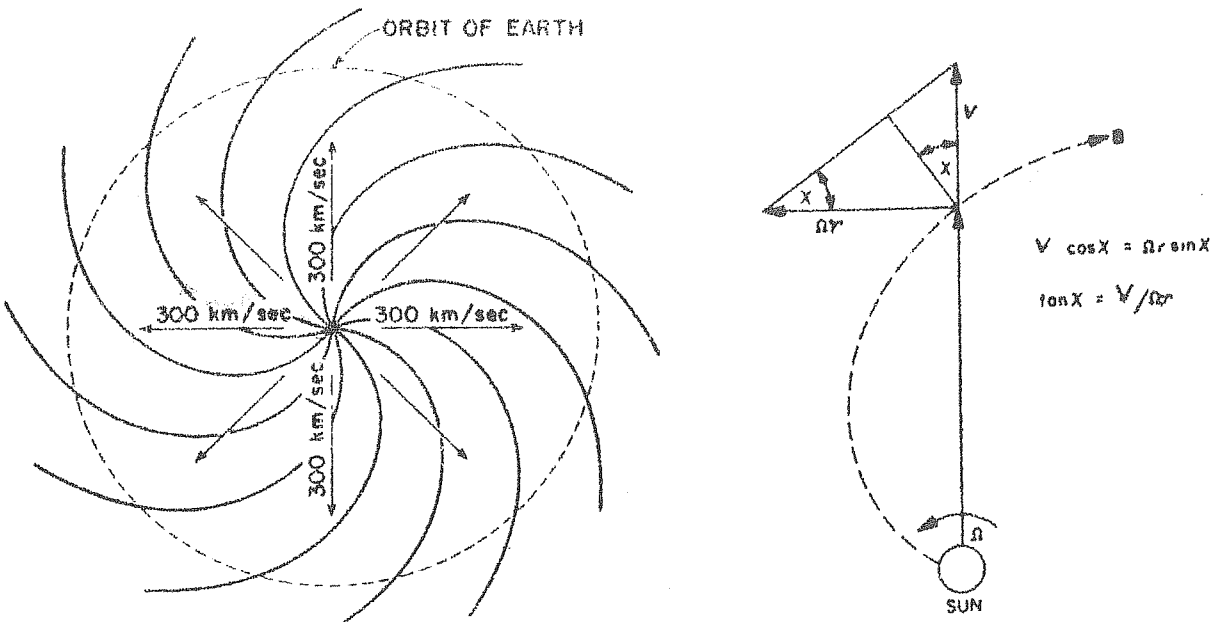

(a) (b)

Fig.1.03 (a) Archimedes spiral structure of the interplanetary magnetic field for a symmetric solar wind velocity of 300 kms/sec.(Parker, 1963).

(b) Garden-hose geometry of the interplanetary magnetic field (Dessler, 1967).

shown in figure (1.03). As seen from the figure, the angle χ (complement of θ) at any radial distance R from the sun is given by

$$\tan \chi = \frac{V}{\Omega R} \qquad \ldots\ldots\ldots 1.11$$

The three vector components of the interplanetary magnetic field are given by

$$\left.\begin{aligned} B_r &= B_1 \left(\frac{R_\odot}{r}\right)^2 \\ B_\theta &= 0 \\ B_\phi &= B_1 \frac{\Omega R_\odot}{V} \left(\frac{R_\odot}{r}\right) \sin\theta \end{aligned}\right\} \qquad \ldots\ldots\ldots 1.12$$

where B_1 is the radial component of the magnetic field at $r = R_\odot$ where 'r' is the radial distance, $R_\odot$ is the radius of the sun. Variation in V, with θ, ϕ and t; instabilities in the solar wind and the variation of B (θ, ϕ) with 't', will superimpose a variety of both small and large scale magnetic irregularities on the general spiral pattern of the magnetic field given above.

The first experimental demonstration of the predicted spiral structure of the interplanetary magnetic field was obtained by McCracken, (1962); from a study of the initial arrival directions of the solar flare cosmic rays. Most of the direct interplanetary magnetic field measurements, made very near the ecliptic plane, have now shown a fair agreement between the predicted Archimedes spiral and the interplanetary field

as projected on the ecliptic plane. The interplanetary magnetic field has an average value of $\approx 5\gamma$. (Ness and Wilcox, 1964, 1966; Davis et al., 1966; Coleman, 1966; Coleman et al., 1966 a, b; Schatten, 1971) with a small north-south component of magnetic field ($< 1\gamma$) perpendicular to the ecliptic plane.

1.4.3 Sector structure

One of the major features of the interplanetary magnetic field is its large scale sector structure configuration first reported by Wilcox and Ness (1965). The interplanetary magnetic field seems to be well ordered into sectors; the field in one sector being predominantly away from the sun for several consecutive days, followed by another sector having the magnetic field predominantly towards the sun(Figure 1.04). The entire sector pattern corotates with the sun. The observations by several authors (Coleman et al., 1966b; Wilcox and Colburn, 1969, 1970) over a long period of time between 1962 to 1968, have indicated that even during the period of maximum solar activity, the sector structure remains well established. During 1963-1964 there were four well established sectors (Figure 1.04). During the rest of the period two prominent quasi-stationary sectors have been observed with a mean period of 27 $\pm$ 0.1 days. A good correlation is obtained between the polarity of the mean solar photospheric field and the direction of the interplanetary magnetic field observed near earth (Ness and Wilcox, 1966;

Wilcox and Ness, 1967) with a lag of about 4.5 days corresponding to the transit time of solar wind from the sun to the earth. This indicates that the interplanetary magnetic field has its origin in the general solar photospheric field (Severny et al., 1970). Cosmic ray solar-flare particle-anisotropy observations on various Pioneer and IMP spacecrafts have shown that the field lines within each sector are in the form of inter-twined filaments.

1.4.4 Small scale irregularities and Power Spectrum of the Interplanetary Magnetic Field

Superimposed on such a large scale structure of the average interplanetary magnetic field, there exist small scale magnetic field irregularities (or kinks), which are essentially frozen into the solar wind and corotate with the sun. Michael (1967) and Jokipii and Parker (1968, 1969) have pointed out that since the magnetic lines of force are imbedded in turbulent fields on the sun they must necessarily be stochastic. The fluctuations in the velocity fields lead to a random-walk of adjacent lines of force. A large part of the random-walk is probably due to the horizontal displacement of the feet of the lines of force resulting from the motion of granules and supergranules. A granularity with a nominal size of 5×10^3 km on the solar surface, when projected on the earth's orbit, corresponds to a size of $\sim 10^6$ km, which is in agreement with

the typical scale sizes of filamentary inhomogeneities observed by McCracken and Ness, (1966) and Bartley et al. (1966) during solar flare events and the correlation length 'D' derived from magnetic field observations (Jokipii and Coleman, 1968). Thus the flux tubes in the 'Wet-spaghetti' model of interplanetary field suggested by Bartley et al. (1966) and McCracken et al. (1967); can be considered as a direct proof for the existence of random-walk of field lines.

The introduction of random small scale irregularities into a uniform field will cause random changes in the pitch angle of the cosmic ray particles, as they move along the lines of force. The integrated effect of a large number of scattering irregularities is maximum for particles whose cyclotron radius is of the same order as the scale size of the irregularities. Thus the scattering for particles of rigidity R(GV), depends mainly on the power in the transverse component of the field in the vicinity of the 'resonant frequency' which is given by $f(R) = 10^{-4} R^{-1} H_z$. Figure (1.05) shows the representative power spectra of the interplanetary magnetic field during 1962-1966, obtained by several authors (Coleman, 1966; Holzer et al., 1966; Jokipii and Coleman, 1968; Sisco et al., 1968; Sari and Ness, 1969).

The power spectral density of the interplanetary magnetic field shows a large variation from day to day. The

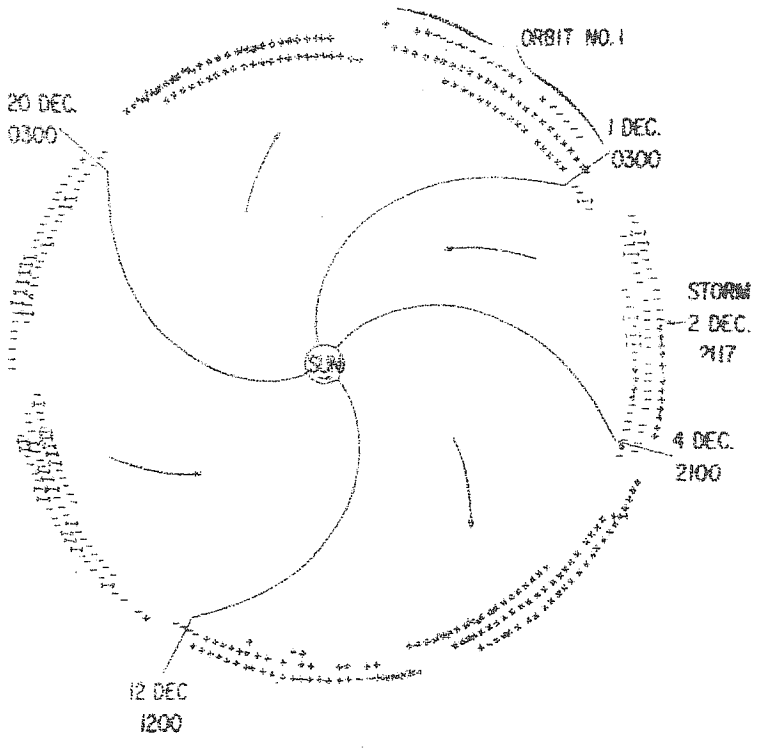

Fig.1.04

The observed sector structure of the interplanetary magnetic field during November 1963 to February 1964 (Wilcox & Ness, 1965).

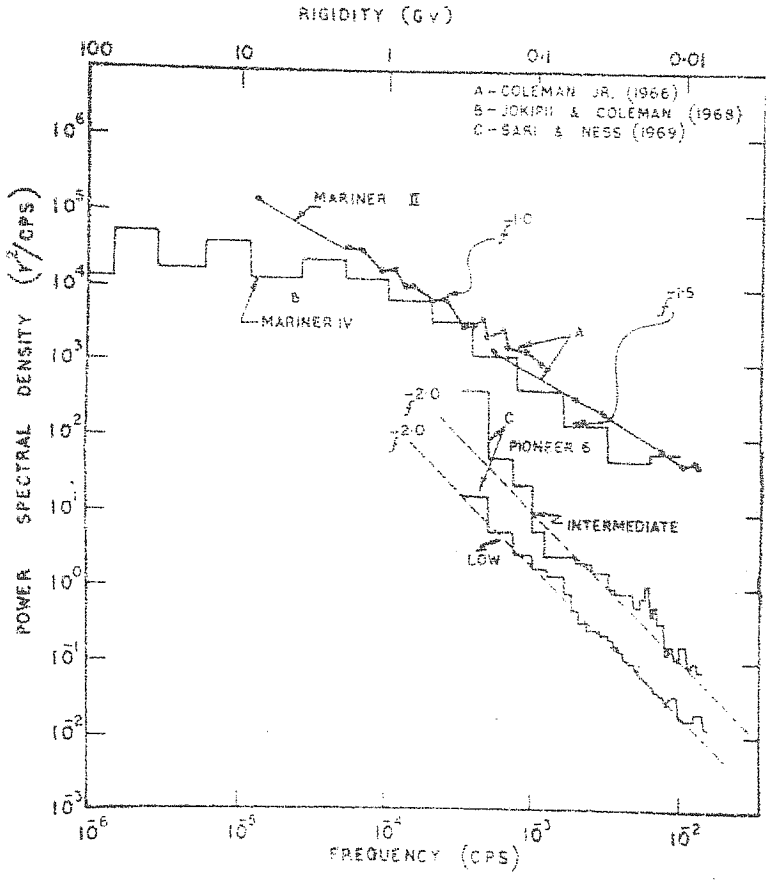

Fig.1.05

The representative power spectra of the co-latitudinal component of the interplanetary magnetic field, near the orbit of the earth. The epochs are: Mariner II, 1962; Mariner IV, late 1964; Pioneer 6, early 1966. The two graphs for Pioneer 6 correspond to low and intermediate disturbance of the magnetic field.

spectral density on a disturbed day often shows an increase by as much as a factor of 10 compared to the spectral density on a quiet day with the spectral shape, however remaining practically unaltered. For particles in the rigidity range ($10\ MV < R < 5\ GV$), the spectral exponent α of the power density shows significantly different values at different epochs indicating different rigidity dependence for the parallel diffusion coefficient (K_{II}). The available power spectral density information corresponding to rigidities above 1 GV is scanty and unreliable and there are some indications that it is constant at frequencies below 5×10^{-4} Hertz (corresponding to rigidities above 5 GV). Hence the magnetic field observations, presently available, are not adequate to derive quantitative conclusions regarding the propagation of high rigidity cosmic ray particles.

1.5 Modulation mechanisms and theories for the daily variation of cosmic ray intensity

Various theoretical models have been proposed to account for the experimental observations of cosmic ray modulation. These can be classified under two main headings, models which invoke modulation by static or time varying electric fields and the diffusion convection models. A number of reviews on this subject are available in literature. We mention here a few of them (e.g. Nagashima et al., 1966; Webber, 1969;

Rao, 1972). It is now generally accepted that the elegant formulation of the diffusion-convection model including the energy loss term (Gleeson and Axford, 1967, 1968 a, b) leads to a satisfactory explanation of the observed long term modulation, the radial density gradient and anisotropy. Here we will therefore briefly discuss this model before we describe the different mechanism that have been put forward to explain the daily variation of cosmic ray intensity.

1.5.1 Diffusion-Convection Model

The diffusion-convection model originally proposed by Morrison (1956) and later by Parker (1958 a) has since been modified greatly by a number of workers to include the energy loss term due to adiabatic deceleration in the solar wind (Parker, 1965, 1966; Gleeson and Axford, 1967, 1968 a, 1968 b, Skadron, 1967; Jokipii and Parker, 1967, 1968 a; Jokipii, 1967; Fisk and Axford, 1968, 1969). According to this model the modulation of the galactic cosmic ray intensity is attributed to the motion of cosmic ray particles in a spherically symmetric model of the interplanetary medium, in which the cosmic ray particles undergo convection, diffusion and energy changes as they move in the irregular magnetic fields. The cosmic ray particles undergo energy losses due to adiabatic deceleration in the expanding solar wind (Parker, 1965); the deceleration resulting from repeated scattering by the magnetic field

irregularities, which are moving outward from the sun at the solar wind speed. Jokipii and Parker (1967) and Jokipii (1971) have treated the cosmic ray transport problem as a problem of diffusion in the frame moving with the solar wind and have included the adiabatic deceleration. Gleeson and Axford (1967) and Fisk and Axford (1969) have considered the scattering processes. Both treatments lead essentially to similar equations.

Assuming an isotropic velocity distribution of cosmic ray gas, the differential number density U (r,E) and the differential streaming current density S (r,E) in a steady state for particles having a kinetic energy E and at a radial distance 'r' from the sun is given by (Gleeson and Axford, 1967; Fisk and Axford, 1969, 1970; Gleeson, 1971)

$$\frac{1}{r^2}\frac{\delta}{\delta r}(r^2 S) + \frac{V}{3}\frac{\delta^2}{\delta r\,\delta E}(\alpha E U) = 0 \qquad \ldots\ldots\ 1.13$$

$$S = CUV - K\frac{\delta U}{\delta r} \qquad \ldots\ldots\ 1.14$$

where

$$C(r,E) = 1 - \frac{1}{3}\frac{1}{U}\frac{\delta}{\delta E}(\alpha E U) \qquad \ldots\ldots\ 1.15$$

is the Compton-Getting factor (Gleeson and Axford, 1968 b; Forman, 1970 a), V(r) is the solar wind velocity, K(r,E) is the diffusion coefficient and $\alpha = (E+2m_o c^2)/(E+m_o c^2)$. $m_o c^2$ being the rest energy of the particle under consideration.

Eliminating 'S' between equations (1.13) and (1.14) one obtains the well known Fokker-Planck equation similar to the one derived by Parker (1965) and Jokipii and Parker (1967).

$$\frac{1}{r^2}\frac{\partial}{\partial r}(r^2UV) - \frac{1}{3r^2}\frac{\partial}{\partial r}(r^2V)\frac{\partial}{\partial E}(\alpha EU) - \frac{1}{r^2}\frac{\partial}{\partial r}\left(r^2K\frac{\partial U}{\partial r}\right) = 0 \quad \ldots\ldots 1.16$$

The second term on the left hand side of equation(1.16), arises as a result of energy changes suffered by cosmic ray particles in the expanding solar wind. Using this equation the intensity at any point and epoch can be derived, knowing the diffusion coefficient valid for that energy and epoch.

1.5.1.1 Isotropic diffusion

The solution of the equation (1.16), in the steady-state convection diffusion theory can be obtained by neglecting the energy loss term. Substituting $\alpha = 0$, the solution of the equation yields the well known expression for the modulated cosmic ray density $U(R, \beta, t)$ at a time 't' at the orbit of the earth.

$$U(R, \beta, t) = U_o(R, \beta, t) \exp - \int_r^L \frac{V(r,t)\, dr}{K(R, \beta, r, t)} \quad \ldots\ldots 1.17$$

$\beta = v/c$

where 'K' is the isotropic diffusion coefficient and 'L' is the dimension of the modulating region beyond which the cosmic ray flux is assumed to be the same as the intersteller cosmic ray density $U_o(R, \beta, t)$.

The cosmic ray intensity at any point, therefore depends upon V, L and the diffusion coefficient (K), which may be a function of rigidity and distance. Moreover the theory also predicts the change in modulation at any given rigidity, the change being caused by the change in any of these parameters (V, L or K). Whereas the changes in V are easily measured, the changes in L and K are to be inferred from the observed changes in the inter-relationship between cosmic ray intensity and solar activity parameters and the changes in the power spectral density of the interplanetary magnetic field respectively.

1.5.1.2 Radial Gradient

The magnetic irregularities moving with the speed of solar wind sweep back the galactic cosmic ray particles and a positive outward radial density gradient is produced inside the solar system. It can be approximated by

$$G = \frac{1}{U}\frac{\partial U}{\partial r} = \frac{V(r,t)}{K(R, \beta, r, t)} \qquad \ldots\ldots\ldots 1.18$$

It is seen from the above expression that the rigidity dependence of the radial gradient, will depend on the rigidity dependence of K. At low energies the energy losses may be quite significant and consequently it is not possible to obtain explicit analytic solutions of equation (1.16) valid at all energies. However, useful deductions can be made by

assuming simple forms for the diffusion coefficient K and α (α = 2 at very low energies and α = 1 at extreme relativistic energies).

1.5.1.3 Anisotropic diffusion

The cyclotron frequency of cosmic ray particles is generally more than the scattering frequency, hence the diffusion process is generally anisotropic. The diffusion coefficient along the field line (K_{II}) is more than the diffusion coefficient perpendicular ($K_{\perp}$) to the field line. For an idealized spiral interplanetary magnetic field, the cosmic ray density at a radial distance 'r' and co-latitude θ is given by

$$U(r,\theta) = U_o \exp\left[\frac{-V}{K_{II}}(R-r)\left\{1+\frac{1}{3}\left(\frac{\Omega \sin^2\theta}{V}\right)(R^2+Rr+r^2)\right\}\right] \quad \ldots\ldots 1.19$$

where Ω is the angular velocity of the sun and V and K_{II} are independent of r. The radial gradient for anisotropic diffusion is given by

$$G = \frac{1}{U}\frac{\partial U}{\partial r} = \frac{V}{K_{II}}\left[1 + \frac{r^2 \Omega^2 \sin^2\theta}{V^2}\right] \quad \ldots\ldots\ldots 1.20a$$

Near the orbit of the earth, $r\Omega = V$ and $\theta \approx 90^\circ$

$$\therefore G = \frac{1}{U}\frac{\partial U}{\partial r} = \frac{2V}{K_{II}} \quad \ldots\ldots\ldots\ldots 1.20b$$

1.5.2 Theories for the Diurnal Variation

To explain the observed diurnal variation of cosmic ray intensity, several mechanisms have been proposed. We will briefly discuss here only those mechanisms (Ahluwalia and Dessler, 1962; Parker, 1964; Axford, 1965; Krimsky, 1964; Gleeson, 1969; Forman and Gleeson, 1970; Jokipii and Parker, 1969, 1970), which take into account the well established solar wind theory and the spiral interplanetary magnetic field configuration.

Considering a smooth spiral magnetic field, Ahluwalia and Dessler (1962), showed that such a field corotating with the sun in the equatorial plane, produces an electric drift which results in the diurnal variation of cosmic ray intensity whose amplitude can be calculated using the well known Compton-Getting (1935) effect. The direction of the anisotropy according to this theory is perpendicular to the interplanetary magnetic field direction and is dependent on the solar wind velocity. This is completely at variance with the observed properties of the average diurnal anisotropy, viz. its time of maximum along 1800 hour direction (Rao et al., 1963; Bercovitch, 1963) and its lack of any correlation with solar wind velocity (Snyder et al. 1963). Further, the cosmic ray streaming as envisaged in this theory will have a component radially outwards from the sun which would make the sun appear to be a continuous source.

Severe theoretical objection to this model was made by Stern (1964) on the basis of Liouville's theorem according to which the cosmic ray density in phase space should be preserved in a conservative system. In other words, if the cosmic ray intensity is the same in all directions at any given point outside the solar system, it must be the same in all directions at any accessible point inside the solar system. Consequently time independent magnetic field$\left(\frac{\delta B}{\delta t} = 0\right)$ system can not produce a diurnal anisotropy.

Solution to this problem was pointed out by Parker(1964) and Axford (1965), who showed that for a realistic model of the interplanetary magnetic field $\frac{\delta B}{\delta t}$ is, in fact not equal to zero. Magnetic field irregularities would wipe out a major portion of the cosmic ray density gradient which is established by the electric field $E = -V \times B$. Parker (1964), considered the presence of magnetic field irregularities beyond the orbit of the earth, while Axford (1965) considered the existence of the scattering centers throughout the interplanetary medium. Under the assumption that $K_{II} \gg K_{\perp}$ and the gradient perpendicular to the ecliptic is zero, their results lead to the same conclusion that the cosmic ray gas will rigidly corotate with the sun. In this mechanism, the streaming velocity does not depend either on the solar wind velocity or on the interplanetary magnetic field. The corotation amplitude of the anisotropy produced by azimuthal streaming at a distance 'r' from the sun

is given by the well known Compton-Getting effect as

$$a_1(r) = \frac{3CV_{co}}{v} \qquad \ldots\ldots\ldots 1.21$$

Where 'V_{co}' is the velocity of the rotating spiral magnetic field and 'v' is the particle velocity (v=c), C is the Compton-Getting factor.

For protons of energies $\gg 1$ GeV, equation (1.21) reduces to $a_1 = \frac{(2+\nu)V_{co}}{C}$ at the orbit of the earth (r = a), where ν is the primary differential energy spectral index. Substituting V_{co} = 400 km/sec. and ν = 2.60 for the solar minimum the expected value of the diurnal anisotropy would be $\simeq$ 0.6%, which exceeds the observed average amplitude of $\simeq$0.4% (McCracken and Rao, 1965) by about $\approx$ 50 percent.

The mechanism put forward by Parker and Axford explains satisfactorily most of the features of the average diurnal variation such as the time of maximum, the spectral behaviour and the declination dependence. The only major discrepancy between the experimental observation and the theoretical prediction is in the amplitude of the diurnal variation.

Considering a general magnetic field (B) and also an electric field (E), the generalised expression for the differential current density can be given by (Gleeson, 1969)

$$S = \left(CU\underline{V} - K \frac{\partial U}{\partial \underline{r}} + C \frac{\omega\tau U}{B} \underline{E} \right)_{\parallel} + \frac{1}{1+(\omega\tau)^2} \left(CU\underline{V} - K \frac{\partial U}{\partial \underline{r}} + C \frac{\omega\tau U}{B} \underline{E} \right)_{\perp} + \frac{\omega\tau}{1+(\omega\tau)^2} \left(CU\underline{V} - K \frac{\partial U}{\partial \underline{r}} + C \frac{\omega\tau U}{B} \underline{E} \right) x \frac{\underline{B}}{B} \quad \ldots\ldots\ldots 1.22$$

Where C is the Compton-Getting factor, 'U' is the differential number density, 'V' is the solar wind velocity, $K = \frac{1}{3} v^2 \tau$ is the isotropic diffusion coefficient (v = the velocity of the particle), 'r' the radial distance from the sun, $\omega = \frac{eB}{m}$ is the gyrofrequency of the particles ('m' is the relativistic mass) and τ is the average collision time.

Assuming $\omega\tau >> 1$, Gleeson (1969) approximated the expression of differential current density 'S' as

$$S = -K \left(\frac{\partial U}{\partial r}\right)_{\parallel} - \frac{1}{3} \frac{v^2}{\omega} \left(\frac{\partial U}{\partial r}\right) x \frac{\overline{B}}{B} + CU \frac{\underline{E} \times \underline{B}}{B^2} \quad \ldots\ldots 1.23$$

In this approximation however the term $CUV_{\parallel}$ is left out. Assuming further that the gradient perpendicular to the ecliptic plane $\left(\frac{\partial U}{\partial r}\right)$ is zero and that there are no energy sources or sinks of cosmic ray particles within the interplanetary region, Gleeson (1969) equated the radial component of streaming vector to zero. He showed that the streaming in the azimuthal direction will be given by

$$S = CUV \tan\chi = CU \Omega r \quad \ldots\ldots 1.24$$

Where Ω is the angular velocity of the sun and r = 1 A.U.

Considering electric field $E = -\underline{V} \times \underline{B}$, generated by the magnetic field in the interplanetary region, Forman and Gleeson (1970) showed that the equation (1.22) for 'S' in terms of the electric field 'E' can be written as

$$S = CU\underline{V}_{||} - K_{||}\left(\frac{\partial U}{\partial r}\right)_{||} - K_{\perp}\left(\frac{\partial U}{\partial r}\right)_{\perp} - \frac{v^2}{3\omega}\frac{(\omega\tau)^2}{1+(\omega\tau)^2}\left(\frac{\partial U}{\partial \underline{r}} \times \frac{\underline{B}}{B}\right) + CU\frac{\underline{E} \times \underline{B}}{B^2} \quad \ldots 1.25$$

Where $K_{||}$ and $K_{\perp}$ are the parallel and perpendicular diffusion coefficients respectively. They are given by

$$K_{||} = K, \quad K_{\perp} = \frac{K}{1+(\omega\tau)^2} \quad \ldots\ldots\ldots 1.26$$

Forman and Gleeson (1970) also showed that in the interplanetary space, the electric field drifts and the convection of the cosmic ray particles parallel to the interplanetary magnetic field, combine as a simple convective flow along the solar wind. (Figure 1.06).

$$\text{i.e.} \quad CUV = CUV_{||} + CU\frac{\underline{E} \times \underline{B}}{B^2} = S_c \quad \ldots\ldots\ldots\ldots 1.27$$

$$\therefore S = S_c - K_{||}\left(\frac{\partial U}{\partial r}\right)_{||} - K_{\perp}\left(\frac{\partial U}{\partial r}\right)_{\perp} - \frac{v^2}{3\omega}\frac{(\omega\tau)^2}{1+(\omega\tau)^2}\left(\frac{\partial U}{\partial r} \times \frac{\underline{B}}{B}\right) \quad \ldots\ldots\ldots 1.28$$

Thus the streaming of cosmic ray particles $S(r,E)$ in the interplanetary space is given by the radially outward convection and the diffusion along and perpendicular to the

field line. Fourth term represents the anisotropy due to the gradient and the interplanetary magnetic field. This anisotropy is perpendicular to the interplanetary magnetic field and the gradient of the cosmic ray density. The anisotropy reverses its direction with the reversal of the interplanetary magnetic field or with the reversal of the gradient. Hence for average anisotropy (average of 27 day or more) the fourth term will average out to zero or become negligible. In general all the terms of equation (1.26) have to be considered to account for the magnitude and direction of the observed anisotropy.

Assuming that the gradient perpendicular to the ecliptic plane is zero, $K_\perp$ negligible and that there is no radial streaming, Forman and Gleeson (1970) showed that the streaming in the azimuthal direction will be given as

$$S = CUV \tan\chi = CUV_{co}.$$

This is shown in Figure 1.06.

The anisotropy ξ is given by $\xi = \frac{3S}{Uv}$ 1.29

$$\therefore \quad \xi = \frac{3CV_{co}}{v} \qquad \text{..... 1.30}$$

which is in the 1800 hour direction. For particles having energies above 1 GeV/nucleon,

$$C(r,E) = (2 + \gamma)/3$$

$$\therefore \xi = (2 + \gamma)\frac{V_{co}}{v} \qquad \text{..... 1.31}$$

V_{co} = 400 km/sec.(at the orbit of the earth), v = C (the speed of light) and γ = 2.6, $\therefore \xi$ is $\approx$ 0.6%.

At lower energies ($\lesssim$ 1 GeV) the condition that the radial streaming or current density is zero (or negligible) is not generally valid. Hence strictly azimuthal streaming cannot be expected at very low energies. In this energy region the Compton-Getting factor is greatly reduced and may even become negative (Gleeson and Axford, 1968 c).

To explain the discrepancy between the observed and expected amplitude of the diurnal anisotropy, a cosmic ray pressure gradient, perpendicular to the solar equatorial plane was suggested by McCracken and Rao, (1965); Parker, (1967); Gleeson and Axford, (1968) and Jokipii and Parker (1969). Gleeson (1969) attributed the entire discrepancy between the observed and expected value to the perpendicular gradient through the fourth term in equation (1.26). This implied a gradient (Forman and Gleeson, 1970) with magnitude $\sim$45/P(GV) per cent per A.U., which appears to be large and has not been confirmed experimentally.

Jokipii and Parker (1969) have attempted also to take into account the effect of the 'random-walk' of the magnetic field lines which enhances $K_\perp$ even to the order of $K_\parallel$ particularly at low energies. Inclusion of this effect introduces an additional term in K, which as Jokipii and

Parker (1969), pointed out could readily account for the observed reduction in the amplitude, by providing an additional component of the differential current density as shown in Figure (1.07). The anisotropy becomes

$$\xi = 3C \left(\frac{V}{v}\right) \frac{(K_{\parallel} - K_{\perp}) \tan \chi}{(K_{\parallel} - K_{\perp} \tan^2 \chi)}$$

$$\xi = 3C \left(\frac{V}{v}\right) \frac{(1 - \epsilon) \tan \chi}{1 + \epsilon \tan^2 \chi} \quad \text{where } \epsilon = \frac{K_{\perp}}{K_{\parallel}} \qquad \ldots\ldots 1.32$$

When $K_{\perp} << K_{\parallel}$ in equation 1.32, the anisotropy corresponds to the rigid corotation of the cosmic ray gas. On the other hand if diffusion coefficient is isotropic i.e. $K_{\perp} = K_{\parallel}$ the diurnal anisotropy will completely vanish.

Subramanian (1971 a) has recalculated the expected amplitude according to equation (1.31) for the period of high solar activity. Using appropriate values for coupling constant W(E), and the spectral index γ (R), he finds that the expected amplitude is in reasonable agreement with the observed amplitude. This implies that it is no longer necessary to invoke a density gradient perpendicular to the solar equatorial plane, during this period and that $K_{\perp} << K_{\parallel}$. This conclusion is in essential agreement with the low energy flare observations by McCracken et al. (1968, 1971).

From a study of the decay of solar flare cosmic ray events McCracken et al.(1968, 1971), showed that even late in

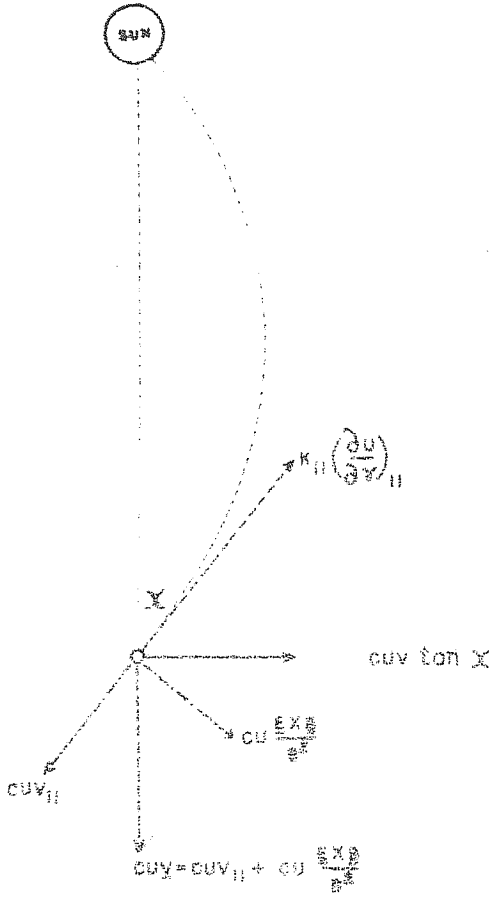

Fig.1.06 Cosmic ray streaming in the plane of the ecliptic. Dot-dashed line shows the diffusion component of the convective vector along the interplanetary magnetic field line and the E x B drift perpendicular to the field line. The dark dashed lines show the vectors due to radial convection and anisotropic diffusion along the field line. The solid line shows the resultant vector in the 1800 hour direction.

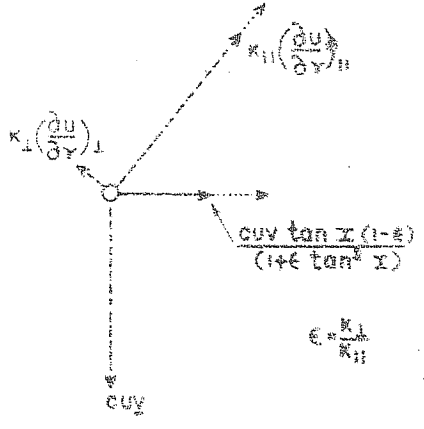

Fig.1.07 Cosmic ray streaming same as in Fig.1.06 where a correction due to finite diffusion perpendicular to the magnetic field lines is shown.

the decay, convection is the dominant mechanism in the interplanetary medium and that $K_{\perp}$ is completely negligible. Very late in the decay, they observed an easterly anisotropy which has been attributed to a balance between outward convection and an inward field aligned diffusion due to density gradients. The convection which is given by Compton-Getting effect, is observed to be of the order of 10% at 1 MeV energy, and about 0.6% at GeV energy. Extending these results from low energy solar cosmic rays to higher energies, these authors suggested that the diurnal variation could be simply considered as a superposition of convection and field aligned diffusion. Specific mathematical formulation of this concept for both solar cosmic ray events and the diurnal variation, has been given by Forman and Gleeson (1970); Gleeson (1969) and Ng.and Gleeson (1971). The model earlier developed by Krimsky (1964) is also in many respects similar to the above model even though it is not as detailed.

According to this concept, on an average it may be assumed that the sun is neither a sink nor a source. Consequently the inward radial component of the field aligned diffusive streaming should just balance the outward convection on an average basis leaving only a net azimuthal or 'corotational component' (Figure 1.08). On a day to day basis, however, the properties of the interplanetary medium vary over a wide range, resulting in an imbalance between the two components. Because

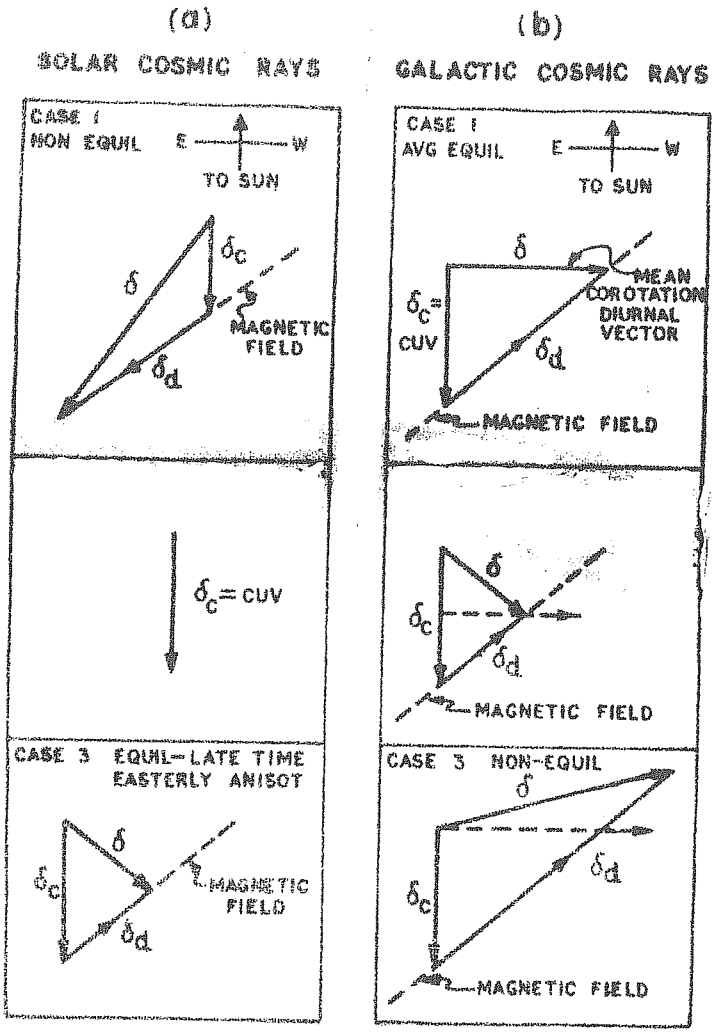

Fig.1.08 Unified model to explain the cosmic ray diurnal as well as solar flare anisotropy in terms of convective and diffusive flows. (Rao et.al.)

of the fluctuations in any of the relevant interplanetary parameters (solar wind velocity, magnetic field direction or diffusion coefficient), the departure from the equilibrium corotational streaming will result on a day to day basis. Since this concept is able to explain the observed anisotropic behaviour of low energy cosmic ray particles of solar origin as well as of galactic cosmic ray particles, it looks to be more attractive.

Experimental verification of the above concept has emerged from the study of Hashim et al. (1972) and Rao et al. (1972). Hashim et al.(1972) have shown that this concept is valid for explaining enhanced diurnal variation on individual days by demonstrating the field aligned nature of the diffusive vector on such days. From a detailed analysis of data over a long period (1964-1970), Rao et al.(1972) have shown that this concept is valid for both average quiet day variations and enhanced diurnal variations. Subtracting the convection vector from the observed diurnal variation, the residual diffusive vector has been shown to be field aligned during both quiet and disturbed periods. The residual field aligned diffusive vector is explainable in terms of a positive radial density gradient of $\approx 4.5\%$/A.U. during quiet periods and $\gtrsim 10\%$/A.U. during selected periods. These estimates are quite consistent with the observed radial density gradients. The observations also

indicate that on an average $K_{\perp}/K_{||} \leq 0.05$ confirming the correctness of the assumption $K_{\perp} << K_{||}$.

1.5.3 Theories for the Semi-diurnal Variation

Subramanian and Sarabhai, (1967); Lietti and Quenby, (1968) and Quenby and Lietti, (1968) have independently suggested that the semi-diurnal component in the cosmic ray intensity can arise, as a result of the symmetrically rising cosmic ray density gradient, perpendicular to the solar equatorial plane. The difference between the two models which are proposed to explain the semi-diurnal variation of cosmic ray intensity is mainly in the assumed nature of the density gradient away from the equatorial plane. Subramanian and Sarabhai assume the perpendicular gradient based on the dependence of the solar activity inferred from the coronal observations at different heliolatitude. On the other hand Lietti and Quenby have assumed a symmetrical density gradient based on the considerations of simple geometry of the interplanetary magnetic field and the consequent loosening of the spiral at higher heliolatitudes. Both the models predict essentially similar properties for the semi-diurnal anisotropy.

Viewing along the interplanetary magnetic field lines in the equatorial plane, a detector on earth measures cosmic ray flux characteristics of the equatorial plane. Viewing in a direction perpendicular to the magnetic field a detector samples particles arriving from higher heliolatitudes, corresponding to

the gyroradius of the particle under consideration. Since a cosmic ray detector on the spinning earth measures cosmic ray intensity twice a day along the interplanetary magnetic field and twice perpendicular to the field lines, a positive density gradient in the perpendicular plane will give rise to a semi-diurnal component with a maximum perpendicular to the inter-planetary magnetic field. The higher the energy of the particle, the higher would be the heliolatitude of sampling and hence the higher would be the resulting amplitude of anisotropy. Thus the model radily explains the observed time of maximum as well as positive energy dependence of the semi-diurnal variation.

According to Lietti and Quenby (1968) and Quenby and Lietti (1968), the perpendicular gradient of the cosmic ray flux is a consequence of the random scattering of particles by scattering centres superimposed on the simple Archimedean spiral. The galactic particles that arrive over the poles experience easy access, since, they diffuse along almost straight field lines, whereas those entering in the solar equatorial plane are constrained to follow many spiral loops. Consequently the cosmic ray density at a given distance should be less at the equatorial plane as compared to the intensities at $\Theta = 0^{o}$. With typical values of V = 400 km/sec., $\lambda = 10^{12}$ p cm. and r_s = 40 A.U., they described the cosmic ray density distribution in the interplanetary space as

$$N_e = N_s \exp \left\{ \frac{-2.4}{P} \sin^2 \Theta \right\} \qquad \ldots\ldots\ldots 1.33$$

Where N_e and N_s are the density at earth and at the boundary of the modulating region respectively, 'P' is the rigidity and θ is the colatitude. Taylor expansion of equation (1.33) gives peak to peak amplitude of the second harmonic component. For a detector that looks at an asymptotic latitude λ with respect to the solar equatorial plane and at an asymptotic longitude ψ measured from the spiral field direction, Quenby and Lietti have shown that the expression for peak to peak amplitude is given by

$$a_2 = 0.005\ (1-\mathrm{Cos}^2\psi\ \mathrm{Cos}^2\lambda)^{3/2}\left(1-\frac{\tan^2\lambda}{\mathrm{Sin}^2\psi}\right) \quad \ldots\ldots\ldots 1.34$$

Subramanian and Sarabhai (1965), on the other hand considered also other types of cosmic ray density distributions. If the density distribution, instead of being symmetrical about $\phi = 0$, is symmetrical about another heliolatitude($\phi \neq, \neq 0$), they find that the amplitude of the semi-diurnal anisotropy will still vary as $\mathrm{Cos}^2\lambda$ and the energy spectrum will still be positive. However, such a distribution will also give rise to a diurnal component which will reverse its direction of maximum with the reversal of interplanetary magnetic field or with the reversal of the north-south asymmetry of solar activity.

Theoretically both the models predict that the semi-diurnal anisotropy, has a positive exponent of the energy spectrum of variation, anisotropy varies as $\mathrm{Cos}^2\lambda$ and has a maximum flux in a direction perpendicular to the interplanetary

magnetic field direction. All these predicted properties are in agreement with the experimental observations.

Theoretical estimates, assuming the perpendicular gradient to be of the same order as the heliocentric radial density gradient (G $\simeq$ 12-15% per A.U.), have yielded amplitudes for the semi-diurnal anisotropy in reasonal agreement with the observations.

Accurate theoretical calculation of the semi-diurnal amplitude is however difficult because of the lack of any direct measurement of the latitudinal gradient. Taking advantage of the change of the earth's position between $\pm 7.25^{\circ}$ in an year with respect to solar equatorial plane, it is possible to estimate the characteristics of the perpendicular gradient from observations during different seasons (Dorman and Fischer, 1965). From such an analysis, however, Subramanian (1971 b) has concluded that the cosmic ray intensity distribution observed in the heliolatitude range $\pm 7.25^{\circ}$ cannot explain the observed semi-diurnal variation. It should also be noted that a semi-diurnal component can arise through a day to day variations of the interplanetary magnetic field. It is reasonable to assume that the particles of rigidity $\simeq$ 200 GV., whose gyroradius corresponds to about 1 A.U. will not show a significant semi-diurnal anisotropy.

C H A P T E R - II

EXPERIMENTAL DETAILS.

2.1 Introduction

Neutron and meson monitors are being very extensively used for continuous monitoring of cosmic ray intensity. Comparison of time variation observations from the low latitude meson monitors having a high energy response with the high latitude neutron monitor observations, provides valuable data, covering a large energy range. Even though both Geiger-Muller counters as well as scintillation detectors have been used for monitoring mu-meson intensity, the fast response of the plastic scintillator (10^{-9} sec.), ease in machining and fabrication and the practically unlimited life-time have favoured the choice of scintillators for time variation studies. With such scintillators, it is possible to measure cosmic ray intensities collected from a large area of the order of several square meters, thus providing a good statistical accuracy.

The operation of a scintillation counter is based on the conversion of the energy of a single particle into light quanta. The incident particle impinging on the scintillator dissipates part of its energy in the ionization and excitation of molecules, a fraction of which is converted into photons. These photons are detected by the photocathode of the photomultiplier, the output pulse of which is amplified, discriminated

and finally recorded automatically. In the succeeding sections, a brief description is given about the experimental set up of scintillation detectors as well as the electronic assembly used for the continuous registration of mu-meson intensity.

2.2 Scintillation Detector set up

2.2.1 Working Principle

The technique of scintillation counting for the detection of ionizing radiation is extensively described in literature by Birks, (1953); Curran, (1953); Mott and Sutton, (1958); and Akimov, (1965). The sequence of events in this technique is briefly summarised here.

An incident particle having an energy E_i, in passing through a scintillator dissipates a part (fraction) FE_i of its energy in ionization and excitation of molecules of the scintillators, which is converted into photons. The number of photons (I_o) radiated, which depends on the conversion efficiency (C_i) of the scintillator may be written as

$$I_o = \frac{FE_i \times C_i}{E_p} \qquad \ldots\ldots\ldots 2.01$$

where E_p is the energy required to produce a single photon in the scintillator. The number of units of these photons decay as $I = I_o e^{-t/t_o}$ where 't_o' is the decay time, which is of the order of 10^{-9} sec. for fast (organic) scintillators. Out of

these photons only a fraction of the photons are generally detected by the photomultiplier.

The number of emitted photons that reach the photocathode is governed by the following two factors (i) the optical transparency (T) of the scintillators to its own radiation and (ii) the light collection efficiency(C_d)of the detector set-up. In other words the number of photons I' reaching the photocathode is given by

$$I' = I \times T \times C_d \qquad \ldots\ldots\ldots 2.02$$

In the case of organic scintillators, the system efficiency is vastly improved by appropriately shifting the spectrum of emitted photons to match the photocathode response of the multiplier tube by adding suitable substances known as wave length convertors and wave-length shifters. In order to improve the collection efficiency (C_d) of the detector box, where multiple reflections are likely to occur a reflector with a high reflectance and low absorption coefficient, in the wave length region of interest, is generally used.

The number of photoelectrons (n) produced, when I' photons impinge on the photocathode is given by

$$n = I' \times C_{pe}f(\lambda_p) \qquad \ldots\ldots\ldots 2.03$$

where $C_{pe}f(\lambda_p)$ is the photoelectric conversion efficiency of the photocathode at its optimum frequency. The photoelectrons

released from the photocathode get multiplied at the subsequent dynode stages of the photomultiplier by secondary emission. The output of the photomultiplier is further amplified prior to discrimination and final recording. The signal to noise ratio is generally unaffected by the multiplication process in the photomultiplier since both are similarly amplified. Thus it is important that the signal (n) should be large. Hence the factors, F, C_{ip}, T, C_d and $C_{pe}f(\lambda)$ affecting the value of 'n' must be optimised.

2.2.2 Design considerations

The response of the scintillation detector to a particle depends on the efficiency of the scintillators, the attenuation length of the emitted light and the design of the detector box, which includes the geometry of the counter, reflectivity of the counter walls and the fraction of the wall area covered by the photomultiplier.

Since large area counters are needed for giving better statistical accuracy, fast response scintillators (i.e. organic scintillators) are preferable for monitoring purposes.

Eventhough both liquid and solid scintillators can be used as large area detectors, liquid scintillators (such as toluene, terphenyl) are unsuitable because of several reasons. The liquid is usually volatile, inflammable and toxic. It is difficult to avoid the leakage and spillages. The liquid being

in contact with the walls of the detector it becomes difficult to provide a good reflecting surface. For long term monitoring purposes, where stability is an essential requirement, solid, plastic scintillators are generally employed. To obtain high quality plastic scintillators, a mixture of three aromatic hydrocarbons is used. The bulk of the mixture is usually made up of the solvent (base) and other two ingredients (wavelength convertor and wavelength shifter) in minute quantities which serve the function of suitably modifying the frequency spectrum emitted by the solvent to match the photomultiplier response.

For cosmic ray work the organic plastic scintillators are generally composed of (1) polystyrene ($\simeq$ 99%), (2)p.Terphenyl ($\simeq$1%) and (3) POPOP ($\simeq$0.05 to 0.1%) by weight. The manufacturing process of solid plastic scintillators involves the following steps: (a) mixing the ingredients (b) heating the mixture to initiate polymerization (c) cooling to remove heat evolved during exothermic polymerization (d) further heating to complete the polymerization (e) shock cooling to break the polymerised mass from the reactor vessel (f) annealing (g) machining and polishing. Details of such processes for the manufacture of large and small size plastic scintillators are available in literature (Schorr and Torney, 1950; Koski, 1951; Buck and Swank, 1953; Wouters, 1955; Fisher, 1955; Clark et al., 1957; Deshpande and Bhide, 1961).

For the registration of relativistic cosmic ray particles, the detector system ideally should have the following characteristics:

(i) Stability

Cosmic ray time variation experiments which require continuous monitoring over long periods of time demand that the efficiency of the detector should remain stable over a long period. In other words, it is important to ensure that the reflecting properties of the reflector or the transmitting properties of the scintillators do not appreciably deteriorate with time.

(ii) Uniformity of response

The response of the detector over the whole of the effective counting area should be fairly uniform. However when one is concerned with counting the particles only, the condition of uniformity is not so strict as in experiments where one desires to measure the energy of the particles also.

In addition to the normal statistical fluctuations in the scintillation processes and in the photomultiplier, the following factors also contribute to the broadening of the pulse height distributions and thereby influence the performance of the large area detector.

(a) Non-uniform luminescence efficiency of the scintillators, due to defects in the manufacturing processes of the slabs (for example, presence of bubbles, white patches or any other optical

flaws in the scintillators). The variations in the efficiency of different slabs, when a number of slabs are used in one detector.

(b) Variations in the light collection efficiency of the detector, which can be minimized by suitable choice of the reflector and the optical geometry of the detector.

(iii) Counting efficiency

All the particles incident on the effective counting surface of the detector within the allowed solid angle of the telescope must be counted. The counting efficiency depends on the (i) number of photoelectrons emitted by the photocathode and (ii) the resolution time of the counting circuits.

2.2.3 Scintillation Telescope set-up at the Physical Research Laboratory

From the known properties of the average diurnal and the semi-diurnal anisotropy of cosmic radiation, it has been recognised that for carrying out further significant investigations on time variation of cosmic radiation, on a day to day basis, a large counting rate of the order of about 1 million/hour is necessary. Therefore, large area scintillation telescopes, consisting of eight plastic scintillation detectors each having an area of 4 sq.meters, have been installed at the Physical Research Laboratory, Ahmedabad. Absorber of about 200 gms/cm^2 surrounds the detector set-up which serves to cut-off

the soft component of the secondary cosmic rays. The entire detector set-up with its electronic instrumentation is placed in an air-conditioned room, where the temperature is maintained at $70 \pm 2^{\circ}F$.

Figure (2.01) shows the geometrical set-up of four detectors (which is only a part of the total set-up) to illustrate the geometry of the two vertical and the two inclined telescopes. The entire set-up with eight detectors, four on the ground and the remaining four, two metres above the ground (Figure 2.02) provide a total of four vertical telescopes of cubical geometry and two telescopes each in directions inclined at 51° to the zenith, pointing to east, west, north and south. The horizontal separation distance between the centres of two adjacent detectors is 2.5 metres. The mean direction of the inclined telescope is $\sim 51^{\circ}$ with respect to the vertical. The opening angle of the directional telescope is $\simeq 52^{\circ}$, having 14° and 66° as the minimum and maximum angle of response. For checking the long term stability and the reliability of operation, the set-up is divided into two independent identical sections of four scintillators each, each section comprising of two vertical telescopes.

2.2.3.1 Description of each detector

The detector of 4 m^2 area consists of sixteen slabs of plastic scintillators, each of 50 cms x 50 cms size, placed in

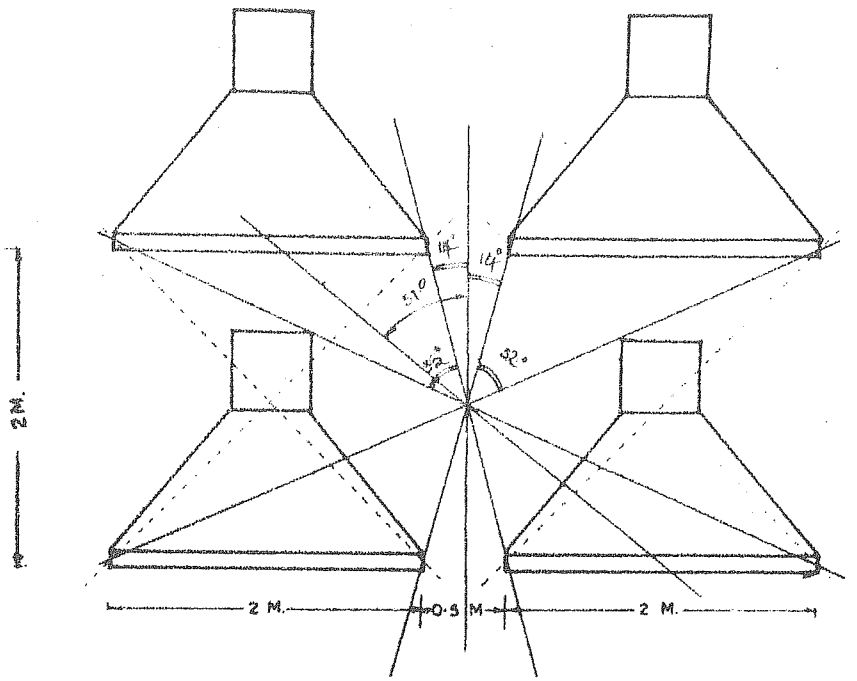

Fig. 2.01 Geometrical set-up of four scintillation detectors forming two vertical and two inclined telescopes.

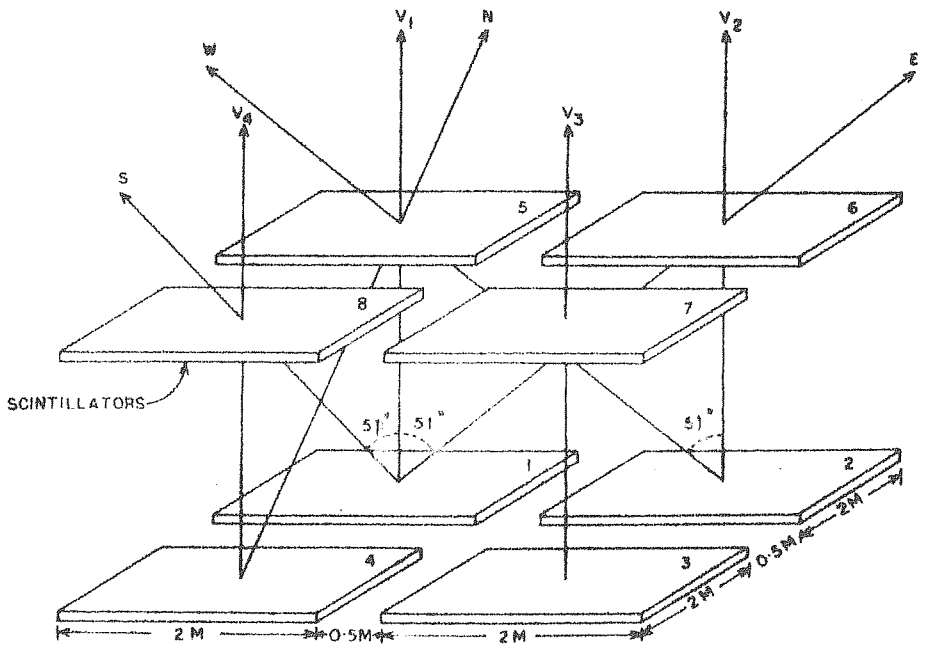

Fig. 2.02 Geometry of the multi-directional meson telescopes at Ahmedabad with eight scintillation detectors.

a light-proof wooden box having a pyramidal shape (Figure 2.01). One side of the box can be opened for service purposes. All the inner sides of the box and the bottom surface of the scintillators are coated with a high reflectance white paint (Titanium dioxide). Scintillators are of a trapezoidal form and placed in close optical contact with each other. Thickness of these scintillators at each of their corner is shown in Figure (2.03). The entire tray of sixteen scintillators is shaped such that the thickness is greatest at the corners and decreases smoothly towards the centre. The increased thickness at the corner compensates for the light losses due to the path length variation in the detector box. The entire tray of scintillators is viewed by a single 14" Du'Mont (K-1328) photomultiplier tube mounted at the top of the pyramidal box.

Great care need to be exercised in the choice of the paint which has to satisfy the conditions of very high reflectance in particular wave-length region and the ability to maintain its optical properties over a long period of time. Small scale experiments were conducted with a number of reflectance paints and were compared with the performance of the aluminium foil. It was found that the water based Tio_2 paint which has a reflectivity of $\simeq$ 0.8 in the transmission band of $\sim$4000-7000^{o} A, was the most suitable diffuse reflector for the geometry of our present set-up. Figure (2.04) shows the comparison of Tio_2 with aluminium foil for a typical set-up. The light output obtained

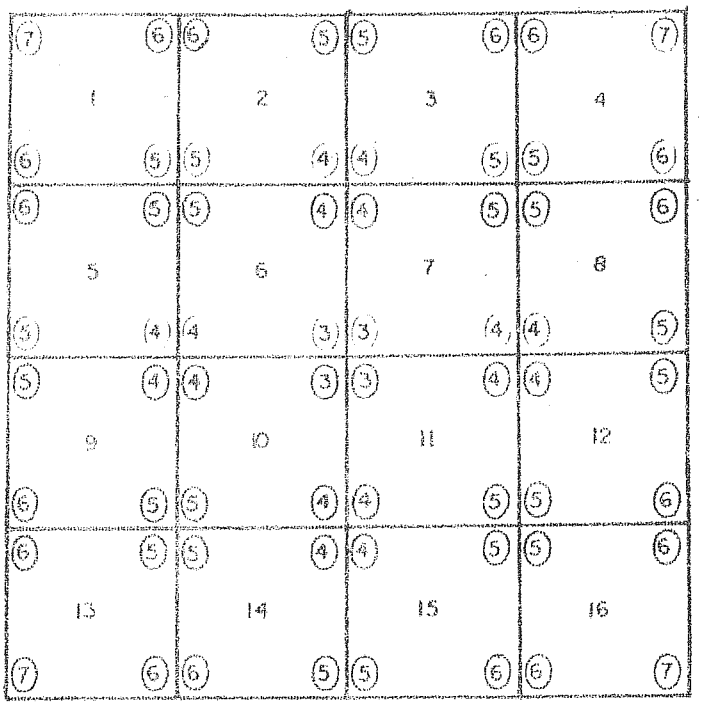

Fig.2.03 Arrangement of 16 scintillator slabs in one detector. Number in the circle indicates the thickness of the scintillator slab at that corner.

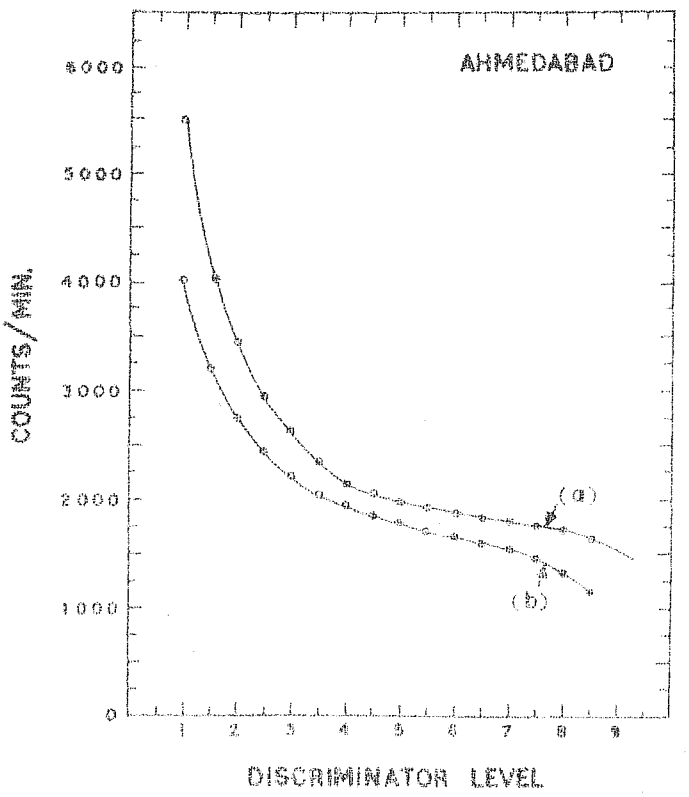

Fig.2.04 Counting rate as a function of discriminator level for proto-type scintillation detector with (a) TiO_2 and (b) crumpled aluminium foil as a reflector.

by using TiO_2 as a reflector is at least ~ 15% more than that obtained using aluminium foil. A reasonably uniform response can be obtained by placing the photomultiplier at a great distance from the scintillators, so that the optical path length from photocathode to different parts of the scintillator tray becomes approximately same. However this will sharply reduce the photon intensity. Hence a choice is being made of a reasonable optimum distance. In the present set-up, the increased thickness of the corners of the scintillation detector provides some compensation for the increased path length. The vertical separation between the photocathode and the scintillator which is 95 cms in our set-up has been worked out for optical performance taking into consideration, the conflicting requirements mentioned above.

The scintillator slabs were manufactured by the Technical Physics Division of the Atomic Energy Establishment, Trombay, according to our specifications and using the raw materials (a) Styrene Monomer PL 50 TBC (b) P-terphenyl (NE-504) and (c) POPOP (NE-502) of scintillators grade. The composition of these material by weight was ~ 99%, 1% and 0.05% respectively.

The scintillators were subjected to infra-red radiation treatment for removing the white patches and other minor manufacturing defects. They were further machined and polished with a fine grade 2/0 and 4/0 waterproof emery papers and aluminium oxide and buffed with a buffing wheel to obtain optically high quality scintillators for the present usage.

A 12 stage Du'Mont K-1328 photomultiplier tube having a photocathode of 14" diameter and an S-11 spectral response is used in the present set-up. The phototube has a rated average gain of ~8 x 10^5. This photomultiplier tube has a metal support cone for the cathode surface, which also provides some magnetic shielding and a focussing electrode whose potential can be varied to give optimum overall electron collection efficiency.

2.3 Electronic Circuits

The block diagram of the entire electronic circuitary associated with one typical channel of meson telescope is shown in Figure (2.05). The circuits are fully transistorized except for the high voltage units. In order to avoid the losses along the coaxial cable, the preamplifier is mounted near the base of the photomultiplier tube. The recording system including the high voltage units, is fed from the mains through a radio frequency suppressor and a constant voltage-transformer to provide better stability.

Two stabilized high voltage units, supply the voltages to the eight photomultipliers. The high voltage unit has a continuously variable output from 500 to 2000 volts. Stability of the power supply is 1 part in 1000 and has a current capacity of 1 mA. The high voltage supplies are well tested to ensure that spurious pulses due to discharge or leakage across the capacitors are absent.

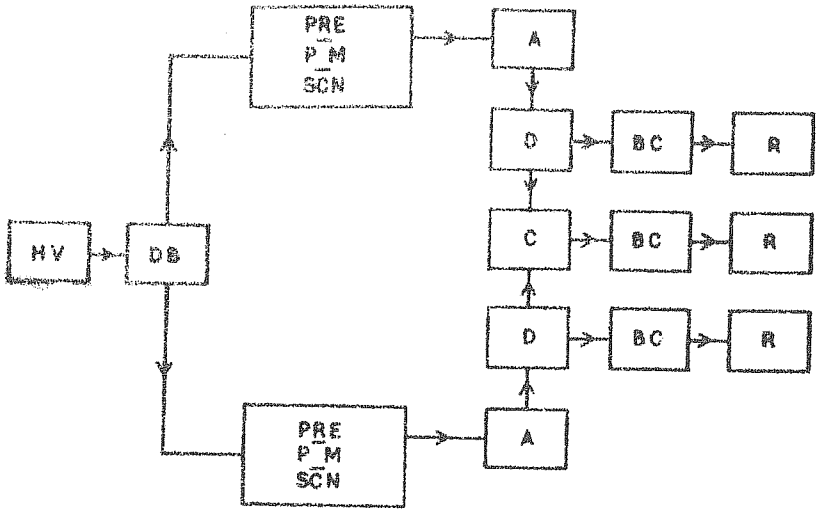

HV	-	High Voltage Supply	A	-	Main Amplifier
DB	-	Distribution Box	D	-	Discriminator
SCN	-	Scintillators	C	-	Coincidence
PM	-	Photomultiplier	BC	-	Binary Counter
PRE	-	Preamplifier	R	-	Recorder

Fig. 2.05 Block diagram of the electronic circuits for one channel of meson telescope.

To provide independent adjustment of voltages on individual photomultipliers, a distribution box containing four, five-step switches is connected with each high voltage supply. High voltage connection to each photomultiplier is decoupled to ensure from any radio-frequency and microphonic pick-up. The high voltage connection to the photomultiplier base is shown in Figure (2.06).

Positive voltage is applied at the anode of the tube. The output of the photomultiplier is a negative pulse of ~ 3 to 10 millivolts height.

2.3.1 Preamplifier

The preamplifier circuit is shown in Figure (2.07). To match the high output impedance of the photomultiplier the effective input impedance and high frequency response of the input circuit of preamplifier is increased by cascading three emitter followers with feedback from the third emitter to the input base resistor. The effective input impedance being nearly two megaohms, the time constant of the exponential decay of the photomultiplier pulse is not affected by the transistor characteristics. The rest of the preamplifier consists of a feedback, commonbase voltage amplifier (gain ≈ 10), with an emitter follower output to drive the coaxial cable (of 120 Ω impedance), which carries the signal to the main amplifier.

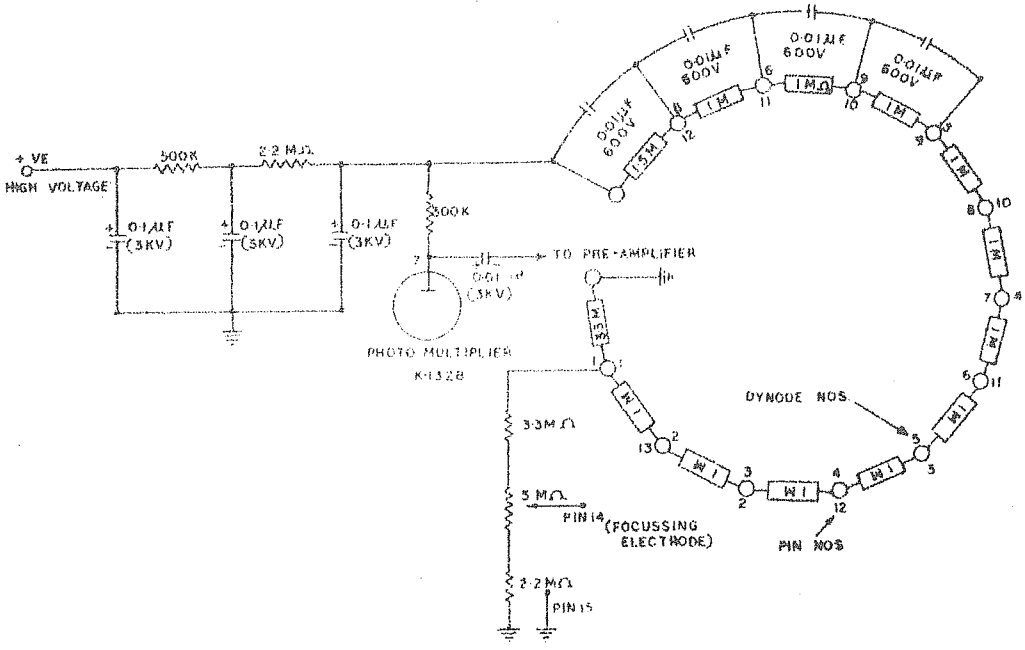

Fig.2.06 High voltage connection to the photomultiplier tube.

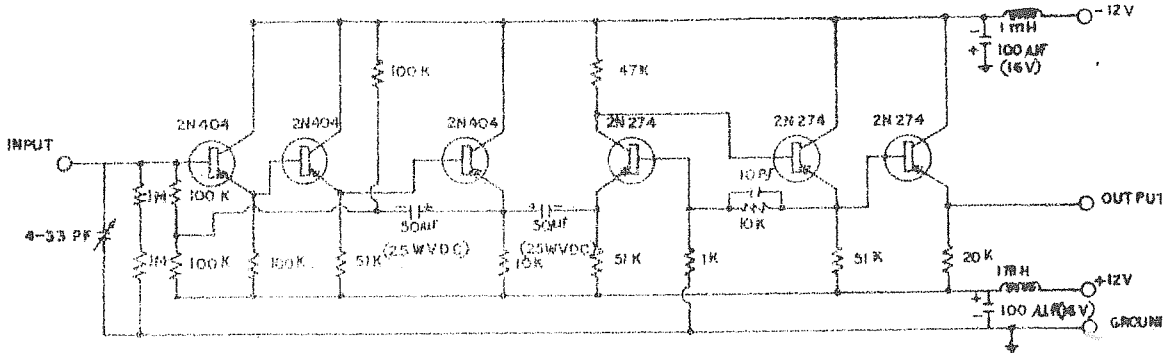

Fig.2.07 Pre-amplifier

2.3.2 Main amplifier

The main amplifier shown in Figure (2.08) consists of three feed-back loops. The total gain of the preamplifier and amplifier combination is about 3000 which is adjustable from 300 to 3000. The amplifier has a rise time of 0.2 μ sec. and provides an output of $\leq$ 11 volts. The signals after amplification are fed to the discriminator circuit which is shown in Figure (2.09).

2.3.3 Discriminator circuit

The level discriminator used in the present set-up is adjusted to eliminate the background noise from the photomultiplier. The discriminator circuit is followed by a pulse shaper, which provides a constant square wave output. Negative output from the pulse-shaper is used for monitoring the tray rate for test purposes. The sharp positive output from the pulse-shaper after differentiation, is fed to the coincidence circuit. Discriminator level, is adjusted using a ten turn linear potentiometer.

2.3.4 Coincidence circuit

Figure (2.10) shows the schematic of the coincidence circuit. The resolving time of the circuit is adjusted at 0.4 μ sec. The output pulses from the coincidence circuit, which are of the order of 6 volts and of 1 μ sec. duration, are fed to the scalers for counting.

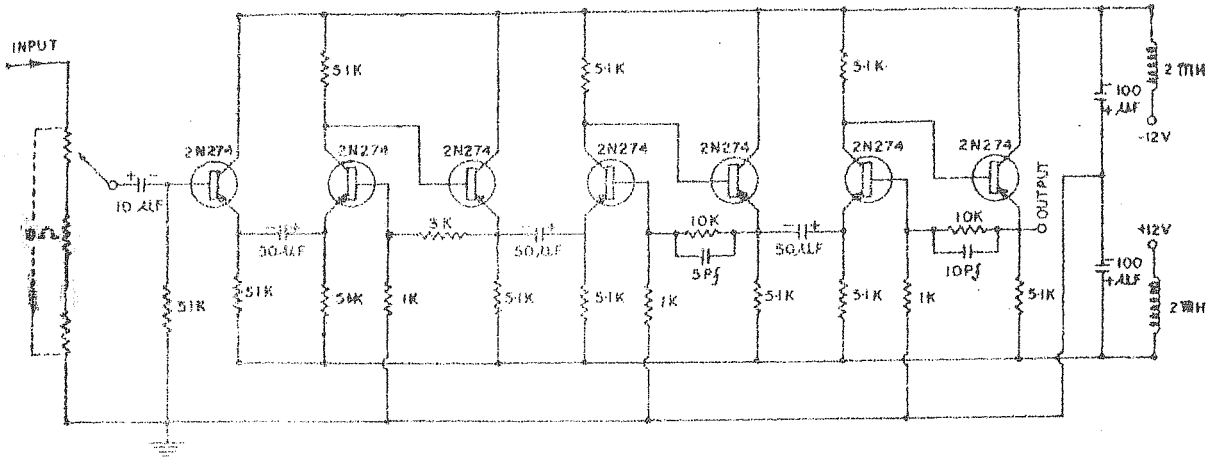

Fig.2.08 Main Amplifier(Linear)

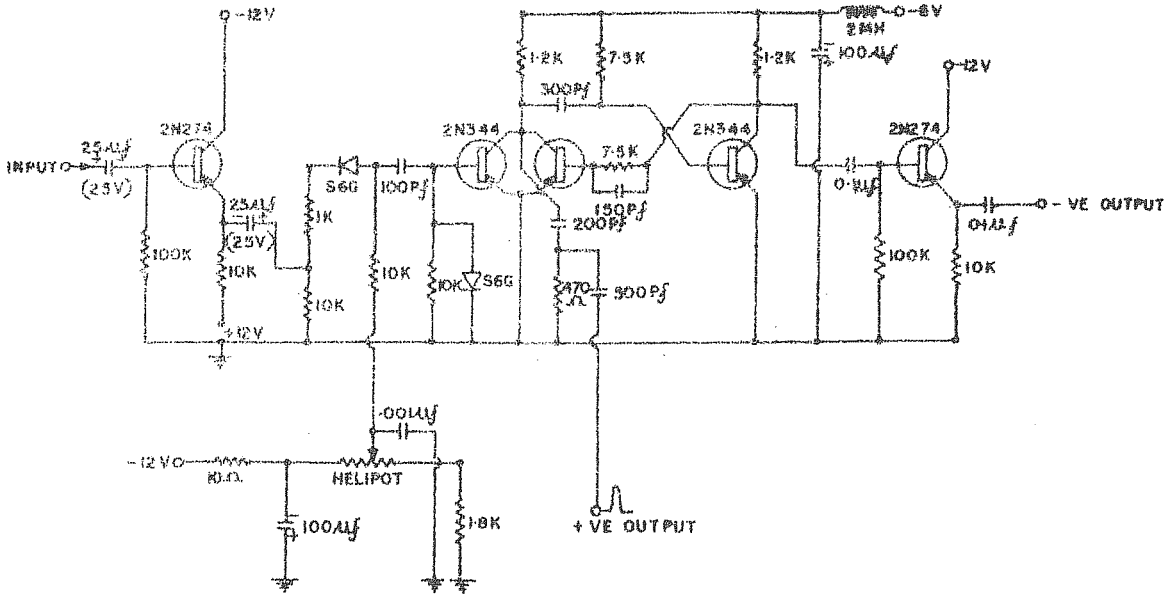

Fig.2.09 Discriminator circuit.

2.3.5 Scaler and Recording System

The basic binary scaler shown in Figure (2.11), is of Eccles-Jordan type bistable multivibrator. Scaling factors of 128 and 512 are used for inclined and vertical telescopes respectively. Output of the scaler is recorded by a telephone type mechanical recorder (Figure 2.12). A panel consisting of all recorders which are attached to different vertical and inclined telescopes, along with information giving the year, date and the time is automatically photographed every twelve minutes, through a motor clock control circuit (Figure 2.13). The description of the operating charactertistics and testing procedure is discussed in the next section.

2.4 Operating Characteristics and Test Procedure

2.4.1 Choice of operating conditions

The three governing factors which control the complete operation of the scintillation detector set-up are the choice of the high voltage to the photomultiplier tube, the adjustment of the amplifier gain and fixation of the discriminator level. Appropriate choice of these parameters is necessary to obtain the optimum operating conditions of the detector and maximum stability of the counting rate against instrumental drift.

It is customary to initially adjust the photomultiplier high voltage to a reasonable value and then fix the amplifier gain to bring the response of the detector within the operating region

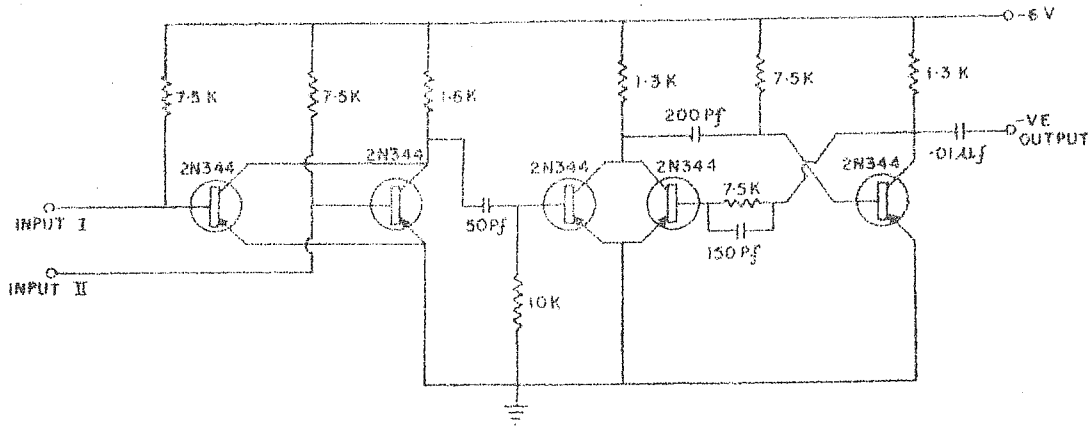

Fig.2.10 Coincidence circuit

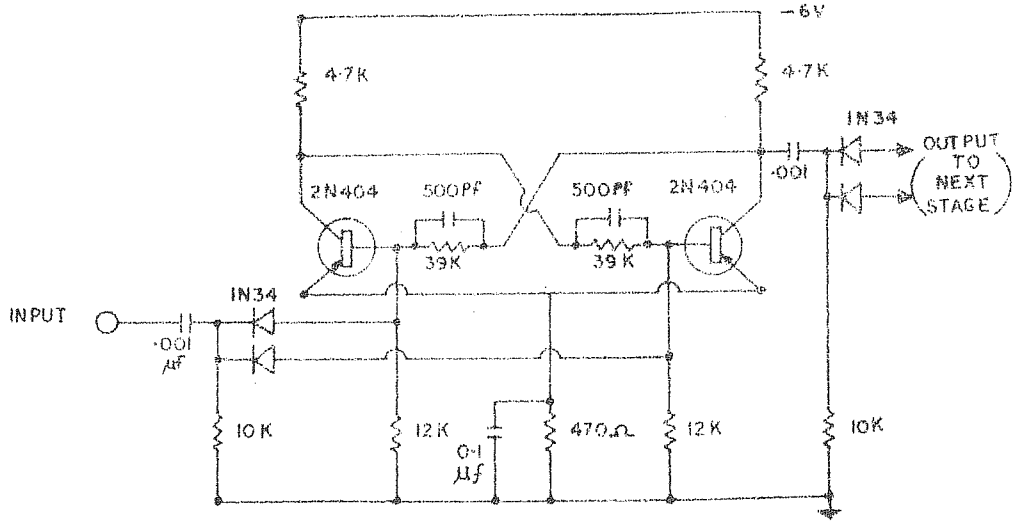

Fig.2.11 Scaler circuit

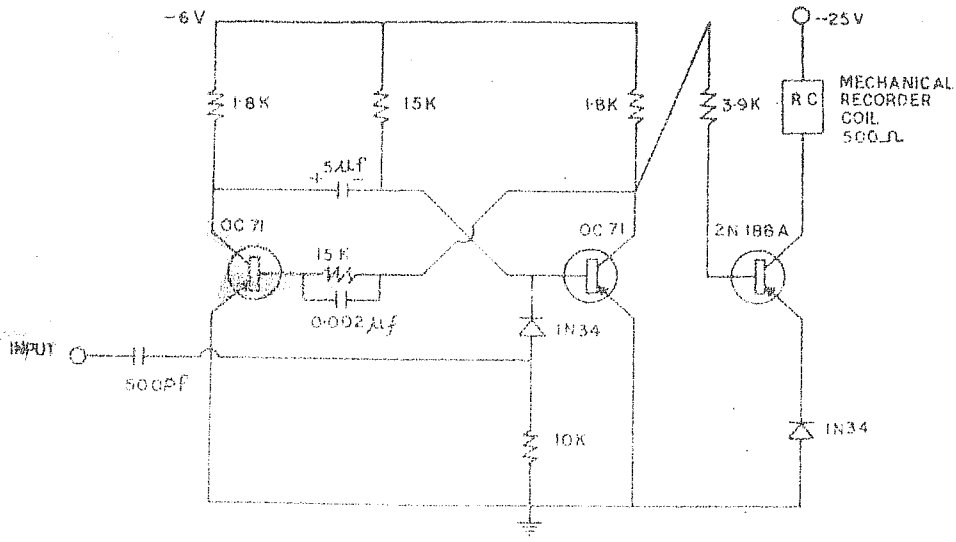

Fig.2.12 Recorder circuit

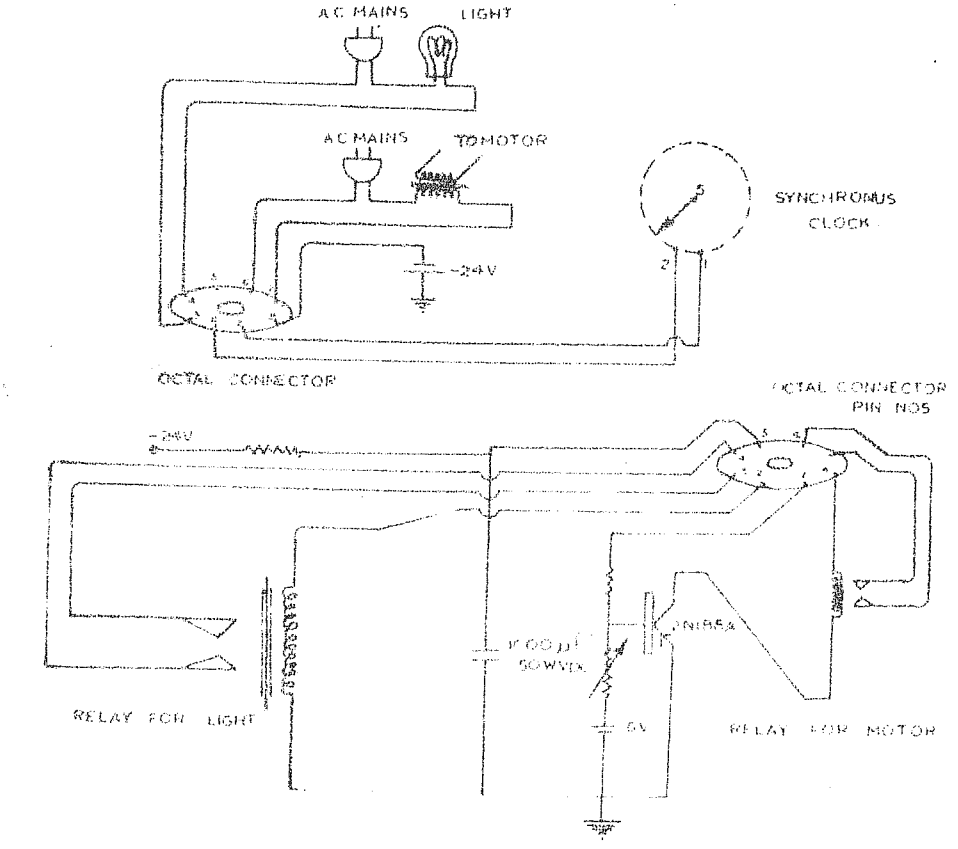

Fig.2.13 Camera control circuit

of the discriminator. Once the amplifier gain is fixed, the performance of the scintillation detector depends primarily upon the photomultiplier voltage and the discriminator level. An optimum combination of these parameters is obtained by determining the characteristic dependence of the counting rate as a function of the photomultiplier voltage and the discriminator level.

2.4.1.1 High Voltage

Figure (2.14) shows the dependence of the count rate of the detector on the high voltage of the photomultiplier for two different discriminator levels. Curve (a) and (b) shown in the figure represents the count rate variation of any single detector with the applied photomultiplier voltage for two discriminator levels 3 and 4 volts respectively. Curve (c) shows the counting rate characteristics of a typical vertical telescope (i.e. two detector units in coincidence), the discriminator level being adjusted at 3.5 volts. All the curves display a minimal plateau of about 50 to 75 volts with a slope of about $\simeq 0.16\%$/volt, for a single detector and of about $\simeq 0.07\%$/volt or less for the coincidence arrangement. The high voltage for the photomultiplier tubes are carefully adjusted taking into consideration the slope and the extent of the plateau region to provide the maximum possible long term stability.

2.4.1.2 Discriminator setting

After fixing the appropriate high voltage for the photomultipliers, the appropriate discriminator level settings can be

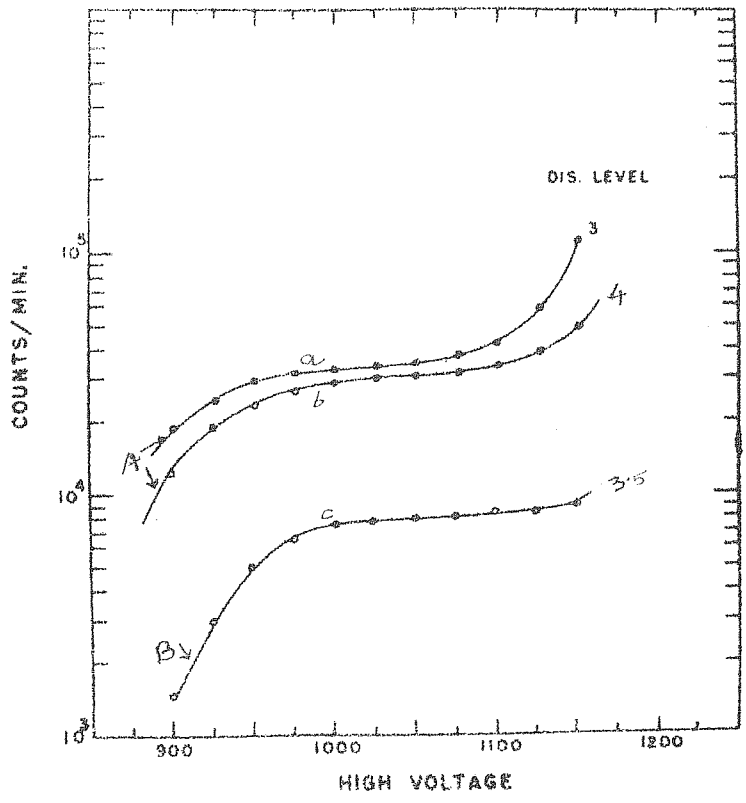

Fig.2.14 (A) The counting rate of a single scintillation detector as a function of the photomultiplier voltage for two descriminator levels.

(B) The coincidence counting rate of a vertical telescope as a function of the photomultiplier voltage.

determined by knowing the counting rate of the individual detectors and the telescope arrangement as a function of the discriminator threshold levels. The integral counting rates of two individual detectors (upper and lower detector, forming vertical telescope) and of the vertical telescope are shown in the Figure (2.15). In this figure, curves 1 and 2 represent the integral counting rate of one upper and lower detector respectively. Curve 3 shows the integral counting rate of a vertical telescope formed by the above two detectors. These curves which represent the integral pulse height distribution of the scintillator, are also contaminated with the background noise, besides the genuine counting rate due to cosmic ray muons. Since, ideally such background can be almost completely eliminated by coincidence arrangement, one should expect to obtain a flat plateau region at the maximum meson counting rate. However, due to the broadening of the meson pulse-height distribution in a large area detector, a completely flat plateau is seldom realised in practice.

The slope of the plateau at the operating level provides a direct measurement of the stability of the instrument against drift in gain. For individual detectors, even near the plateau, the count rate change is observed to be 8 to 10% for one volt change in the discriminator threshold. The corresponding change in count rate for the coincidence (telescope) arrangement is observed to be only 4 to 6%. Because

of the increase in the chance coincidence, curve (3) shows a rising trend at the lower discriminator level.

In the coincidence arrangement an accurate adjustment of two discriminator levels (say D_1 and D_2, for two detectors) have been achieved by using the following procedure. Coincidence rate (integral rate) of the telescope was measured as a function of the discriminator threshold voltage D_2, for different fixed values of D_1. Results obtained for one typical telscope in the present set-up are shown in the Figure (2.16). From such a curve it is possible to identify the region in which the change in the coincidence rate is very low for change in the discriminator level D_1 and D_2. From figure (2.16) the optimum threshold level for the discriminators is observed to be between 3 & 4 volts.

In the actual set-up, the focussing electrode of each of the photomultiplier is operated at the appropriate voltage, to achieve maximum collection efficiency. Typical curve showing the counting rate efficiency as a function of the focussing electrode voltage is shown in Figure (2.17).

2.4.2. Uniformity of response of the detector

To test the uniformity of response of the detector, the following experiment was carried out. A proto-type unit with a scintillator of 50 cms. x 50 cms. size was built. The positions of all the sixteen scintillators inside the large area detector box were numbered (marked) according to the thickness of the

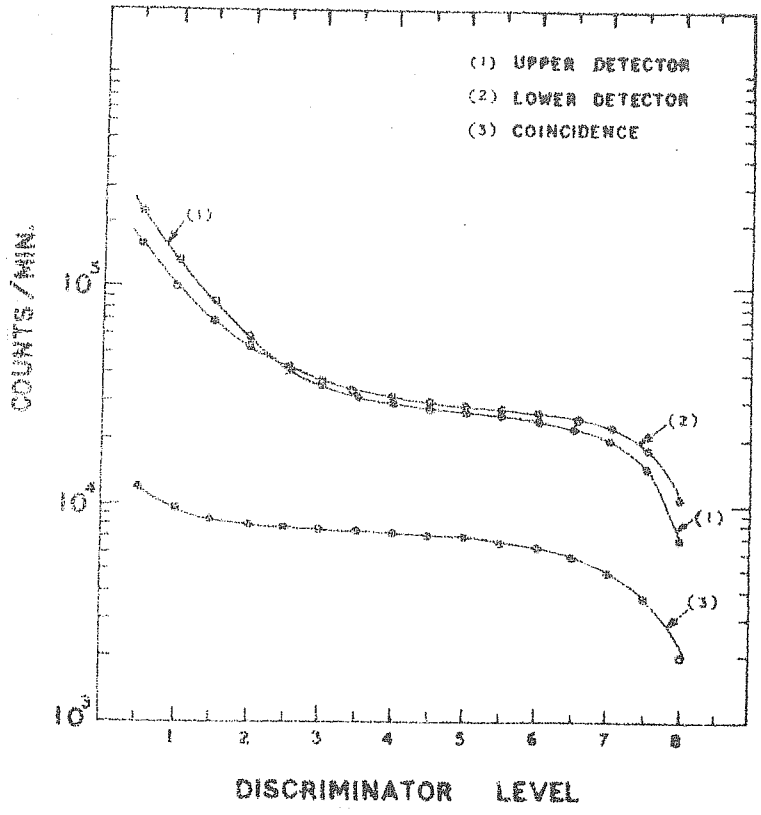

Fig.2.15 The counting rate of the individual scintillation detectors (1) & (2) and the coincidence counting rate of a vertical telescope (3) as functions of discriminator level.

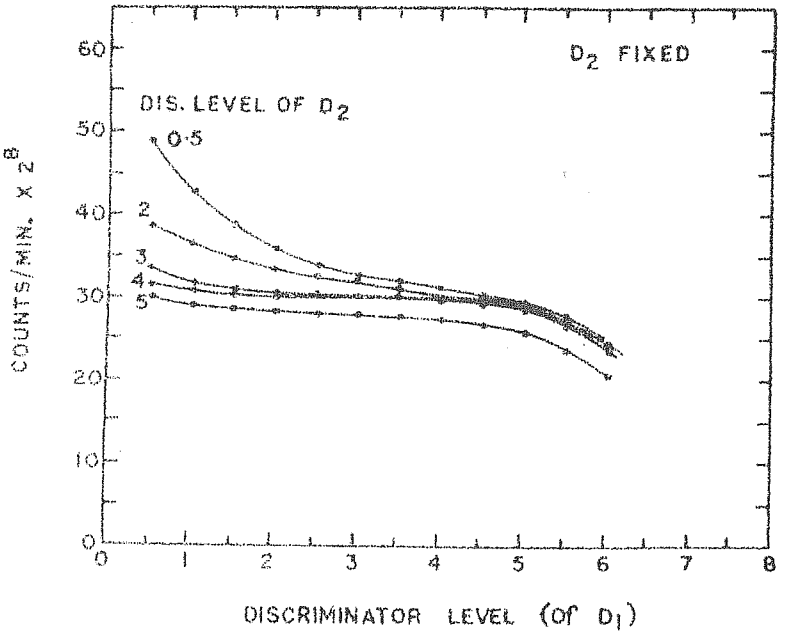

Fig.2.16 Coincidence counting rate of a typical vertical telescope versus the discriminator level of the upper detector(D_1), for different fixed discriminator levels of the lower detector(D_2).

scintillator (as shown in figure 2.03). All the scintillators were removed from the detector box. Then one scintillator was placed at its proper place inside the detector box. The proto-type unit was kept directly below this scintillator and integral coincidence rates were taken between the detector and the proto-type unit for different discriminator levels. The first scintillator was removed and a second scintillator was placed at its appropriate place. Proto-type unit was brought directly below the second scintillator and again coincidence rate was taken between the detector and the proto-type unit. This method was repeated for all the sixteen scintillators. Since the position of different scintillators being different with respect to the position of the photomultiplier in the detector-box, the count rates obtained from the above experiment for all the scintillators will provide an estimate of the uniformity of response of the detector.

Three positions 'a', 'b' and 'c' are shown in Figure (2.18) where 'a' corresponds to the four innermost scintillators while 'c' corresponds to the four outermost scintillators. The integral counting rate obtained for these three positions 'a', 'b' and 'c' are shown in Figure (2.19). It is found that the change in the count rate efficiency between the centre and the corner scintillators, i.e. 'a' & 'c', is less than 8 to 10%.

2.4.3 Routine Check-up

The regulated output from the high voltage supplies, the

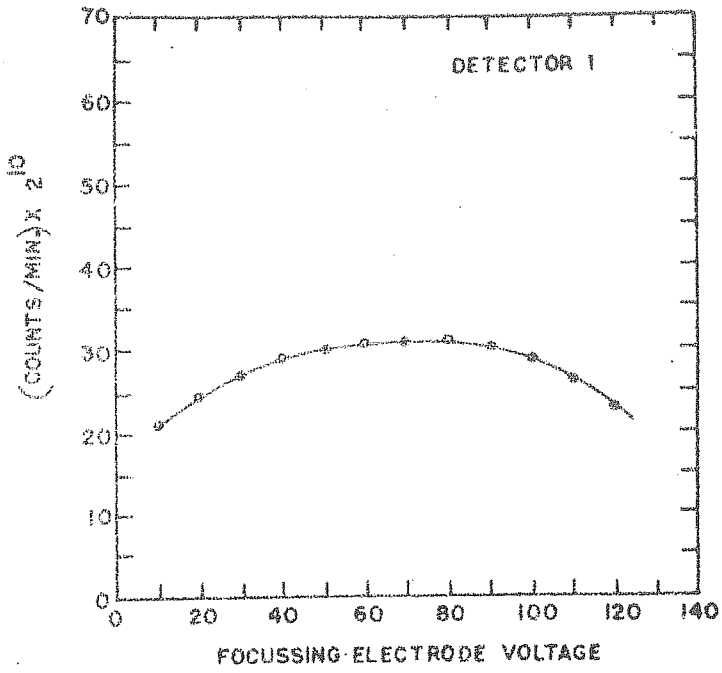

Fig.2.17 Counting rate of a scintillation detector as a function of the focussing electrode voltage of the photomultiplier tube.

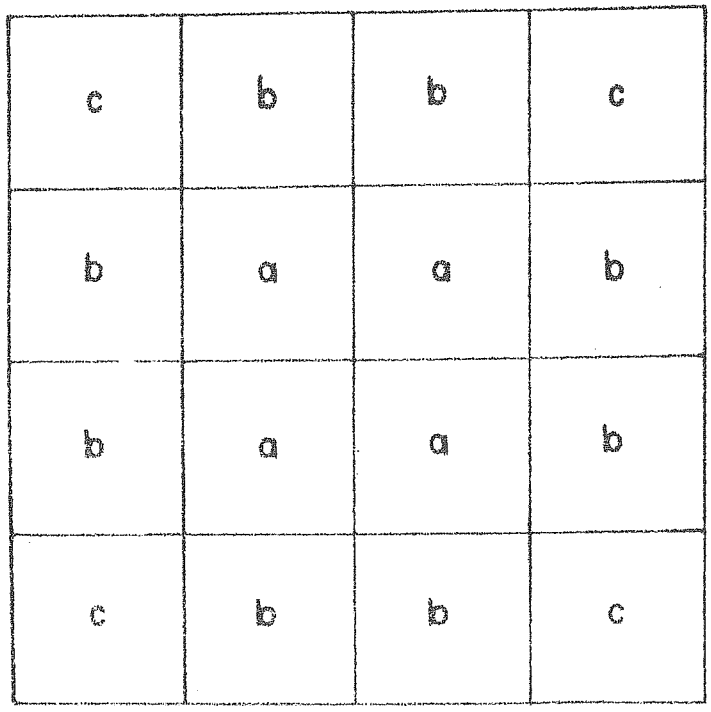

Fig.2.18 Bottom-view of the scintillation detector showing the three different positions 'a', 'b' and 'c' of the scintillator slabs.

photomultiplier voltages, the low voltage supplies and the focussing electrode voltages are checked every day. The performance characteristics of the telescopes are tested by well known statistical methods. The overall stability of the detection system is tested at frequent intervals, by determining the counting rate plateau.

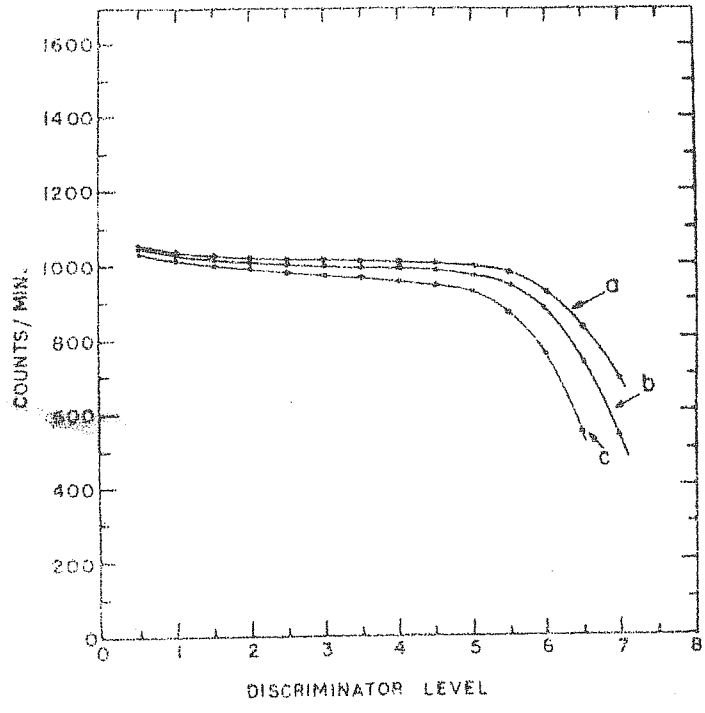

Fig.2.19 Integral coincidence counting rate between the proto-type unit and the detector with a single scintillator slab placed at three different positions 'a', 'b' and 'c'.

C H A P T E R - III

DATA PROCESSING AND METHOD OF ANALYSIS

3.1 Data recording and self-consistency check

From the hourly photographs of the mechanical recorder, the readings of different telescopes for 00, 01, 02 ..... 23, 24 hours local time are noted. The difference between successive readings gives the hourly values of cosmic ray intensity centred at 0.5, 1.5 ..... 23.5 hours. Data recorded by independent but identical telescopes are added together after ensuring their self-consistency. Appropriate normalisation procedures were adopted to obtain the total counting rate of each set of telescopes, even when data from one or more of such set is not available.

3.2 Data processing

Before being able to use the observed data for investigating the time variations, the data has to be corrected for variations due to meteorological changes. The data will have to be further processed to quantize information relevant to the daily variations.

3.2.1 Correction for Barometric Variations

It has been shown by a number of workers (Elliot and Dolbear, 1951; Bachelet and Conforto, 1956; Peacock et al., 1968) that the barometric pressure coefficient is not significantly different for vertical and inclined telescopes.

Therefore we have used the same value of the pressure coefficient, namely β = -0.21%/mm. of Hg. for vertical and for inclined telescopes to correct the cosmic ray intensity for pressure variations. The pressure values used for correcting the cosmic ray data were obtained at each hour from the pressure records at 0.5, 1.5.....23.5 local hours.

3.2.2 Temperature correction

An accurate estimate of the temperature induced meson-intensity variations is possible, only when a precise knowledge of temperature variations, from the ground level to about 50 mb is available, at different times of the day. However, data are normally available only twice a day. Further, it is usually available only up to 100 mb, which is completely inadequate for our purposes. Besides, their accuracy is also limited due to radiation errors. In order to overcome this difficulty, various workers have attempted to use the ground temperature for correcting the meson-intensity variations, assuming certain empirical relationships between the variations at ground level and at higher levels.

The first systematic attempt in arriving at a satisfactory empirical approach was made by Dorman and Feinberg(1955). They divided the whole atmosphere into eleven layers, each layer having its temperature coefficient, as shown in Table-3.01.

The total temperature correction is given by

$$\frac{\delta N_\mu}{N_\mu} = \sum_{i=1}^{11} K_i \, \delta T_i \qquad \ldots\ldots 3.01$$

where $\frac{\delta N_\mu}{N_\mu}$ is the resultant variation in the meson intensity due to atmospheric temperature variations at different layers. K_i and δT_i are the partial temperature coefficients and the mean temperature variations for the i'th layer respectively. The values of K_i for different isobaric levels are given in Table-3.01.

TABLE - 3.01

Height in mb.	1000	900	800	700	600	500	400	300	200	100	50
$K_i \times 10^{-3}$	20	21	22	24	25	25	28	33	38	31	23

Because of the non-availability of upper air temperature data, at least for four times a day, we have not corrected cosmic ray intensity for the daily variation of atmospheric temperature. However, we emphasise that the atmospheric temperature effects being equal in all directional telescopes inclined at the same zenith angle, the difference in intensity between any two telescopes from East, West, North and South will be free from the atmospheric contribution, at least to the first degree of approximation.

3.2.3 Moving averages

Before attempting to derive the parameters describing

the daily variation, it is essential to remove the effects due to gradual or slowly varying day to day changes of cosmic ray intensity. The method of 24 hourly moving averages has been adopted, to separate out the daily variation from changes having periodicity of more than a day. Even though this method is quite satisfactory in eliminating the 'slope effects' on the daily variation, the curvature effects and effects due to short term, world-wide changes of intensity still persist. However, such residual effects are generally small and can be ignored in a study of daily variation on a day to day basis (Rao and Sarabhai, 1961).

3.2.4 Harmonic Analysis

After removing the long term trend by the method of moving averages from the pressure corrected hourly intensity, the phase and amplitude of the first and second harmonic of the daily variation is obtained by subjecting the data to harmonic analysis. In addition, the time of maximum 'T_{max}', time of minimum 'T_{min}' and the peak to peak amplitude of the daily variation are also obtained by fitting the data with sinusoidal curves having 24 hour and 12 hour periodicity.

3.3 The response Characteristics of the Telescopes

3.3.1 Calculation of geometrical sensitivity

In order to relate the daily variation of μ meson intensity measured by a directional telescope to the anisotropy

of primary cosmic radiation, it is necessary to know the response characteristics of a telescope. Response characteristics of a telescope for any direction can be calculated by knowing the sensitive area of the telescope for the particles coming from that direction and the intensity of radiation in that direction. Newell (1948) and Newell and Pressly (1950) have discussed the geometrical sensitivity (sensitive area x solid angle) of a two G.M.counter telescope. Calculation of geometrical sensitivity of more complicated set up such as cylindrical, cubical and rectangular parallelopiped geometries have been discussed by Brunberg, (1958); Parsons, (1957) and Kane and Rao, (1958) respectively.

Kane and Rao (1958) have given the formula for the geometrical sensitivity of a rectangular telescope with vertical axis in terms of the length, breadth and separation between the extreme trays. Following their method, we have calculated the geometrical sensitivity of the vertical telescopes in the present set-up. Kane and Rao (1958) have also calculated the geometrical sensitivity of inclined telescopes where the detector trays are inclined at an angle α to the zenith. In the present set up however, detector trays are kept horizontal. The size of each detector tray is 'bxb' metres (b = 2 metres). The adjacent trays are separated by a horizontal distance 'C' = 0.5 metre. The vertical separation between two trays of the telescope is 'a'= 2 metres. Considering the above geometry and following the method

given by Kane and Rao (1958) we have calculated the geometrical sensitivity for our inclined telescopes. The minimum angle of response θ_1, the maximum angle of response θ_3 and the mean direction of the inclined telescope θ_2 in the present set up are given by

$$\theta_1 = \tan^{-1}\frac{c}{b} \qquad \theta_2 = \tan^{-1}\frac{a+c}{b}$$

$$\theta_3 = \tan^{-1}\frac{(2a+c)}{b} \qquad \text{.....3.02}$$

The radiation sensitivity calculated for inclined telescopes is shown in figure(3.01). An important point that emerges from this study is that even though the mean direction of the telescope is $\sim 51^\circ$, the radiation sensitivity is maximum at about 45° zenith angle.

3.3.2 Cut-off rigidity

The cut-off rigidities for different zenith and azimuth angles at Ahmedabad have been obtained by (Daniel and Stephens, 1966) using the Finch and Leaton (1957) expansion of the geomagnetic field which includes upto sixth harmonic. The calculated cut-off rigidities as a function of zenith and azimuth angles at Ahmedabad are plotted in figure (3.02)

3.3.3 Asymptotic directions and Cones of acceptance for vertical and inclined telescopes at Ahmedabad.

In order to relate the directions of arrival (θ and ϕ) at the top of the atmosphere to the directions of the asymptotic

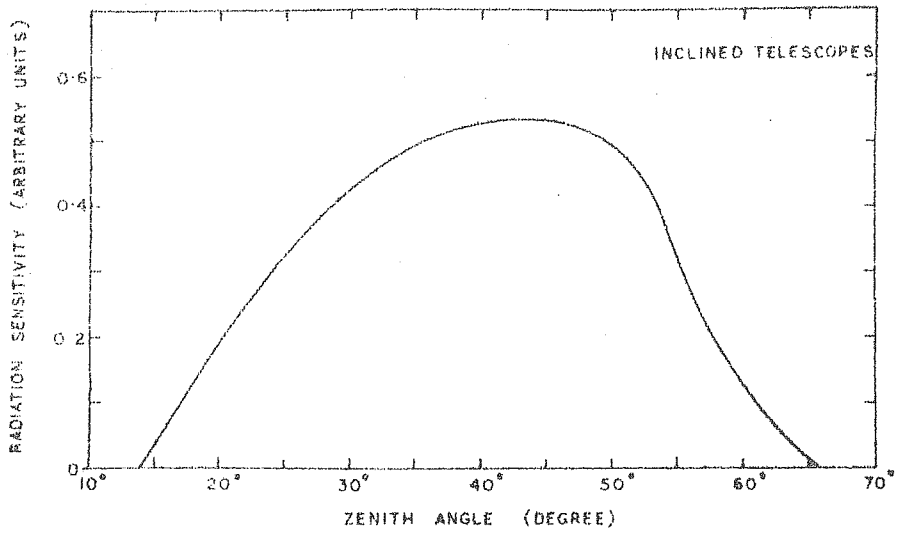

Fig.3.01 Radiation sensitivity of the directional telescopes inclined at 51° to the zenith at Ahmedabad

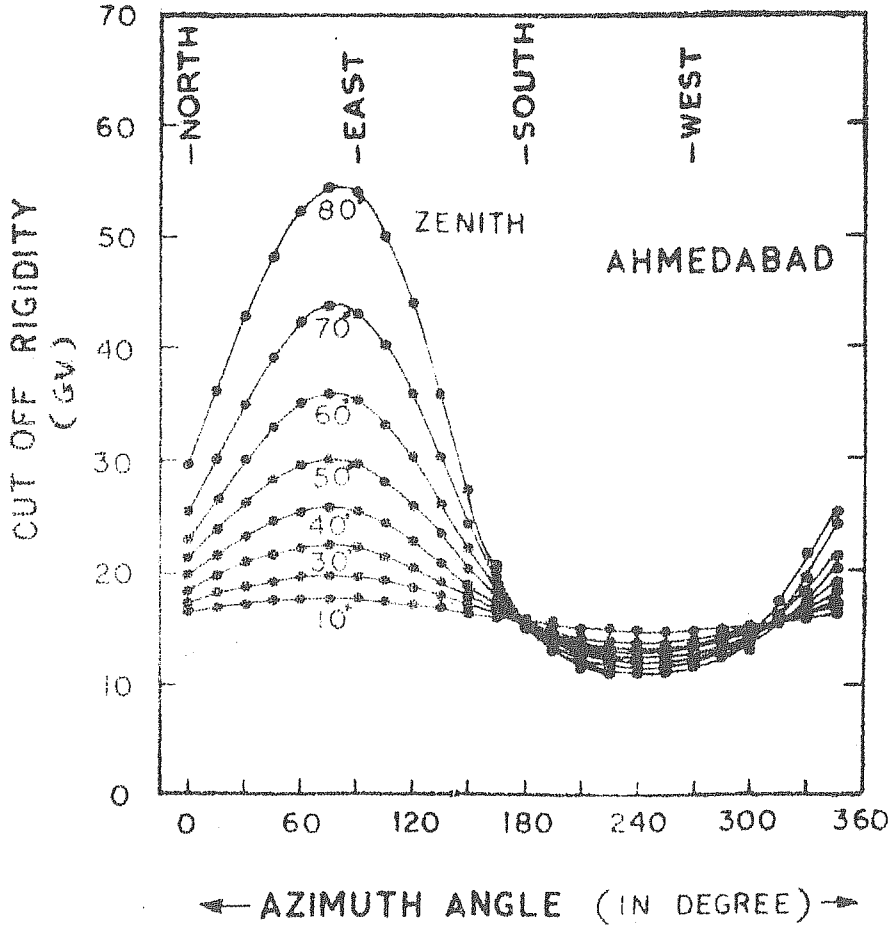

Fig.3.02 Geomagnetic cut-off rigidity as a function of azimuth for different zenith angles at Ahmedabad.

velocity vectors, (λ and ψ) it is necessary to know the detailed trajectory information of cosmic ray particles in the geomagnetic field. McCracken et al.(1962) have determined the trajectories using the sixth degree simulation of the geomagnetic field. For number of stations the asymptotic directions of approach for particles incident from 0, 16^{o} and 32^{o} zenith angles in east, west, north and south azimuths have been published by McCracken et al.(1965). For the present work the asymptotic directions for zenith angles greater than 32^{o} have been obtained from Brunberg and Dattner's (1953) experimental observations. Since these observations are made using only a dipole simulation of the geomagnetic field, by comparing these values with the calculated values of McCracken et al.(1965) appropriate correction have been made to take into account the non-dipole nature of the geomagnetic field. At energies above about 25 GeV these extrapolated asymptotic directions of approach are reasonably correct. At very near the cut-off rigidities, however, these may be in error by as much as $\pm\ 8^{o}$. Figure (3.03) shows the asymptotic directions of approach along 45^{o} zenith for particles incident from east, west, north and south azimuths at Ahmedabad.

Figure (3.04) shows the asymptotic cones of acceptance for these telescopes. The cone-envelope contains the asymptotic directions for zenith angles which has radiation sensitivity more than 0.37 (Figure 3.01). From an examination of the

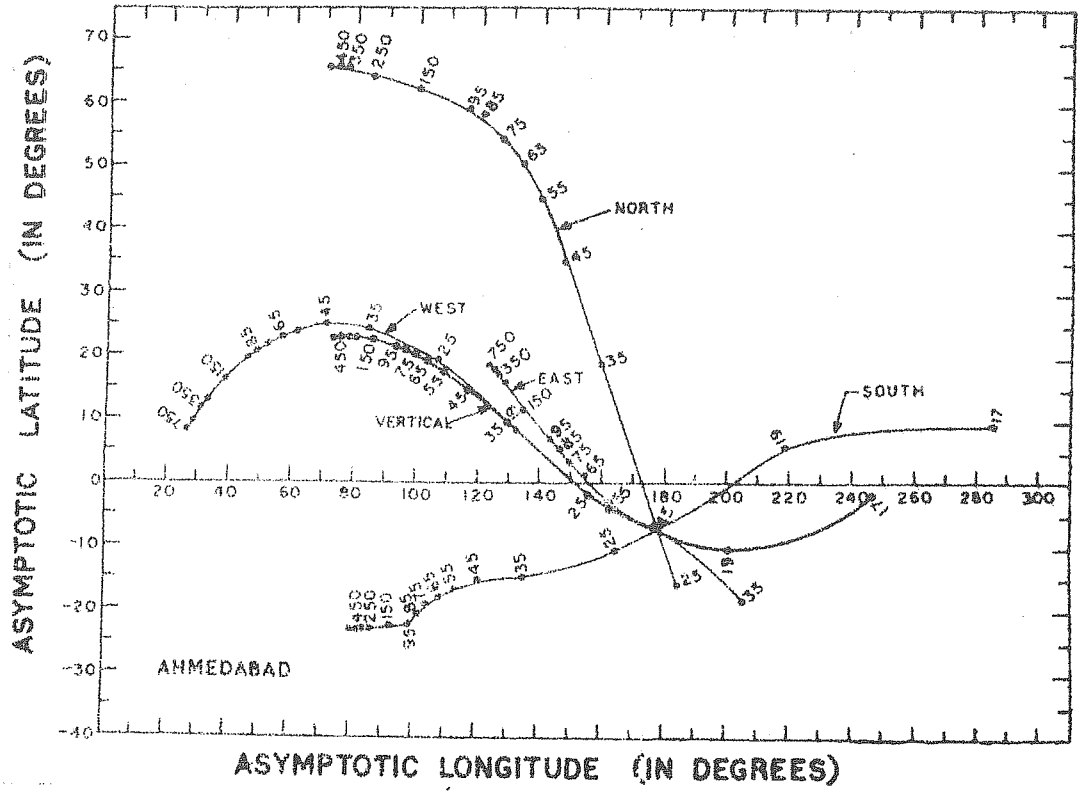

Fig.303 Asymptotic directions of approach for primary cosmic ray particles arriving along East (45°), West (45°), North (45°), South (45°) and vertical at Ahmedabad. (Numbers on curves indicate rigidity in GV.)

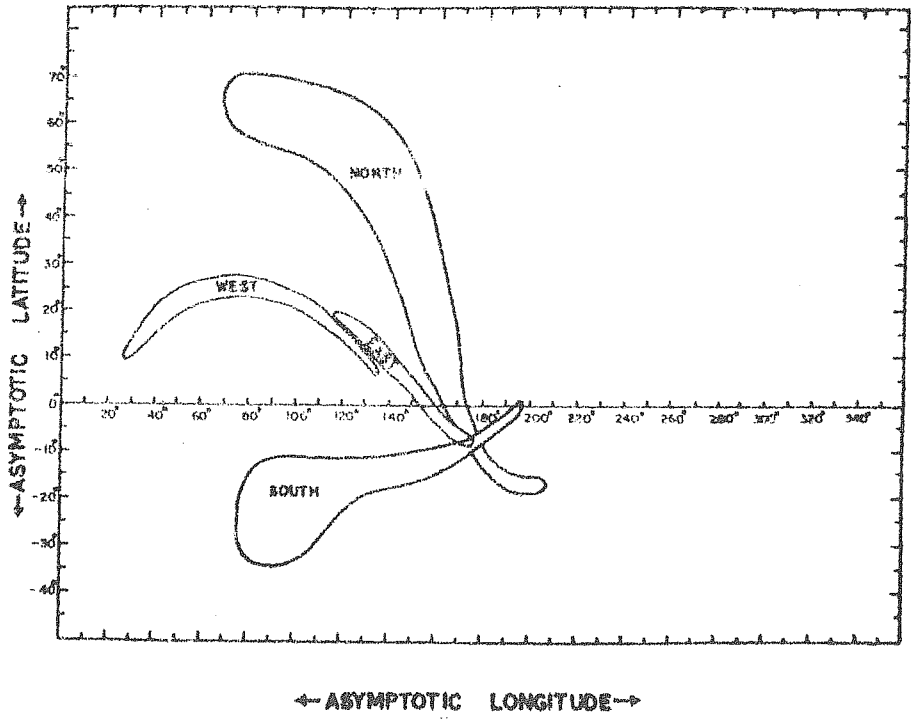

Fig.3.04 Asymptotic cones of acceptance for East, West, North and South telescopes at Ahmedabad.

figure (3.04) we may summarise the general properties of the asymptotic cones as follows:

(1) East pointing telescope leads the west pointing one, by about 6 hours, with the former scanning almost entirely along the equator.

(2) North pointing telescope leads the west pointing one, by about 4 hours, with the latter scanning mostly in the 10°-25° latitude belt. The north pointing one, however, scans almost upto 65° declination.

3.3.4 Coupling coefficients for vertical and inclined meson telescopes

From the observed latitude effect, Dorman, (1957) and Quenby and Webber (1959) have evaluated coupling coefficients for vertically incident nucleons and mesons upto 15 GeV. Coupling coefficients for particles above this energy have been obtained by extrapolation method. As described in Chapter I, Krimsky et al.(1966) have calculated the coupling coefficients for meson component arriving from zenith angles 0°, 8°, 16°.....64° which is shown in Figure (1.02 Chapter I). From that figure it is seen that the maxima of the response-function-curves shifts to higher energies with increase in the zenith angle. In all our calculations of variational coefficients we have utilised the coupling constants given by Krimsky et al. (1966). To achieve a measure of confidence in the coupling

constants we have checked that the expected relative intensities at different inclined telescopes using this coupling coefficients agree reasonably well with the observed values (Table 3.02).

TABLE 3.02

Telescope	Cut-off rigidity GV.	Relative intensity %	
		Calculated	Observed
West	12.2	100.0	100.0
South	15.3	98.6	98.0
North	21.3	94.1	93.9
East	29.7	86.2	87.8

3.3.5 Calculation of variational coefficient and its application to the daily variation

In order to relate the observed cosmic ray secondary variations at ground after correcting for meteorological effects, to primary anisotropy, it is necessary to calculate the effects due to geomagnetic bending, the relationship between the primary and secondary cosmic rays and the detector response on the observed amplitude and phase. This has been achieved through the use of 'variational coefficients' which have been derived by Rao et al.(1963). Using the coupling coefficients, the detector response and the trajectories of primary cosmic ray particles in the geomagnetic field it has become possible

to derive the characteristics of the anisotropy in outer space (Rao et al. 1963; Bercovitch, 1963; McCracken and Rao, 1965; Jacklyn et al., 1970) from the observed daily variations at ground.

Following the method given by Rao et al.(1963), we have derived the applicable variational coefficients for vertical and inclined meson telescopes at Ahmedabad. The method is briefly summarised here.

The fractional counting rate ($dN\Omega_i$) due to cosmic ray intensity from solid angle Ω_i is given by

$$\frac{dN\Omega_i}{N\Omega_i} = \int_0^{\infty} W(E) \frac{\delta D(E)}{D(E)} \quad \frac{Y(\Omega_i, E)}{Y(4\pi, E)} \, dE \qquad \ldots\ldots 3.03$$

where $\frac{Y(\Omega i, E)}{Y(4\pi, E)}$ is the ratio of the asymptotic directions accessible from the solid angle Ω_i and the total solid angle from all accessible directions. Assuming the energy spectrum of variation to be of the form

$$\frac{\delta D(E)}{D(E)} = AE^{-\beta} \quad \text{for} \quad E_{min} < E < E_{max}$$
$$= 0 \qquad\qquad E < E_{min}, \quad E > E_{max} \qquad \ldots\ldots 3.04$$

and substituting it in equation 3.03 we get

$$\frac{dN_{\Omega i}}{N_{\Omega i}} = A.v \ (\Omega_i, \beta) \qquad \ldots\ldots 3.05$$

where 'A' is the strength of the primary anisotropy and

$$v\ (\Omega_i, \beta) = \int_{E_{min}}^{E_{max}} W(E).E^{\beta}\ \frac{Y(\Omega_i\ E)}{Y(4\pi\ ,E)}\ dE \qquad \ldots\ldots\ 3.06$$

is defined as the variational coefficients of the detector corresponding to the solid angle Ω_i and spectral exponent 'β'.

Assuming that the strength of the anisotropy varies with declination as $Cos^n\lambda$ the variational coefficient can be evaluated from

$$v\ (\Omega_i, \beta) = \int_{E_{min}}^{E_{max}} W(E)\ E^{\beta}\ \frac{Y(\Omega_i, E)}{Y(4\pi\ ,E)}\ Cos^n\lambda\ ,\ dE \ \ldots\ 3.07$$

The factor $\frac{Y(\Omega_i, E)}{Y(4\pi\ ,E)}$ can be estimated following the method suggested by Rao et al. (1963). In evaluating this factor it is essential to consider the appropriate zenithal weightage equal to the radiation sensitivity of the detector (or telescope) along the all accessible directions.

Assuming that the form of the anisotropy is expressed as

$$\frac{\delta D(E)}{D(E)} = AE^{\beta} = f\ (\psi)\ g\ (\lambda)\ E^{\beta} \qquad \ldots\ldots\ 3.08$$

equation 3.05 reduces to

$$\frac{dN\Omega_i}{N\Omega_i} = f\ (\psi)\ g\ (\lambda)\ v,\ (\Omega_i, \beta) \qquad \ldots\ldots\ 3.09$$

Summing over all Ω_i

$$\frac{dN\Omega_i}{N\Omega_i} = f(\psi)\ \Sigma\ g(\lambda)\ v\ (\Omega_i, \beta)$$

$$\frac{dN_{\Omega i}}{N_{\Omega i}} = f(\Psi) . \; V(\Psi, \beta) \qquad \ldots\ldots 3.10$$

Considering the solid angle between the meridional planes at $\psi = 5i^{\circ}$ and $\Psi = 5(i + 2.5)^{\circ}$ (where i is a positive integer or zero), the flux from within this solid angle is assumed to be essentially that from the mean longitude $5i + 2.5^{\circ}$

Assuming the anisotropy to be an arbitrary function of η and expanding it as a Fourier series

$$f(\eta) = \sum_{m=1}^{\infty} \alpha_m \; \text{Cos } m(\eta - Cm) \qquad \ldots\ldots\ldots 3.11$$

where η is the angle measured to the left of the sun-earth line and α_m and C_m are arbitrary amplitude and phase constants. 'C_m' is a direction of viewing from which a maximum of the m'th harmonic is seen. From figure(3.05),

$$\eta = \Psi + 15T - 180^{\circ}$$

$$\therefore f(\Psi) = \sum_{m=1}^{\infty} \alpha_m \; \text{Cos } m(\Psi + 15T \pm 180^{\circ} - C_m) \qquad \ldots\ldots 3.12$$

where $\Psi = 5(i + 2.5)^{\circ}$. Inserting this value of $f(\Psi)$ in (3.10) and summing over the subscript i, we find that

$$\frac{\Delta N}{N} = \sum_{i=0}^{>1} V(\Psi, \beta) \sum_{m=1}^{\infty} \alpha_m \; \text{Cos } m(5i + 15T + 2.5 - C_m)$$

$$= - \sum_{m=1}^{\infty} \alpha_m B_m \; \text{Cos}\left[m(15T - C_m) + \gamma_m \right] \qquad \ldots\ldots 3.13$$

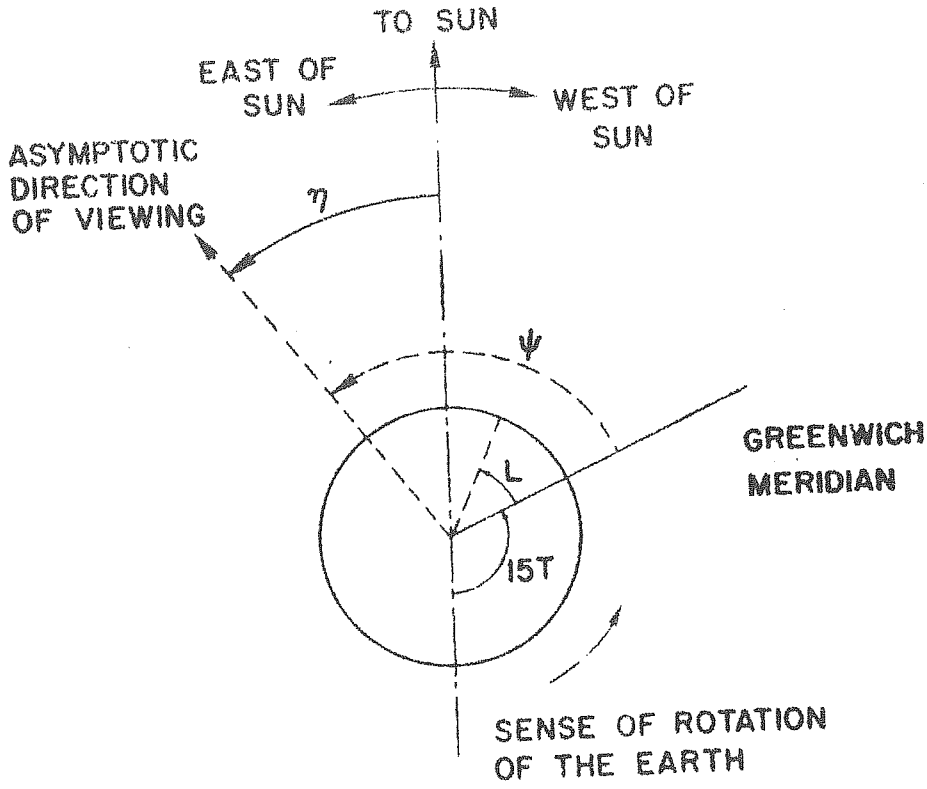

Fig.3.05 Asymptotic direction of viewing of an arbitrary station.

where B_m is called the relative amplitude and is given by

$$B_m^2 = X_m^2 + Y_m^2$$

$$= \left\{ \sum_{i=0}^{71} V(\psi, \beta) \cos m(5i+2.5) \right\}^2 + \left\{ \sum_{i=0}^{71} V(\psi, \beta) \sin m(5i+2.5) \right\}^2 \quad \ldots\ldots 3.14$$

and

$$\tan \gamma_m = \frac{Y_m}{X_m} = \frac{\sum_{m=1}^{71} V(\psi, \beta) \sin m(5i + 2.5)}{\sum_{m=1}^{71} V(\psi, \beta) \cos m(5i + 2.5)} \quad \ldots\ldots 3.15$$

In equation (3.13) $\alpha_m B_m$ and $(-mc_m + \gamma_m)$ represents the amplitude and phase constant of the m'th harmonic.

The universal time at which the maximum intensity is observed is given by

$$T_m = \frac{180m + m\,C_m - \gamma_m \text{ hours}}{15m} \quad \ldots\ldots 3.16$$

and local time of maximum intensity is given by

$$t_m = \frac{180m + C_m - (\gamma_m - mL) \text{ hours}}{15m} \quad \ldots\ldots 3.17$$

where 'L' is the geographic longitude of the station. The term $(-\gamma_m - mL)$ is usually defined as the 'geomagnetic bending' of the cosmic ray particle.

Considering E_{min} = cut-off, E_{max} = 500 GeV and anisotropy as a function of $\cos\lambda$ dependence, McCracken et al. (1965) have evaluated the variational coefficients, relative

amplitude and geomagnetic bending for diurnal and semi-diurnal components for a number of neutron monitors, for different values of 'β' ranging from +0.6 to -1.5. For a detailed study of the anisotropy of galactic cosmic rays on a day to day basis it is necessary to calculate the variational coefficients, relative amplitude and geomagnetic bending for different combinations of 'β', 'E_{min}' and 'E_{max}'. Besides, experimental observations indicate that the average diurnal anisotropy varies as cosine of declination (McCracken and Rao, 1965) and average semi-diurnal anisotropy varies as square of cosine of declination (Subramanian and Sarabhai, 1967; Quenby and Lietty, 1968; Rao and Agrawal, 1970; and Subramanian, 1971). Therefore calculations of variational coefficients need to be extended to inclue $Cos^2\lambda$ dependence.

We have calculated the variational coefficients $V(\Psi)$ relative amplitude (α_m) and geomagnetic bending (τ_m) for a number of neutron monitors and for meson monitors at Ahmedabad. Energy spectrum of variation is assumed to be of the form

$$\frac{\delta D(E)}{D(E)} = AE^{\beta} \quad \text{for} \quad E_{min} < E < E_{max} \qquad \ldots\ldots 3.18$$

The calculations have been carried for 'β' varying from -1.2 to +1.0 (in steps of 0.2) with (i) E_{min} = cut-off, 4 and 15 GeV. Keeping E_{max} = 500 GeV constant and (ii) E_{min} = cut-off and E_{max} = 35, 45, 55, 65, 75, 85, 95, 127.5, 227.5, 350, 450, 500 GeV. In calculating the variational

coefficients for inclined telescopes, particles incident from several zenith angles (30°, 35°, 40°, 45°, 50°, 55°, 60°) have been considered with appropriate weightages as described in Section 3.3.1.

Mori (1968)[a,b] has calculated the variational coefficients for several neutron and meson monitors. However, his calculations are not available for vertical as well as for inclined meson telescopes at Ahmedabad.

3.3.6 Energy spectrum of variation

Data from a large number of stations can be used to determine the energy spectrum of daily variation. From the observations at different stations the amplitude and the time of maximum of the anisotropy 'in space' for different values of 'γ' with different sets of E_{min} or E_{max} can be computed. A goodness of fit is obtained for a particular set of 'γ' and E_{min} or E_{max} which gives the minimum scatter between the computed values of amplitude and phase 'in space' for number of stations. In actual fact we have tried to obtain the goodness of fit by ensuring minimum variance in both the orthogonal components of the individual harmonic component. Following the approach of Subramanian, 1964; Sarabhai and Subramanian, 1966; we define the free space values a^{*}_{ji} and b^{*}_{ji} corresponding to the observed diurnal and semi-diurnal components (a_{ji}, b_{ji}) at any station as

$$a^{*}_{jik} = \frac{a_{ji}\ \mathrm{Cos}\,\gamma_{jik} - b_{ji}\ \mathrm{Sin}\,\gamma_{jik}}{\alpha_{jik}} \qquad \ldots\ldots 3.19\text{-a}$$

$$b^{*}_{jik} = \frac{a_{ji}\,\mathrm{Sin}\,\gamma_{jik} - b_{ji}\,\mathrm{Cos}\,\gamma_{jik}}{\alpha_{jik}} \qquad \ldots\ldots 3.19\text{-b}$$

where j = 1 and j = 2 refers to the first and second harmonic components respectively. k denotes the particular combination of 'β' and E_{min} or E_{max} in the above formula, α_{jik} and γ_{jik} are the relative amplitude and geomagnetic bending respectively for the station 'i'.

The variance S_k^2 between the space values of different stations is determined for different combination of 'β' and (i.e. for different values of k) E_{max}. S_k^2 which provides a measure of the scatter in the derived values r_1^*, ϕ_1^*, r_2^* and ϕ_2^* in space is given by

$$S_k^2 = \sum_{i=1}^{N} \sum_{j=1}^{2} \frac{(a^{*}_{jik} - \bar{a}^{*}_{jik})^2 + (b^{*}_{jik} - \bar{b}^{*}_{jik})^2}{\sigma_{jik}^2} \qquad \ldots\ldots 3.20$$

where the bar denotes values averaged over all stations and

$$\sigma^2_{jik} = \frac{(N^2 - 2N)\alpha^2_{jik}\,\sigma^2_{ji} + \sum_{i=1}^{N} \alpha^2_{jik}\,\sigma^2_{ji}}{N^2} \qquad \ldots\ldots 3.21$$

The minimum values of S_k^2 indicate the best fit for the experimental observations of the cosmic ray anisotropy.

3.4 Characteristics of Ahmedabad Telescopes

Calculated values of α_j and γ_j for E_{max} = 500 GeV, for Ahmedabad meson monitors are presented in Figures(3.06), (3.07), (3.08) where Figure (3.06) shows the ratios of the relative

amplitude of the diurnal and semi-diurnal components of East/West and North/South as a function of 'β'. It is seen from the Figure (3.06) that for $E_{max} \geq 227.5$ as 'β' varies from -1.2 to 1.0, the ratio of the expected diurnal amplitude of

(i) East/West varies from 0.77 to 1.1

(ii) North/South varies from $\sim$ 0.9 to 0.58.

The ratio of the expected semi-diurnal amplitude of

(i) East/West varies from $\sim$ 0.92 to 1.16

(ii) North/South varies from $\sim$ 0.94 to 0.25

The geomagnetic bending ($\mathcal{T}_j$) of the diurnal and semi-diurnal component for East, West, North, South and Vertical telescopes at Ahmedabad as a function of 'β' for E_{max} = 500 GeV is shown in Figure (3.07). Figure (3.08) shows the computed geomagnetic bending difference between West and East $|\mathcal{T}_{jW} - \mathcal{T}_{jE}|$ for diurnal and semi-diurnal component. It may be seen that the difference in geomagnetic bending for E_{max} = 500 GeV., varies between 5 to 6 hours when 'β' changes from +1.0 to -1.2. The calculations of the bending difference for other values of E_{max} also indicate that the geomagnetic bending difference is not very sensitive to the choice of E_{max}. From these detailed calculations we conclude that for values of 'β' ranging within these limits, the geomagnetic bending difference between West and East is almost constant $\sim$ 6 hours.

The greater advantage of having multi-directional telescope is to use the difference component from two directional

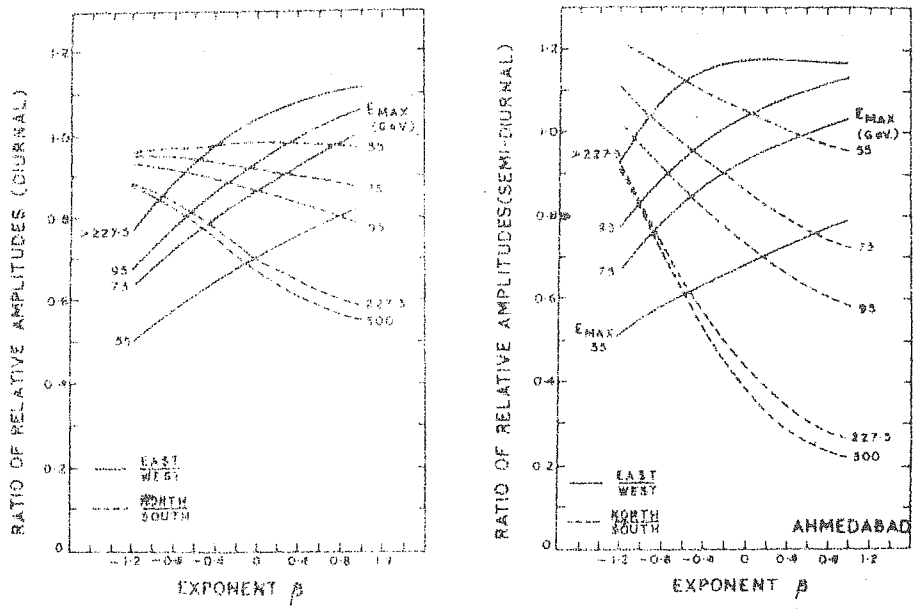

Fig.3.06 Ratio of relative amplitudes of E/W(solid lines) and N/s(dashed lines) for (a) diurnal and (b) semi-diurnal components as a function of ' ' for various values of E_{max}.

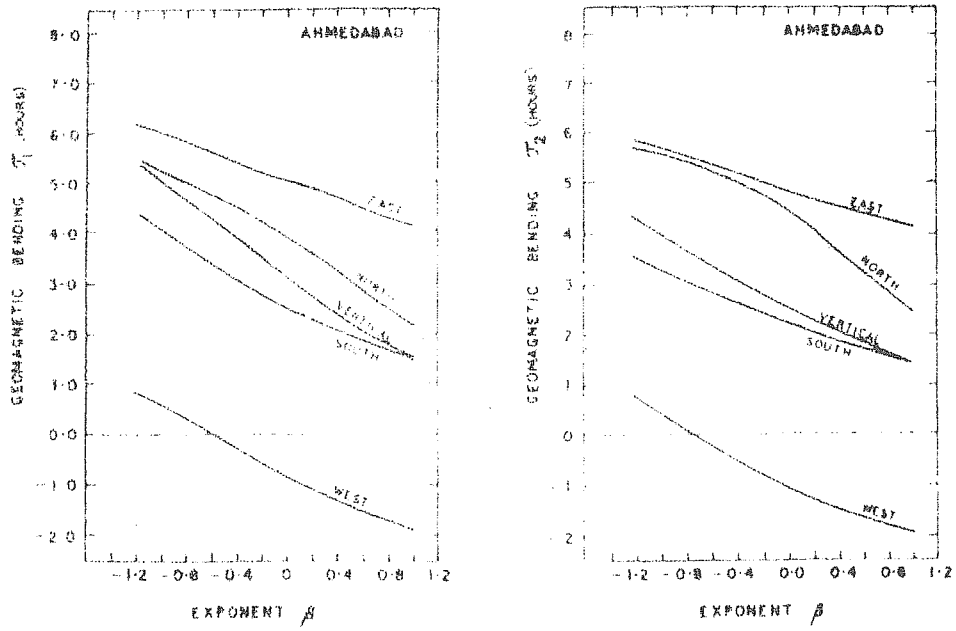

Fig.3.07 Average geomagnetic deflection for (a) diurnal and (b) semi-diurnal component for East, West, North, South and Vertical telescopes at Ahmedabad (E_{max} = 50) GeV).

telescopes inclined at the same zenith angle but in different azimuths. Such a component will be free from the meteorological variations to a first degree of approximation; since secondaries registered by both the instruments would have passed through the same mass of the atmosphere. However in order to understand the behaviour of the difference components, it would be instructive to construct the expected daily variation curve for West and East telescopes. Assuming an arbitrary amplitude for West telescope for both diurnal and semi-diurnal component, we can derive the expected amplitude of the East telescope for different values of the spectral indices of anisotropy. From these two curves we can obtain the difference component (W-E) at the instrument. Figure (3.09) shows the diurnal and semi-diurnal component observed by West and the expected amplitude at the East pointing telescopes for $\beta = 0, +1.0, -1.0$ and the derived (W-E) curve. From an examination of this figure, we can derive the following generalized conclusions related to the anisotropy of (W-E) data.

(1) Diurnal amplitude of (W-E) will be $\sqrt{1 + \left(\frac{\alpha_{1W}}{\alpha_{1E}}\right)^2}$ times the amplitude observed by East telescope, i.e.

$$r_{1(W-E)} = r_{1E} \sqrt{1 + \left(\frac{\alpha_{1W}}{\alpha_{1E}}\right)^2}$$

(2) Phase of the diurnal component $\phi_{1(W-E)}$ will be shifted to later hours compared to the observed phase (ϕ_{1W}) in the West pointing telescope.

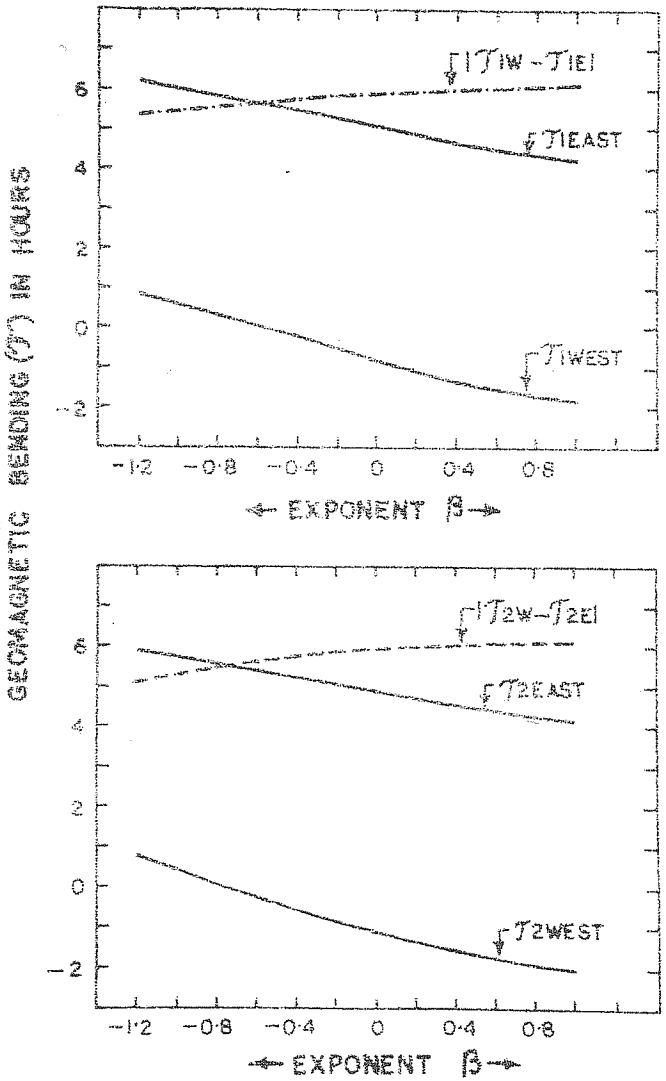

Fig.3.08 Computed difference of geomagnetic deflection between West and East telescopes at Ahmedabad for (1) diurnal and (2) semi-diurnal component with E_{max} = 500 GeV.

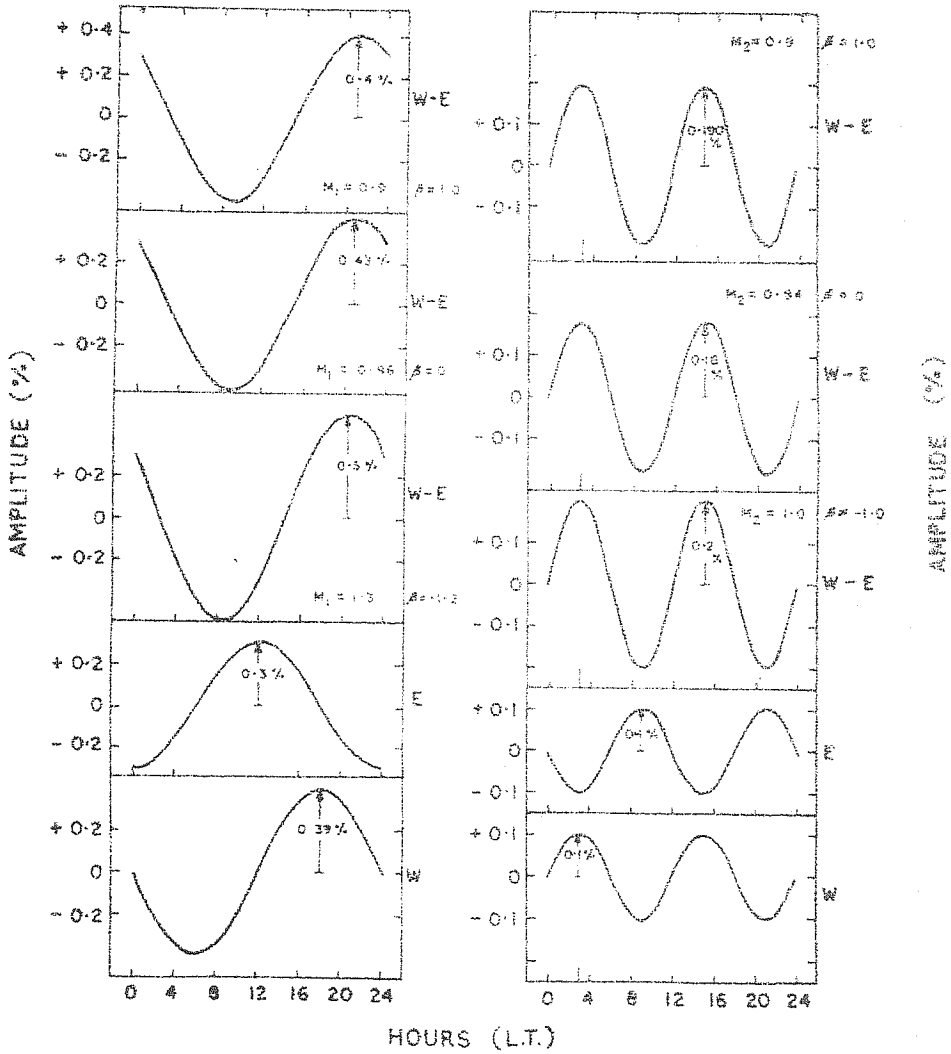

Fig.3.09 With assumed values of the diurnal and semi-diurnal variation in West telescope the (a) diurnal and (b) semi-diurnal variation for (W-E) is shown for three different values of the exponent ' ' (viz. +1.0, 0 and -1.0) with E_{max} = 500 GeV.

(3) Semi-diurnal amplitude of (W-E) will be $1 + (\frac{\alpha_{2W}}{\alpha_{2E}})$ times the amplitude of the East telescope i.e.

$$r_{2(W-E)} = r_{2E}\left[1 + (\frac{\alpha_{2W}}{\alpha_{2E}})\right]$$

(4) Semi-diurnal phase will be the same as that of the West telscope.

$$\phi_{2(W-E)} = \phi_{2W}$$

Because of $\simeq$ 6 hours phase difference between West and East telescopes, the actual semi-diurnal anisotropy in (West + East) data will vanish provided the expected amplitudes of West and East are comparable. Thus in general the semi-diurnal component derived from (W+E) can be attributed to the meteorological or local sources.

As a representative of the above calculations the values of the relative amplitudes α_j and geomagnetic deflection γ_j (for diurnal and semi-diurnal component) for East, West, North, South and vertical telescopes with E_{min} = cut-off and E_{max} = 95 GeV are given in Table (3.03) for different values of 'β' ranging from -1.2 to 1.0.

Since in all our analysis we have utilized mostly the difference components for deriving the anisotropy of galactic cosmic rays, these calculation have been further extended to include West-North, West-South and other similar combinations. For difference-components, the following formulae have been

TABLE 3.03 a

E_{min} = Cut-off E_{max} = 95 GeV. Ahmedabad

	East Telescope				West Telescope			
β	α_1	τ_1	α_2	τ_2	α_1	τ_1	α_2	τ_2
1.0	12.4217	5.88	10.0651	5.69	13.4344	-0.24	10.1923	-0.34
0.8	5.4874	5.95	4.3970	5.74	6.0523	-0.13	4.5082	-0.25
0.6	2.4326	6.02	1.9268	5.80	2.7443	-0.02	2.0043	-0.14
0.4	1.0822	6.10	0.8471	5.87	1.2530	0.10	0.8963	-0.02
0.2	0.4832	6.18	0.3737	5.93	0.5763	0.23	0.4035	0.10
0.0	0.2166	6.26	0.1655	6.00	0.2671	0.36	0.1831	0.24
-0.2	0.0974	6.34	0.0735	6.07	0.1248	0.51	0.0838	0.40
-0.4	0.0440	6.42	0.0328	6.15	0.0588	0.66	0.0387	0.56
-0.6	0.0199	6.51	0.0147	6.22	0.0280	0.81	0.0181	0.73
-0.8	0.0090	6.59	0.0066	6.30	0.0134	0.97	0.0085	0.91
-1.0	0.0041	6.68	0.0029	6.38	0.0065	1.13	0.0041	1.10
-1.2	0.0019	6.76	0.0013	6.46	0.0031	1.29	0.0020	1.28

τ_1 and τ_2 in hours

TABLE 3.03 b

E_{min} = Cut-off E_{max} = 95 GeV. Ahmedabad

	North Telescope				South Telescope			
β	α_1	τ_1	α_2	τ_2	α_1	τ_1	α_2	τ_2
1.0	10.0115	4.62	6.1262	4.73	13.2241	3.04	10.9563	2.82
0.8	4.5582	4.72	2.8110	4.83	5.9227	3.15	4.8325	2.90
0.6	2.0875	4.82	1.2987	4.94	2.6665	3.27	2.1390	2.98
0.4	0.9618	4.92	0.6042	5.04	1.2072	3.40	0.9503	3.06
0.2	0.4458	5.03	0.2831	5.15	0.5498	3.55	0.4238	3.16
0.0	0.2080	5.14	0.1336	5.26	0.2520	3.71	0.1898	3.26
-0.2	0.0976	5.25	0.0635	5.36	0.1162	3.89	0.0854	3.36
-0.4	0.0461	5.37	0.0304	5.47	0.0540	4.08	0.0385	3.48
-0.6	0.0219	5.48	0.0146	5.57	0.0253	4.29	0.0175	3.60
-0.8	0.0104	5.60	0.0071	5.67	0.0119	4.51	0.0079	3.73
-1.0	0.0050	5.71	0.0034	5.77	0.0056	4.74	0.0036	3.87
-1.2	0.0024	5.82	0.0017	5.86	0.0027	4.99	0.0016	4.01

TABLE 3.03 c

E_{min} = Cut-off E_{max} = 95 GeV. Ahmedabad

Vertical Telescope

β	α_1	τ_1	α_2	τ_2
1.0	13.1220	3.59	9.2531	3.24
0.8	5.9920	3.75	4.1453	3.35
0.6	2.7573	3.92	1.8689	3.47
0.4	1.2794	4.11	0.8486	3.59
0.2	0.5990	4.31	0.3883	3.73
0.0	0.2832	4.52	0.1793	3.88
-0.2	0.1352	4.75	0.0835	4.03
-0.4	0.0652	4.98	0.0393	4.19
-0.6	0.0318	5.22	0.0187	4.36
-0.8	0.0157	5.47	0.0090	4.52
-1.0	0.0078	5.71	0.0043	4.69
-1.2	0.0039	5.96	0.0021	4.86

derived and used to determine the space values.

$$a^{*}_{jik} = \frac{a_{j(1-2)}\,(A_{j1k}-A_{j2k}) - b_{j(1-2)}\,(B_{j1k}-B_{j2k})}{(A_{j1k}-A_{j2k})^2 + (B_{j1k}-B_{j2k})^2} \quad \ldots\ldots 3.22$$

and

$$b^{*}_{jik} = \frac{a_{j(1-2)}\,(B_{j1k}-B_{j2k}) + b_{j(1-2)}\,(A_{j1k}-A_{j2k})}{(A_{j1k}-A_{j2k})^2 + (B_{j1k}-B_{j2k})^2} \quad \ldots 3.23$$

where $a_{j(1-2)}$ and $b_{j(1-2)}$ are the observed j'th harmonic component of the difference-data obtained from the telescopes (1 and 2). i = (1-2) or any other difference-conponent e.g., (1-3, (1-4)....

$$A_{j1k} = \alpha_{j1k}\,\mathrm{Cos}\,\gamma_{j1k} \qquad A_{j2k} = \alpha_{j2k}\,\mathrm{Cos}\,\gamma_{j2k}$$

$$B_{j1k} = \alpha_{j1k}\,\mathrm{Sin}\,\gamma_{j1k} \qquad B_{j2k} = \alpha_{j2k}\,\mathrm{Sin}\,\gamma_{j2k} \quad \ldots 3.24$$

Here α_{j1k}, α_{j2k}, γ_{j1k} and γ_{j2k} are the relative amplitudes and geomagnetic bending for j'th harmonic component for telescopes 1 and 2 as shown earlier. k represents the spectra, i.e. particular combination of 'β' and E_{max}.

The equations (3.22) and (3.23) are further simplified as

$$a^{*}_{jik} = \frac{a_{j(1-2)}\,\alpha_{j(1-2)k}\,\mathrm{Cos}\,\gamma_{j(1-2)k} - b_{j(1-2)}\,\alpha_{j(1-2)k}\,\mathrm{Sin}\,\gamma_{j(1-2)k}}{\alpha^{2}_{j(1-2)k}} \quad \ldots\ldots 3.25$$

$$b^{*}_{jik} = \frac{a_{j(1-2)} \alpha_{j(1-2)k} \sin \tau_{j(1-2)k} - b_{j(1-2)} \alpha_{j(1-2)k} \cos \tau_{j(1-2)k}}{\alpha^{2}_{j(1-2)k}} \quad \ldots.3.26$$

where

$$\alpha_{j(1-2)k} = \sqrt{(A_{j1k} - A_{j2k})^2 + (B_{j1k} - B_{j2k})^2}$$

and

$$\tau_{j(1-2)k} = \tan^{-1} \frac{(B_{j1k} - B_{j2k})}{(A_{j1k} - A_{j2k})}$$

The equations (3.25) and (3.26) are similar in form to the equations (3.19-a) and (3.19-b) respectively, which are given for single telescope. Thus $\alpha_{j(1-2)k}$ and $\tau_{j(1-2)k}$ can be considered as the relative amplitude and the geomagnetic bending for a difference-telescope (1-2).

Table 3.04 gives the relative amplitudes ($\alpha_{j(1-2)}$) and the geomagnetic-bending ($\tau_{j(1-2)}$) for diurnal and semi-diurnal variations of the six difference-telescopes (W-E, W-S, W-N, S-E, S-N and N-E) for E_{max} = 95 GeV. and for different values of 'β' ranging from 1.0 to -1.2.

TABLE 3.04 a

E_{min} = Cut-off E_{max} = 95 GeV. Ahmedabad

	(W-E)				(W-S)			
β	α_1	τ_1	α_2	τ_2	α_1	τ_1	α_2	τ_2
1.0	18.6117	-3.03	20.2560	-0.33	11.1325	-4.53	15.6488	-1.82
0.8	8.2746	-2.91	8.9052	-0.25	5.0108	-4.40	6.8744	-1.74
0.6	3.6957	-2.77	3.9309	-0.17	2.2708	-4.25	3.0297	-1.64
0.4	1.6588	-2.62	1.7430	-0.07	1.0368	-4.09	1.3400	-1.53
0.2	0.7486	-2.46	0.7767	0.02	0.4773	-3.91	0.5950	-1.41
0.0	0.3398	-2.28	0.3480	0.13	0.2217	-3.72	0.2654	-1.28
-0.2	0.1552	-2.08	0.1569	0.25	0.1040	-3.51	0.1190	-1.14
-0.4	0.0714	-1.88	0.0712	0.37	0.0493	-3.29	0.0537	-0.97
-0.6	0.0331	-1.65	0.0326	0.51	0.0236	-3.05	0.0244	-0.79
-0.8	0.0154	-1.41	0.0150	0.65	0.0114	-2.81	0.0112	-0.60
-1.0	0.0073	-1.16	0.0070	0.80	0.0056	-2.56	0.0052	-0.38
-1.2	0.0034	-0.90	0.0032	0.96	0.0027	-2.31	0.0024	-0.16

TABLE 3.04 b

E_{min} = Cut-off E_{max} = 95 GeV. Ahmedabad

	(W-N)				(S-E)			
β	α_1	τ_1	α_2	τ_2	α_1	τ_1	α_2	τ_2
1.0	14.2344	-3.06	15.8875	-0.68	9.3553	-1.22	14.3494	1.36
0.8	6.4251	-2.98	7.1259	-0.55	4.1120	-1.06	6.2721	1.43
0.6	2.9164	-2.90	3.2144	-0.50	1.8113	-0.88	2.7484	1.51
0.4	1.3316	-2.81	1.4589	-0.39	0.7994	-0.67	1.2075	1.60
0.2	0.6117	-2.70	0.6666	-0.28	0.3536	-0.44	0.5319	1.69
0.0	0.2828	-2.59	0.3067	-0.16	0.1567	-0.18	0.2349	1.79
-0.2	0.1316	-2.47	0.1422	-0.04	0.0697	0.12	0.1040	1.90
-0.4	0.0617	-2.33	0.0665	0.09	0.0310	0.46	0.0462	2.01
-0.6	0.0291	-2.19	0.0313	0.22	0.0139	0.85	0.0205	2.13
-0.8	0.0138	-2.04	0.0149	0.36	0.0063	1.30	0.0091	2.25
-1.0	0.0066	-1.87	0.0071	0.50	0.0029	1.81	0.0041	2.39
-1.2	0.0032	-1.70	0.0034	0.64	0.0013	2.38	0.0018	2.53

TABLE 3.04 c

E_{min} = Cut-off E_{max} = 95 GeV. Ahmedabad

	(S-N)				(N-E)			
β	α_1	τ_1	α_2	τ_2	α_1	τ_1	α_2	τ_2
1.0	5.7246	0.06	9.2265	1.70	4.3792	-2.93	5.5325	-5.23
0.8	2.5216	0.08	4.1127	1.73	1.8557	-2.63	2.2972	-5.10
0.6	1.1122	0.10	1.8404	1.75	0.7875	-2.27	0.9502	-4.95
0.4	0.4910	0.13	0.8268	1.78	0.3354	-1.86	0.3916	-4.77
0.2	0.2168	0.18	0.3729	1.80	0.1438	-1.37	0.1608	-4.56
0.0	0.0956	0.23	0.1689	1.83	0.0625	-0.81	0.0661	-4.30
-0.2	0.0421	0.31	0.0767	1.85	0.0277	-0.16	0.0273	-3.97
-0.4	0.0185	0.40	0.0350	1.88	0.0126	0.55	0.0114	-3.58
-0.6	0.0080	0.53	0.0160	1.90	0.0059	1.29	0.0049	-3.11
-0.8	0.0034	0.70	0.0073	1.92	0.0029	2.02	0.0023	-2.60
-1.0	0.0015	0.94	0.0034	1.93	0.0014	2.71	0.0011	-2.10
-1.2	0.0006	1.26	0.0015	1.94	0.0007	3.32	0.0005	-1.65

C H A P T E R - IV

RESULTS AND DISCUSSION

4.1 Basic Data Presentation

4.1.1 Energy response of meson telescopes at Ahmedabad

For a qualitative understanding of the energy spectral variations, the concept of mean energy of response of a telescope is generally useful. The mean energy of response for any telescope is generally estimated by using the formula

$$\frac{1}{\bar{E}} = \int_{E_c}^{\infty} W(E)\,\frac{1}{E}\,.dE \Big/ \int_{E_c}^{\infty} W(E).dE \quad \ldots\ldots\ldots\ldots\ldots 4.01$$

Where $\bar{E}$ is the mean energy, $W(E)$ is the coupling constant, E_c is the cut-off energy for the telescope and E is the total energy. In the present set-up the vertical telescope has a cubical geometry whereas the directional telescopes (E,W,N and S) are inclined at 51° to the zenith. The opening angle of each of the directional telescopes is 52°, having 14° and 66° as the minimum and maximum angle of response. The geomagnetic cut-off rigidity for the mean direction of each of the telescope has been calculated using the sixth-degree Finch and Leaton simulation of the geomagnetic field. It is, as expected, found to be lowest for the West pointing (12.2 GV) telescope and is highest for the East (29.7 GV) pointing telescope. The cut-off rigidities for Vertical, South and North telescopes lie within the above two extreme limits. The mean energies of response have been calculated substituting the value of E_c as derived above in

equation (4.01). The calculations indicate that the mean energy of response for Vertical, West, South, North and East telescopes are about 45 GeV, 55 GeV, 59 GeV, 66 GeV and 76 GeV respectively. Table 4.01 gives all the relevant details concerning the cut-off rigidity, the mean energy of response and other counting rate characteristics of each of the telescopes at Ahmedabad. It is

TABLE 4.01

Ahmedabad Meson Telescopes

Telescope		No.of telescopes	Cut-off rigidity (GV.)	Mean energy of response (GeV.)	Mean Asymptotic Latitude Degree	Mean Asymptotic Longitude* Deg.	Counting rate per hour for each telescope.
Vertical (cube)		Four	16.0	45.0	15	44	460,000
Inclined at 51° to the zenith	West	Two	12.2	55.0	25	-12	98,000
	South	Two	15.2	59.0	-17	38	96,000
	North	Two	21.3	66.0	52	58	92,000
	East	Two	29.7	76.2	4	78	86,000

* with reference to local meridian

seen from the table that even though, West telescope has a cut-off rigidity lower than that for the vertical, the mean energy of response of the West telescope is higher than the corresponding values for the Vertical telescope. This is so because the maximum of the response function curve for an inclined telescope

is at higher energies than for the vertical direction as seen in Figure (1.02).

The counting rate of vertical telescope is about 0.46×10^6 counts/hour for each channel. The counting rate of each directional telescope is about ~ 90,000 counts/hour. Standard error in harmonic components derived from the actual scatter in the data is 0.20%/day for inclined telescope and ~0.16%/day for vertical telescope. Though the counting rate of the vertical telescope is about five times the counting rate of the inclined telescope, the r.m.s. errors in harmonic components derived from the actual scatter in the data are approximately same for all the telescopes.

4.1.2 Data Selection

The present meson monitor set-up at the Physical Research Laboratory, Ahmedabad has been in continuous operation since 25th May 1968. Out of these, data for days, on which the air-conditioning plant did not work satisfactorily, have been rejected in the present analysis. Total number of days for which the data is available and used in the present analysis are 205 days in 1968, 330 days in 1969 and 300 days in 1970, which are approximately same for different telescopes.

Before proceeding with the analyses of the data it is imperative to check the goodness of the data by intercomparing with other similar data. In the present analysis, in order to obtain reliable information of the spectral behaviour of the anisotropy, the data from the meson monitors have been used along with the data from superneutron monitors as listed in table 4.02

Table 4.02

Super Neutron Monitor

Station	Altitude m.a.s.l.	Geographic		Cut-off rigidity (GV)	Mean energy of response (GeV)	Asy. lat. for mean energy	Counting rate per hour x 10^5
		Latitude (degree)	Longitude (degree)				
Sulphur Mt.	2283	51.2 N	115.6 W	1.14	10.0	5.6	10.2
Churchill	39	58.4 N	94.1 W	0.21	11.0	34.0	8.0
Deep River	145	46.1 N	77.3 W	1.02	11.0	7.0	21.0
Kiel	54	54.3 N	10.1 E	2.29	13.0	8.7	6.4
Lindau	140	51.6 N	10.1 E	3.00	13.0	2.4	3.7
Dallas	208	32.5 N	96.5 W	4.35	14.0	-21.6	8.0
Pic du Midi	2860	42.9 N	0.2 E	5.36	15.0	-6.2	26.0
Chacaltaya	5220	16.4 N	68.2 W	13.10	33.0	-10.4	60.0

to provide a maximum energy range. Prior to the actual calculations, however, the data from the individual neutron monitors have been intercompared for checking their parallel running. Figure (4.01) shows the plot of daily mean intensity of neutron

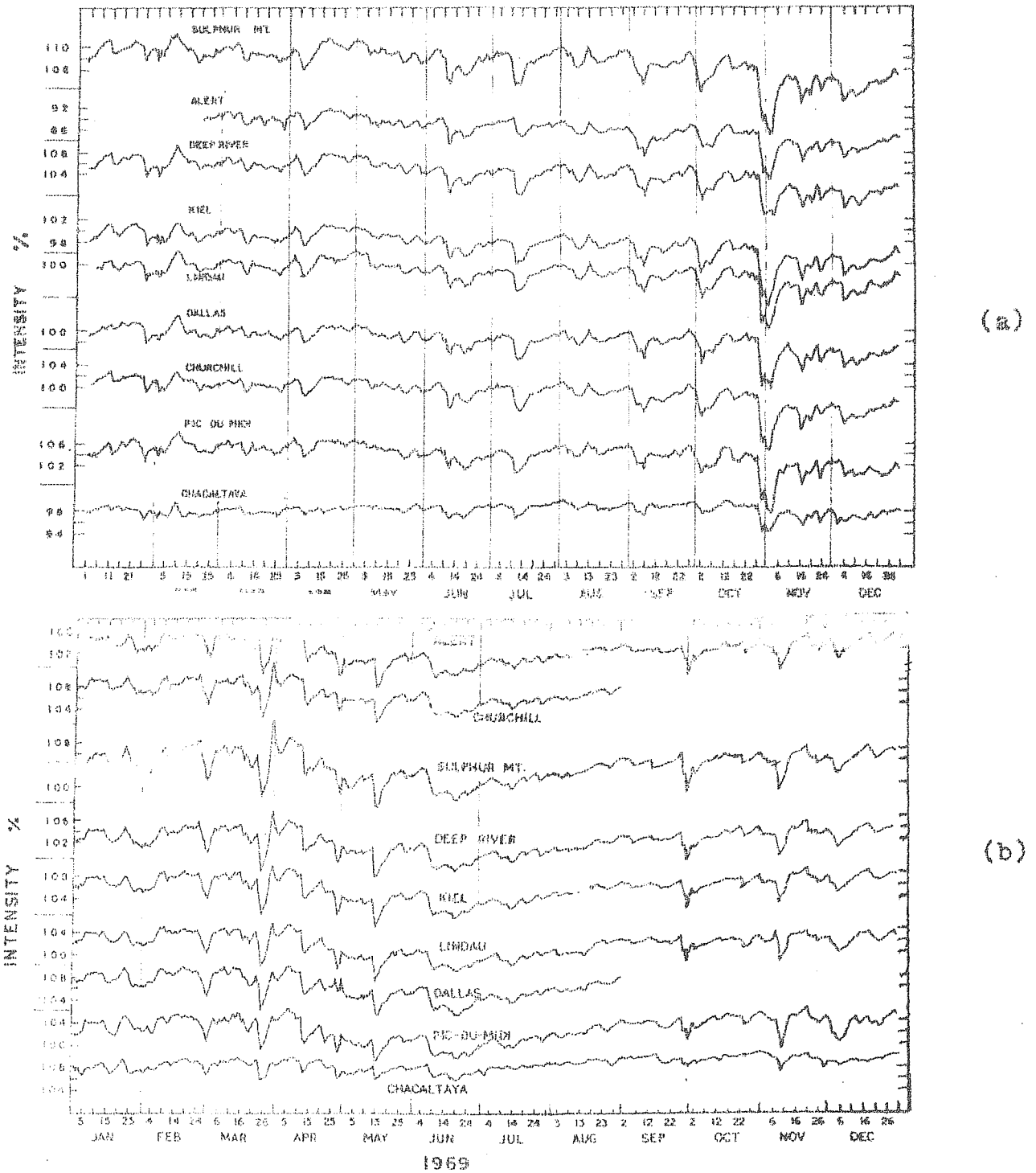

Fig.4.01 Daily mean intensity observed by number of neutron monitors during (a) 1968 & (b) 1969.

monitors during the years 1968 and 1969. A good tracking between super neutron monitors at different stations can be seen from the figures. Correlation coefficients for the daily mean intensity of different neutron monitors have also been obtained during 1968 and 1969. Extremely good correlation coefficients exceeding 0.9 have been obtained between different super neutron monitors except for Chacaltaya for which the correlation coefficient is about 0.7.

Similarly meson data from different telescopes at Ahmedabad have been compared with each other for parallel running. Further, the hourly mean meson data for Ahmedabad during two Forbush-decrease events (one on 29th October 1968 and another on 24th March 1969) have been compared with the corresponding meson observations at Bologna and a few neutron monitor observations. These observations along with the value of the horizontal magnetic field 'H' observed at Alibag are shown in Figure (4.02). During both these events the daily mean intensity at Ahmedabad showed a significant (1%) decrease. It is seen from Fig.4.02 that there is good tracking between different observations. It is further seen that the decreases in different telescopes are not identical, being least in the East pointing telescope and maximum in the West pointing telescope, clearly indicating the characteristic spectral features generally observed in the Forbush-decreases. The meson data have been further checked by comparing their monthly mean diurnal and semi-diurnal vectors as described in the next section.

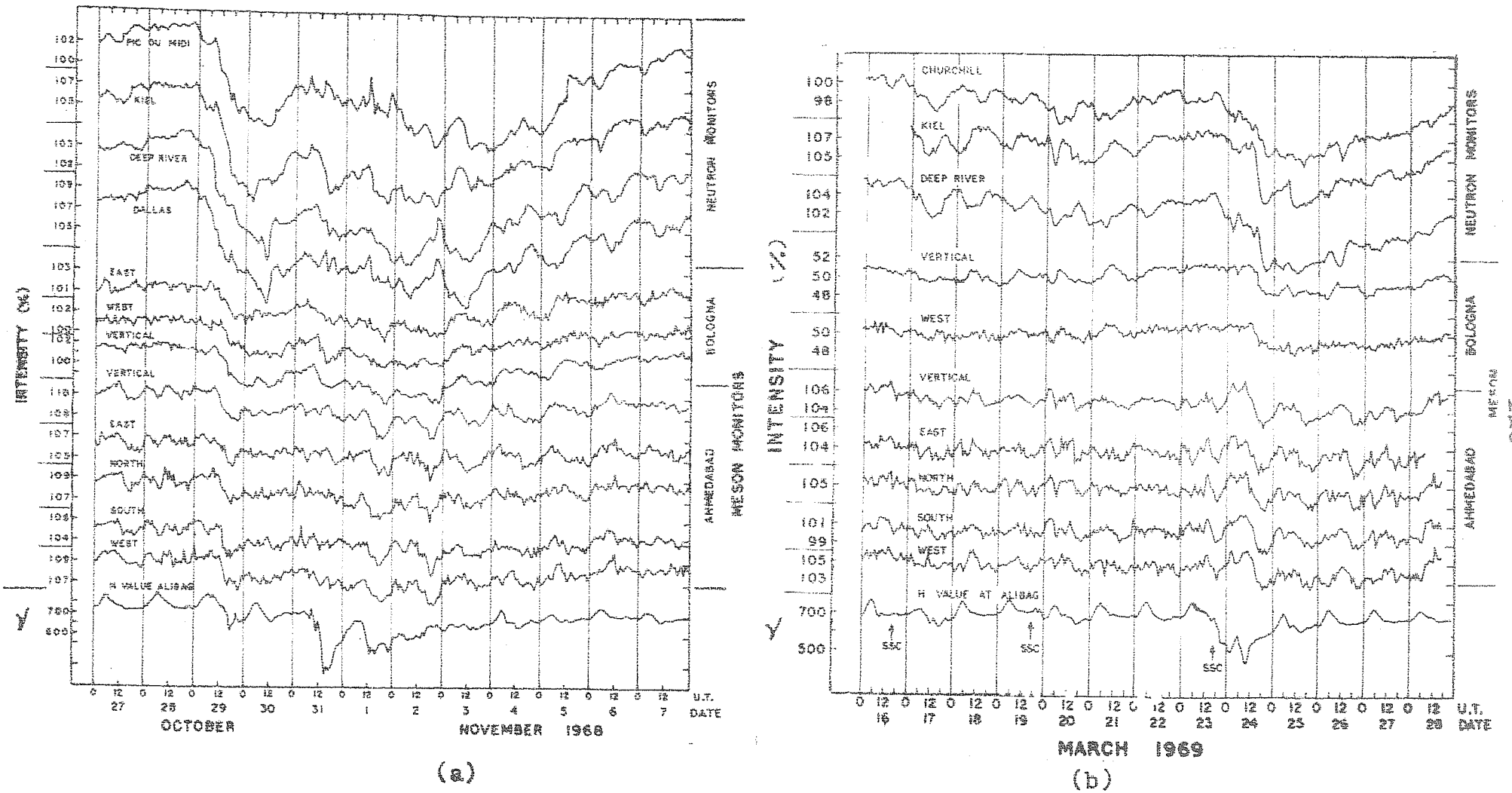

(a) (b)

Fig.4.02 Hourly intensity recorded by number of neutron and meson monitors during two Forbush-decrease events (a) 29th October 1968 and (b) 23rd March 1969.

Meson monitor data have been corrected only for pressure variations as discussed in Chapter III. The six difference-components viz., (West-East), (West-North), (West-South), (South-North), (South-East) and (North-East) are derived from East, West, North and South directional telescopes. To a first degree of approximation these differences will be free from the atmospheric temperature (or any other meteorological) variations. As pointed out by Nagashima et.al.(1971 and also described in Chapter III the difference-components have their characteristic relative amplitudes and geomagnetic bending, from which the amplitudes and phase of the actual anisotropy outside the influence of the geomagnetic field can be calculated. We have therefore used the difference-observations for estimating the anisotropy characteristics at these energies. For simplicity of usage we use the term difference-telescopes for the above six differences.

4.1.3 Observed average diurnal and semi-diurnal variations with meson telescopes at Ahmedabad

The amplitude and phase of the yearly average diurnal and semi-diurnal variations observed by the above difference-telescopes during the years 1968, 1969 and 1970 are given in Table (4.03) along with the three yearly average for the entire period 1968 to 1970. The diurnal and semi-diurnal variations observed by superneutron monitors during 1968 and 1969 are given in Table (4.04). It is seen from the table 4.03 that the

Table 4.03

Ahmedabad Meson Monitor

Year	Telescope	r_1%	ϕ_1(deg.)	r_2%	ϕ_2(deg.)
1968	W-E	0.141 ± 0.017	291 ± 7	0.142 ± 0.015	125 ± 6
	W-N	0.120 ± 0.017	294 ± 9	0.105 ± 0.015	127 ± 8
	W-S	0.079 ± 0.017	301 ± 12	0.103 ± 0.015	154 ± 8
	S-E	0.065 ± 0.017	278 ± 15	0.071 ± 0.015	81 ± 12
	S-N	0.043 ± 0.017	279 ± 23	0.048 ± 0.015	53 ± 18
	N-E	0.022 ± 0.017	275 ± 44	0.080 ± 0.015	199 ± 11
1969	W-E	0.136 ± 0.015	292 ± 6	0.108 ± 0.013	125 ± 6
	W-N	0.121 ± 0.015	287 ± 7	0.061 ± 0.013	128 ± 11
	W-S	0.092 ± 0.015	312 ± 9	0.081 ± 0.013	164 ± 8
	S-E	0.059 ± 0.015	259 ± 15	0.068 ± 0.013	76 ± 10
	S-N	0.054 ± 0.015	241 ± 16	0.048 ± 0.013	31 ± 14
	N-E	0.019 ± 0.015	324 ± 45	0.048 ± 0.013	121 ± 14
1970	W-E	0.146 ± 0.016	288 ± 6	0.090 ± 0.013	136 ± 8
	W-N	0.131 ± 0.016	290 ± 7	0.048 ± 0.013	150 ± 15
	W-S	0.055 ± 0.016	304 ± 17	0.075 ± 0.013	184 ± 10
	S-E	0.094 ± 0.016	279 ± 10	0.069 ± 0.013	81 ± 11
	S-N	0.078 ± 0.016	280 ± 12	0.045 ± 0.013	41 ± 17
	N-E	0.016 ± 0.016	267 ± 57	0.045 ± 0.013	121 ± 17
Mean of 1968 1969 & 1970	W-E	0.141 ± 0.010	290 ± 4	0.113 ± 0.009	128 ± 5
	W-N	0.123 ± 0.010	290 ± 5	0.070 ± 0.009	132 ± 7
	W-S	0.075 ± 0.010	306 ± 8	0.085 ± 0.009	166 ± 6
	S-E	0.072 ± 0.010	273 ± 8	0.082 ± 0.009	80 ± 6
	S-N	0.055 ± 0.010	268 ± 10	0.046 ± 0.009	42 ± 11
	N-E	0.017 ± 0.010	288 ± 34	0.044 ± 0.009	121 ± 12

Table 4.04

Neutron Monitors

		r_1(%)	ϕ_1(deg.)	r_2(%)	ϕ_2(deg.)
Sulphur Mt.	1968	0.326 ± 0.015	245	0.044 ± 0.011	63
	1969	0.328 ± 0.016	249	0.034 ± 0.011	37
Churchill	1968	0.277 ± 0.015	246	0.039 ± 0.011	54
	1969	0.277 ± 0.015	244	0.040 ± 0.012	72
Deep River	1968	0.307 ± 0.014	228	0.058 ± 0.010	34
	1969	0.292 ± 0.015	227	0.045 ± 0.009	31
Kiel	1968	0.282 ± 0.014	220	0.043 ± 0.009	44
	1969	0.290 ± 0.015	220	0.032 ± 0.009	35
Lindau	1968	0.282 ± 0.015	214	0.032 ± 0.010	63
	1969	0.265 ± 0.015	213	0.020 ± 0.010	93
Dallas	1968	0.295 ± 0.016	228	0.043 ± 0.011	63
	1969	0.307 ± 0.017	232	0.035 ± 0.011	98
Pic du Midi	1968	0.315 ± 0.016	194	0.049 ± 0.011	91
	1969	0.299 ± 0.016	189	0.044 ± 0.010	97
Chacaltaya	1968	0.234 ± 0.012	211	0.053 ± 0.006	9
	1969	0.221 ± 0.011	209	0.046 ± 0.006	26

amplitudes of the diurnal and semi-diurnal variations for most of the difference-telescopes are comparable. In the case of the difference-telescope (N-E) even though the diurnal amplitude observed is not significant, the semi-diurnal amplitude of the same difference-telescope is observed to be large and quite significant. This can easily be understood referring to the theoretical treatment given in Chapter III. Due to the existence of bending difference between different telescopes, even a small semi-diurnal anisotropy will cause a large difference in the observed amplitude, whereas a comparable diurnal anisotropy will have much less influence on the difference amplitude. The statistical error being the same for both cases, it is obvious that the semi-diurnal anisotropy can be more accurately studied than the diurnal anisotropy by using data from difference-telescopes which are assumed to be free from the effects due to the meteorological variations.

In Figure (4.03) the harmonic dials for the diurnal variations observed by the difference-telescopes during 1968, 1969 and 1970 have been plotted. Three yearly average of the above diurnal vectors are also plotted in the figure (4.03 d). The error circles drawn at the tip of each vector is the mean standard error derived from the scatter in the data. The vector addition dials for the period 1968 to 1970 for diurnal variation are shown in Figure (4.05 a). From figures (4.03) and (4.05 a) it is evident that, within the statistical uncertainties, the

amplitude and phase of the diurnal vectors remain approximately constant during 1968, 1969 and 1970.

The harmonic dials for the semi-diurnal variations during 1968, 1969 and 1970 are plotted in Figure (4.04). Three yearly average semi-diurnal variation vectors are also shown in figure (4.04 d). The vector addition dials for semi-diurnal variations are shown in figure (4.05 b.). From the above figures it is seen that the amplitude and the phase of the semi-diurnal variation exhibit slight gradual change during the three years. Semi-diurnal amplitude seems to decrease consistently in all the difference-telescopes from 1968 to 1970.

From a qualitative examination of figure 3.04 it may be seen that whereas the bending correction for East, North and South is 4 to 6 hours and is not very much different from each other, the bending correction for West is very small and is quite different from the above three telescopes. Consequently it is qualitatively seen that out of the various difference-telescopes the one involving West viz. (W-E), (W-N) and (W-S) should exhibit significant diurnal and semi-diurnal variation due to primary anisotropy. This is also borne out from the actual observations as shown in figure (4.03) and (4.04) and table (4.03). Therefore, for the detailed determination of the spectral characteristics of the diurnal and semi-diurnal anisotropy we have used the data from only these three difference-telescopes.

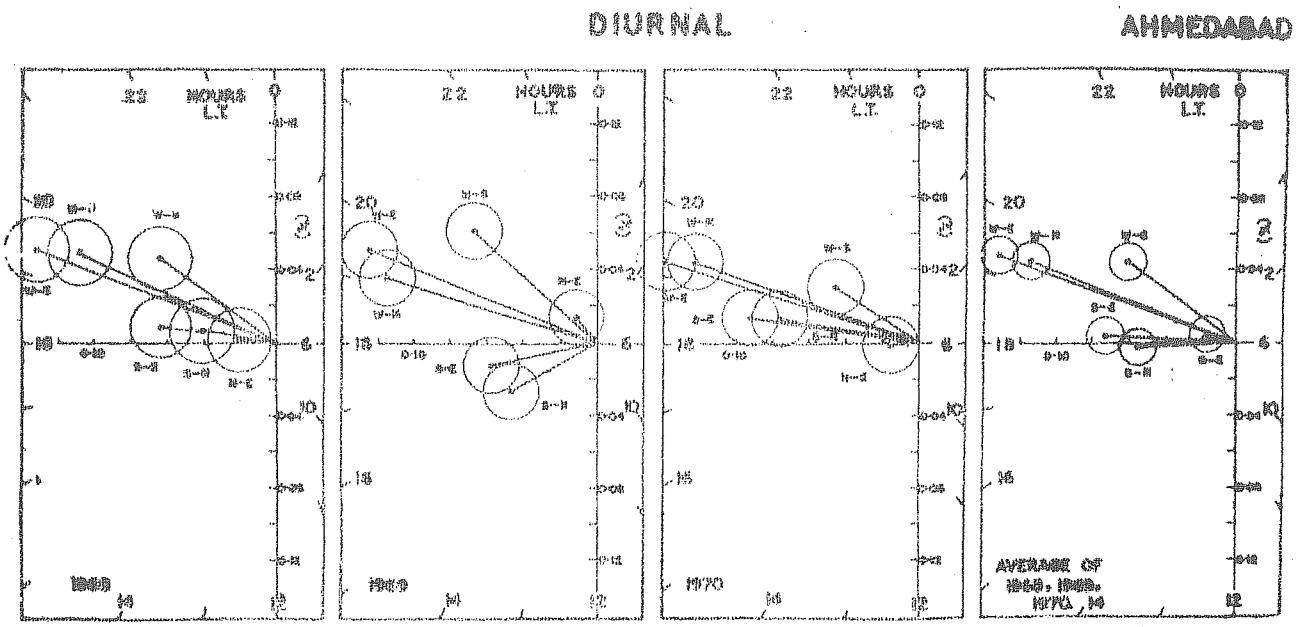

(a) (b) (c) (d)

Fig.4.03 Yearly harmonic dial of the diurnal variation observed by six difference-telescopes at Ahmedabad during (a) 1968, (b) 1969, (c) 1970 and (d) the three yearly average.

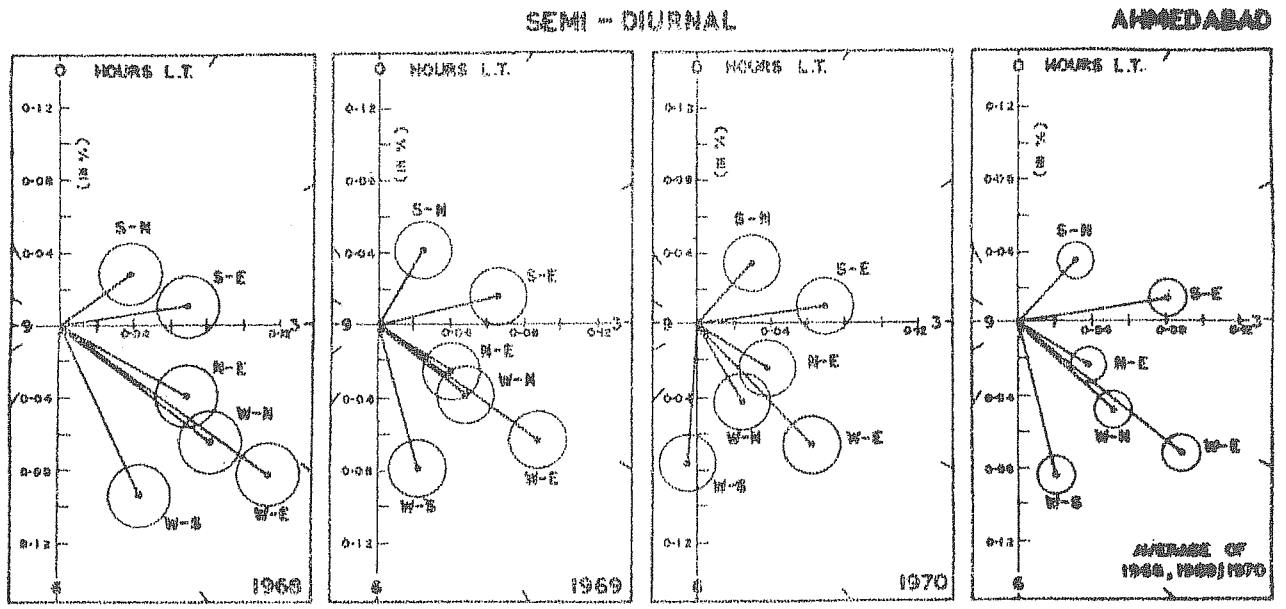

(a) (b) (c) (d)

Fig.4.04 Yearly harmonic dial of the semi-diurnal variation observed by six difference-telescopes at Ahmedabad during (a) 1968, (b) 1969, (c) 1970 and (d) the three yearly average.

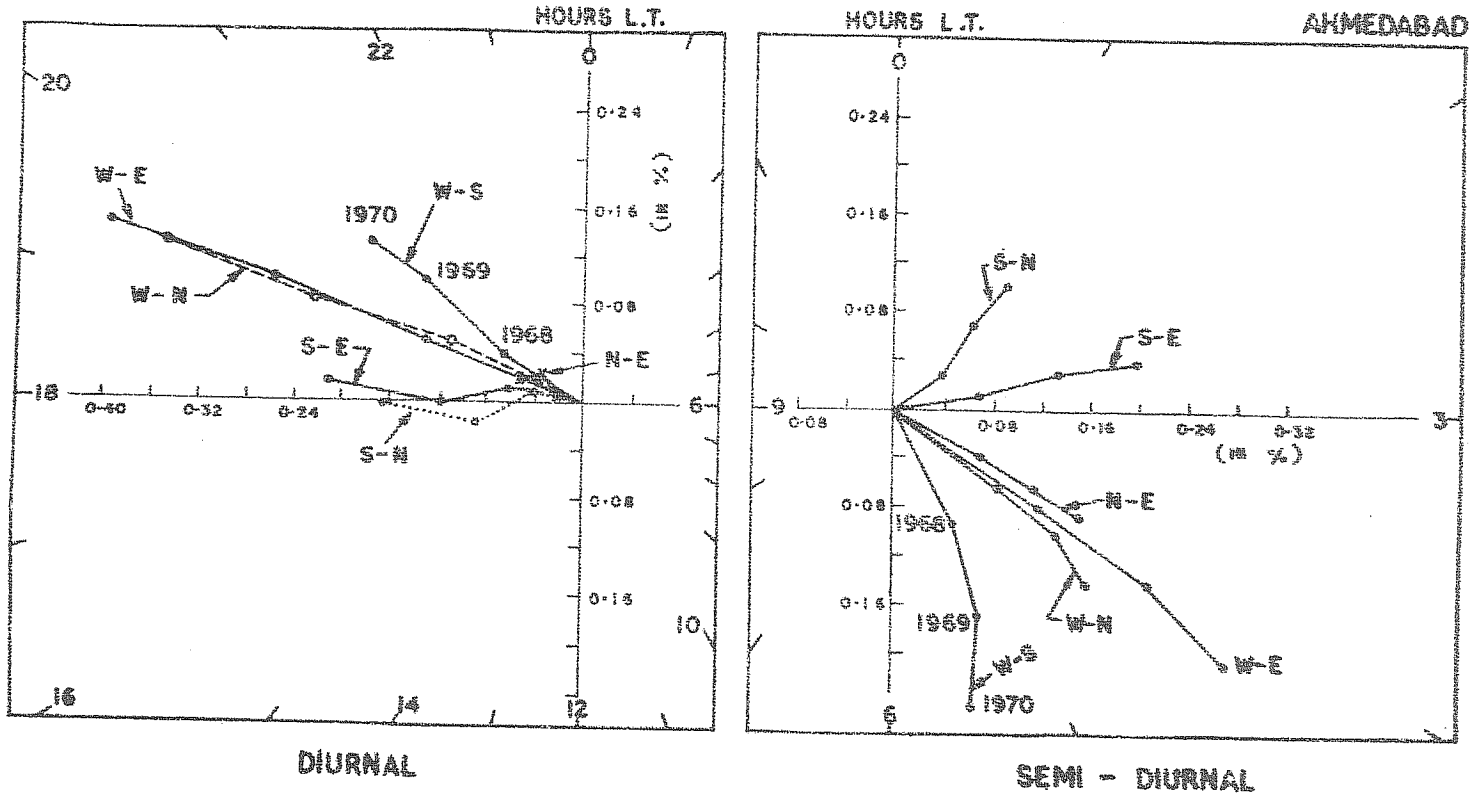

Fig.4.05 Summation harmonic dials of the diurnal and semi-diurnal components observed by six difference-telescopes (mesons) at Ahmedabad.

As a further check for the statistical significance of the observations derived from (W-E), (W-N) and (W-S) telescopes the vector addition diagram of the monthly mean diurnal and semi-diurnal variation as observed by these three difference-telescopes are plotted end to end in figure (4.06). The good tracking on a monthly basis between diurnal and semi-diurnal vectors between these three telescopes also ensure that the observations are quite significant and thus can be used to derive the characteristics of the respective primary anisotropies.

4.2 The characteristics of daily variation on a day-to-day basis

The energy dependence of the daily variation is generally represented in the form of a power law

$$\frac{\delta D(E)}{D(E)} = aE^{\beta} \quad \text{for} \quad E < E_{max}$$
$$= 0 \qquad\qquad E > E_{max} \qquad \ldots\ldots 4.02$$

Where a is the free space amplitude of the anisotropy for 1 GeV particles, E_{max} is the upper limit of the energy of the particles, above which limit the particles do not experience the diurnal or semi-diurnal modulation. Even though the spectral exponent β has been known to vary considerably on a day-to-day basis, the time averaged diurnal variation has been generally found to be consistent with an energy independent spectra. Since, however, the primary cosmic ray spectrum is generally of the form $AE^{-2.5}$, it is evident that the detectors

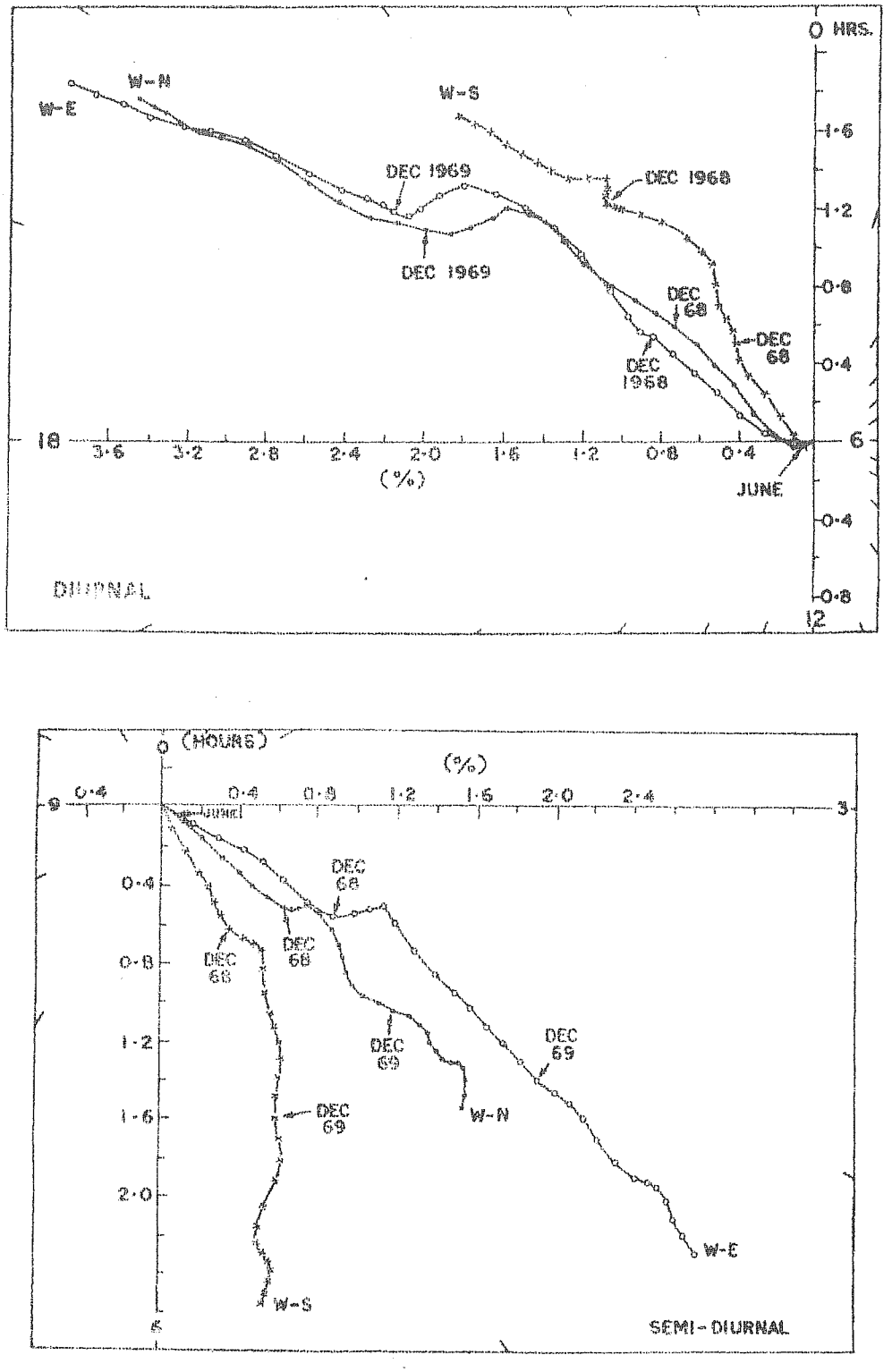

Fig.4.06 Monthly summation harmonic dials of the diurnal and semi-diurnal component observed by W-E, W-N and W-S telescopes at Ahmedabad from June 1968 to December 1970.

responding to lower mean energies of response should be more sensitive to changes in 'β'. On the other hand determination of E_{max} which is generally found to be of the order of 100 GeV, much above the mean energy of response of neutron monitors, is possible only by utilizing the data from meson monitors, particularly the ones located at either low latitudes or underground. The ambiguities caused, due to the meteorological effects on meson data in general and the lack of precise knowledge in the coupling coefficients applicable to underground meson monitors, have in the past, provided only rough estimates of E_{max}, the energy, beyond which the cosmic ray particles do not partake in corotation. Since a precise knowledge of E_{max} is useful in understanding the large scale structure of the interplanetary magnetic field, it is desirable to obtain more accurate estimate of its value. For the determination of anisotropy characteristics, the data from difference-telescopes which are free from meteorological influences have been effectively used in the present work together with neutron data for achieving the objective.

We may also note that for determination of spectral characteristics of semi-diurnal anisotropy whose exponent is reported to be positive, meson data, in particular, the data from the difference-telescopes will be very effective.

Before proceeding to use the data from difference-telescopes we will attempt to understand the gross feature of the energy spectral characteristics of the diurnal variation by

using the temperature uncorrected meson data from Ahmedabad. We shall however not draw fine conclusions from this exercise since the meson data has not been corrected for atmospheric temperature variation. Following the method described in Chapter III and using the data from a number of superneutron monitors, the energy spectral characteristics of diurnal and semi-diurnal anisotropy have been determined on a day-to-day basis for the years 1968 and 1969. Unlike the past work of Patel et al.(1968) which used data from only six neutron monitors ranging in cut-off rigidity from about 1 GV to 4.36 GV, in the present work we have used eight superneutron monitors (as listed in table 4.02) with their cut-off rigidities ranging from 1.00 to 13.1 GV. The mean energy of response of the above neutron monitors used in the present work ranges from about 10 to 33 GeV.

Considering E_{max} to be $\simeq$ 250 GeV and the exponent 'δ' in the range -1.2 to +1.0 (in steps of 0.2) the variational coefficients for each station have been calculated for two values of the lower limit of energy E_{min} (viz. 2 GeV and 4 GeV). From the above variational coefficients the relative amplitude α_j (also called the attenuation or reduction factor) and geomagnetic deflection (bending) γ_j for diurnal (j =1) and semi-diurnal (j = 2) components have been derived.

Using the observed diurnal or semi-diurnal components (a_j, b_j) at each station and using equation (3.19), the free space values of the anisotropy were computed for different

values of β and E_{min}. For each combination of 'β' and E_{min} the parameter called variance S^2 was calculated by using equation (3.20). The parameter S^2 thus determined, provides a measure of the scatter in different estimates of the diurnal (or semi-diurnal) amplitudes and phases in space corresponding to the observed values at each station. The minimum value of variance (S^2_{min}) indicates the best fit value of 'β' and E_{min} operative on that particular day. However, considering the error ($\sigma_{S^2_{min}}$*) in S^2_{min} values which generally depends upon the number of degrees of freedom, other equally good choices of 'β' and E_{min} should also be considered. All combinations of 'β' and E_{min} for which $S^2 = S^2_{min} + \sigma S^2_{min}$ are considered as equivalent spectra amongst which unambiguous determination of a single value is not possible due to the limited resolution inherent in the method. In the present analyses Forbush-decrease days and days on which the resolution between various spectra were completely not possible have been rejected. For each remaining day a spectrum (i.e. β and E_{min}) corresponding to S^2_{min} and other equivalent spectra are identified and noted.

The frequency of occurrence of such equivalent spectra of diurnal and semi-diurnal variation obtained with neutron monitor data during 1968 and 1969 are shown in figure (4.07 a) and (4.08 a) respectively. The same analysis have been repeated for neutron data together with the data from Ahmedabad meson telescopes (E, W, N, S and V) uncorrected for temperature

* $\sigma_{S^2_{min}} \simeq \sqrt{2/N} \cdot S^2_{min}$ when N is large
N = no. of degrees of freedom

variations. The frequency of occurrence of equivalent spectra of both diurnal and semi-diurnal variations obtained with neutron and Ahmedabad meson monitors together are plotted in figures (4.07 b) and (4.08 b) respectively.

Comparing the histograms of diurnal exponent plotted in figures 4.07 a and 4.07 b, it is seen that both neutron and neutron plus meson data show a primary peak corresponding to $\beta = 0$, for both values of E_{min}, indicating that the spectrum is primarily energy independent. The secondary peak corresponding to 'β' = -1.2 observed in Figure 4.07 (b) when meson data is included might be arising because of the use of temperature uncorrected meson data.

Comparing the histograms for semi-diurnal exponents plotted in figures (4.08 a) and (4.08 b) it is seen that the histogram for both neutron and neutron plus meson are alike and both of them show the occurrence of a positive spectral exponent on a large number of days. In fact with the inclusion of meson data as seen in figure 4.08 b, the resolution improves which can be understood because of the larger mean energy of response of the meson telescope and the applicability of positive exponent for semi-diurnal variations.

An important conclusion that can be drawn from the above diagrams is the existence of large variability in the spectral characteristics of both the diurnal and semi-diurnal variation on a day-to-day basis, which is consistent with the conclusions

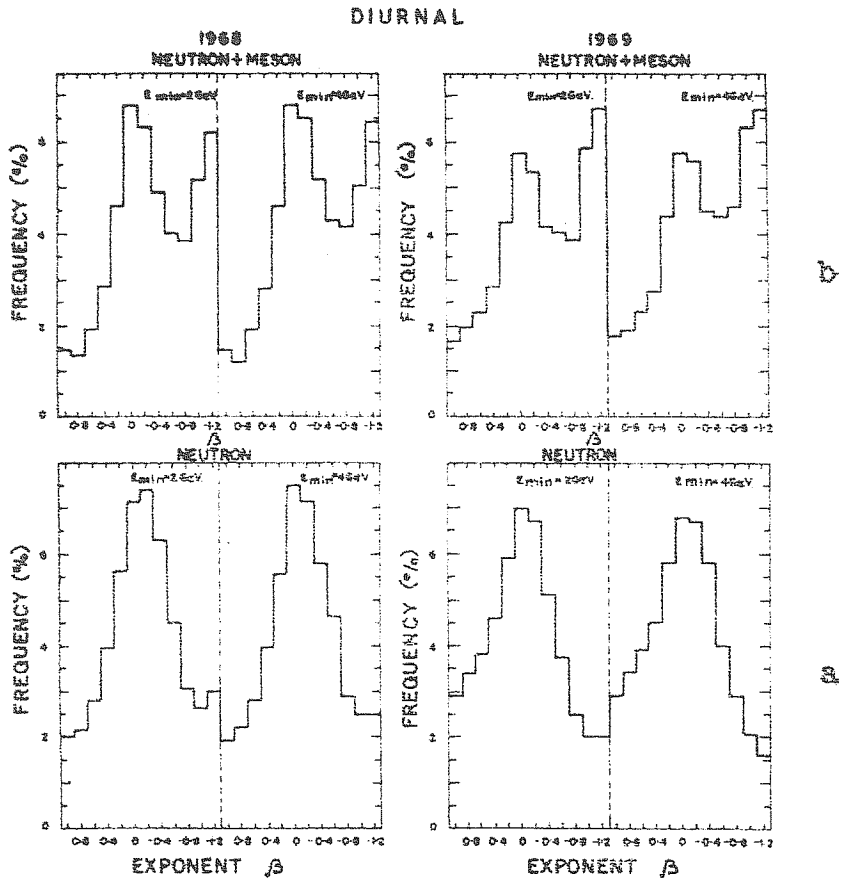

Fig.4.07 Frequency of occurrence of the exponent 'β' of the energy spectrum of diurnal anisotropy during 1968 and 1969.

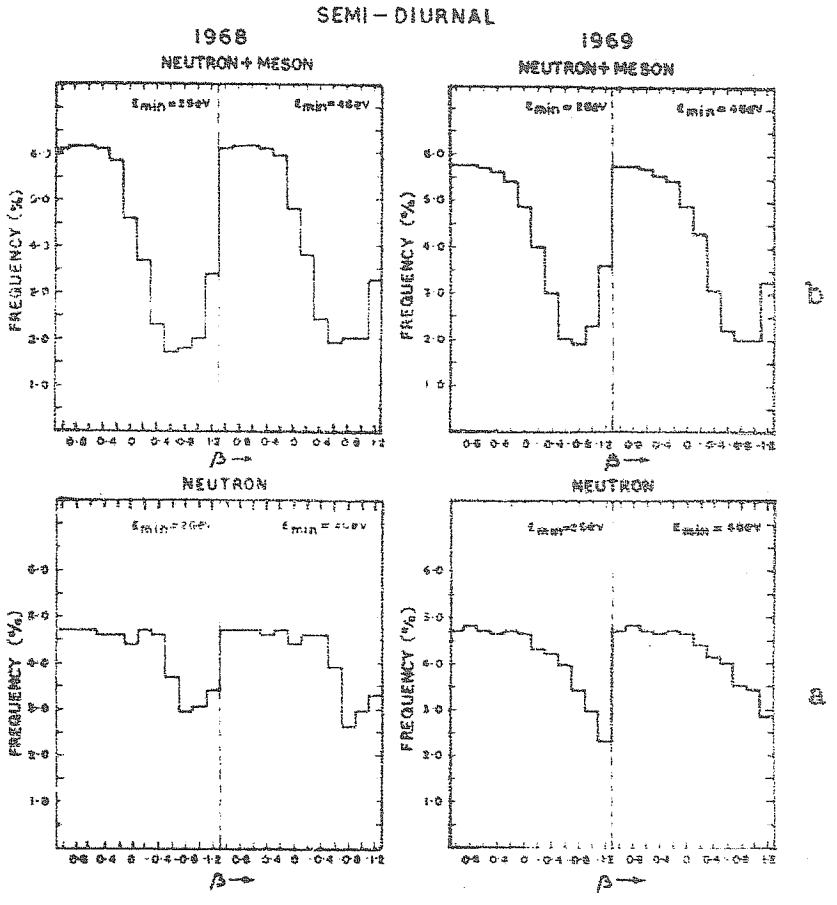

Fig.4.08 Frequency of occurrence of the exponent 'β' of the energy spectrum of semi-diurnal anisotropy during 1968 and 1969.

The spectrum determination has been done (a) using data from neutron monitors only and (b) using data from neutron monitors and also pressure corrected data from East, West, North, South and Vertical meson telescopes at Ahmedabad together.

drawn by previous workers (Rao and Sarabhai, 1964 and Patel et al. 1968). Further detailed investigation of day-to-day variation of diurnal and semi-diurnal component however is not possible with the present data due to poor statistics particularly in the data from difference-telescopes (Ahmedabad meson monitors) which have to be employed in the analysis to avoid ambiguities due to the temperature fluctuations in the atmosphere.

4.3 The characteristics of the average diurnal anisotropy

4.3.1 Determination of the upper limiting energy E_{max}

Assuming the characteristics of the solar diurnal anisotropy (r_1 = 0.58%, ϕ_1 = 1800 hrs. in space and the anisotropy as independent of energy i.e. γ = 0) and using appropriate correction factors for geomagnetic bending and the width of the asymptotic cones of acceptance, the expected diurnal variations for difference-telescopes (W-E, W-N and W-S) at Ahmedabad have been calculated for different values of the upper limiting energy E_{max}. The loci of the end points of the expected diurnal vectors are shown as dot-dash curves in figure (4.09a,b).The number against each of the point denotes the corresponding value of the upper limiting energy E_{max}. The diurnal variations observed by the difference-telescopes during each of the years 1968, 1969 and 1970 are also plotted in Figure 4.09 a. Three yearly average diurnal variation observed by the above difference-telescopes is separately plotted in figure (4.09b) along with the expected diurnal variation curves.

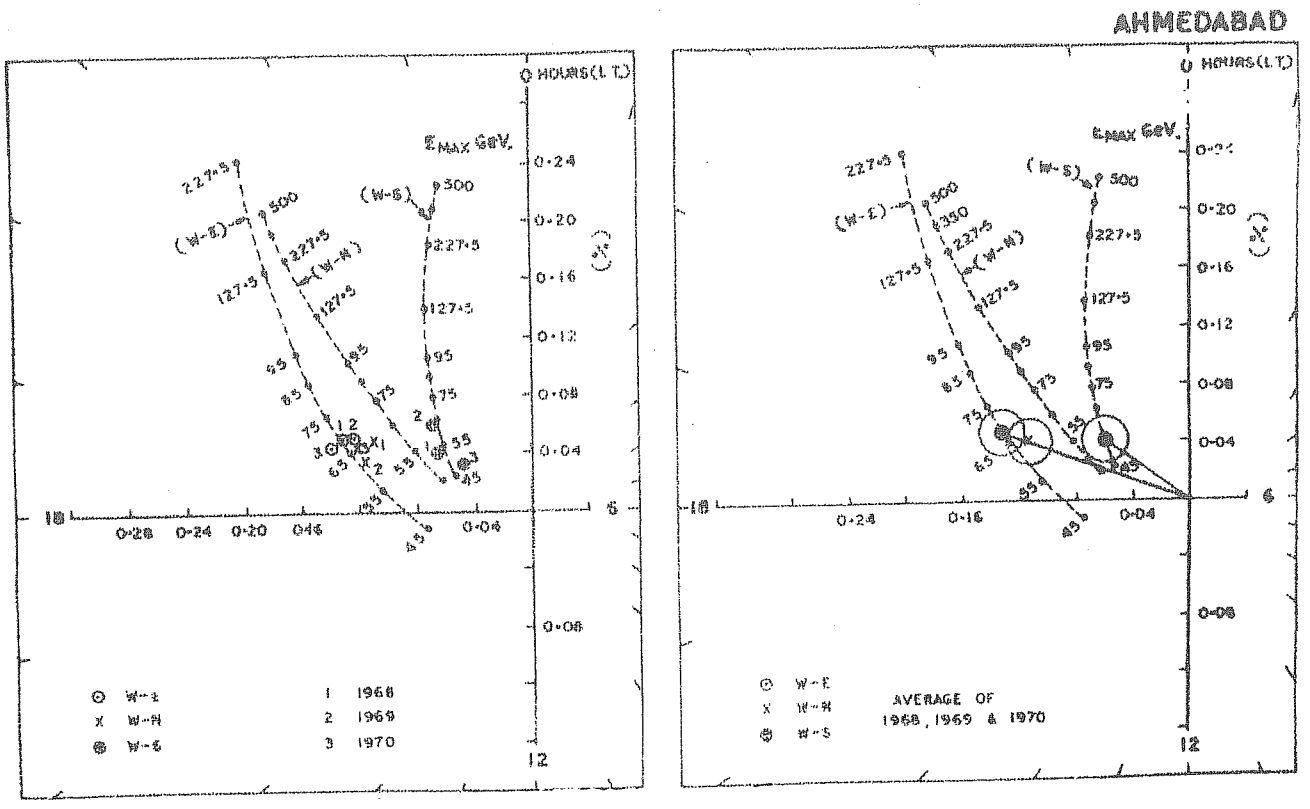

Fig.4.09 Diurnal variations to be expected for difference-telescopes (W-E, W-N and W-S) at Ahmedabad when a corotational anisotropy having an amplitude of 0.5% along 1800 hours direction is considered. The anisotropy is considered to be independent of energy upto an upper limiting energy E_{max}. Values of the limiting energy are marked along the curves. The observed diurnal variations are also shown in (a) for individual years and in (b) for the average of three years from 1968 to 1970.

For a determination of E_{max}, the vector difference between the observed and expected amplitudes of (W-E), (W-N) and (W-S) for different values of E_{max} have been calculated. Using the data from the above three difference-telescopes the variance in the 'observed-expected' values have been obtained for different values of E_{max}. The minimum variance corresponds to the best fit value of E_{max}. The calculated variances for each of the years 1968, 1969 and 1970 and also for the three yearly average are

plotted in figure 4.10 as a function of E_{max}. It is evident from this figure that the variance is minimum for E_{max} = 85, 80 and 100 GeV for the years 1968, 1969 and 1970 respectively. For three yearly average the variance is minimum for E_{max} = 85 GeV. Thus diurnal variations observed by the difference-telescopes at Ahmedabad during 1968 to 1970 are consistent with the corotational anisotropy with E_{max} being 80-100 GeV.

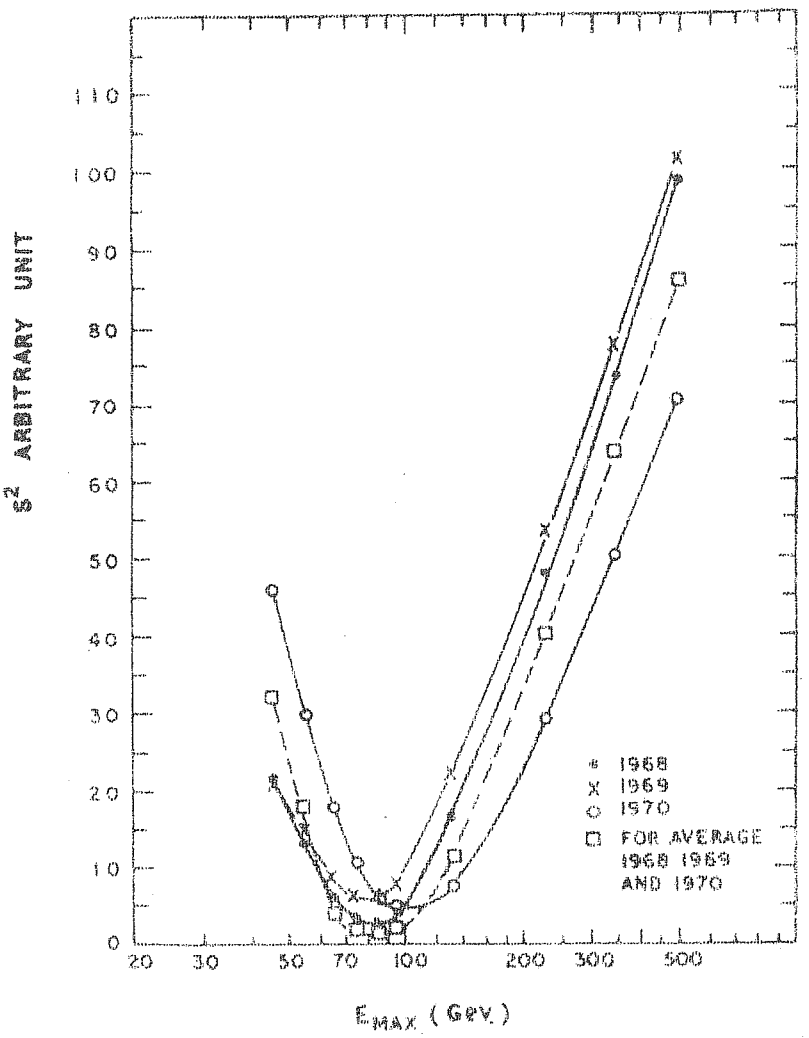

Fig.4.10 Variance 'S^2' in the 'observed minus expected' values (shown in Fig.4.09) of the diurnal variation for W-E, W-N and W-S telescope is shown as a function of the upper limiting energy E_{max} for individual years and for the three year average.

4.3.2 Determination of spectral characteristics of the average diurnal anisotropy using neutron and Ahmedabad meson monitor data

Following the same procedure as discussed in section 4.2 the free space values of the diurnal anisotropy during 1968 and 1969 were computed for various values of 'γ' and E_{max} using the average diurnal variations observed by a number of neutron and Ahmedabad meson (difference-telescopes) monitors separately. The variance 'S^2' in the space values, determined for different assumed values of the exponent 'γ' and for different values of E_{max} for 1968 with neutron data are shown in Figure 4.11 a. It is seen from the figure that even though all the curves for different E_{max} values show a minimum variance for $\gamma = 0.0 \pm 0.2$, the value of E_{max} can not be fixed uniquely with neutron data alone. The corresponding variance calculated using only Ahmedabad meson telescope (difference-telescopes) data is shown in Fig.4.11 b. Examination of the figure indicates that again neither 'γ' nor E_{max} can be uniquely specified, with meson data alone which may probably be due to the fewer number of available data. The curves for other years are also similar to the one shown in figure 4.11 a and 4.11 b.

The variance 'S^2' calculated including both neutron and Ahmedabad meson monitor (difference-telescopes) observations for the years 1968 and 1969 are shown in figure 4.12 a and 4.12 b. During both the years the minimum variance is exhibited for $\gamma = 0. \pm 0.2$ and $E_{max} = 85 \pm 10$ GeV. The value of E_{max} obtained

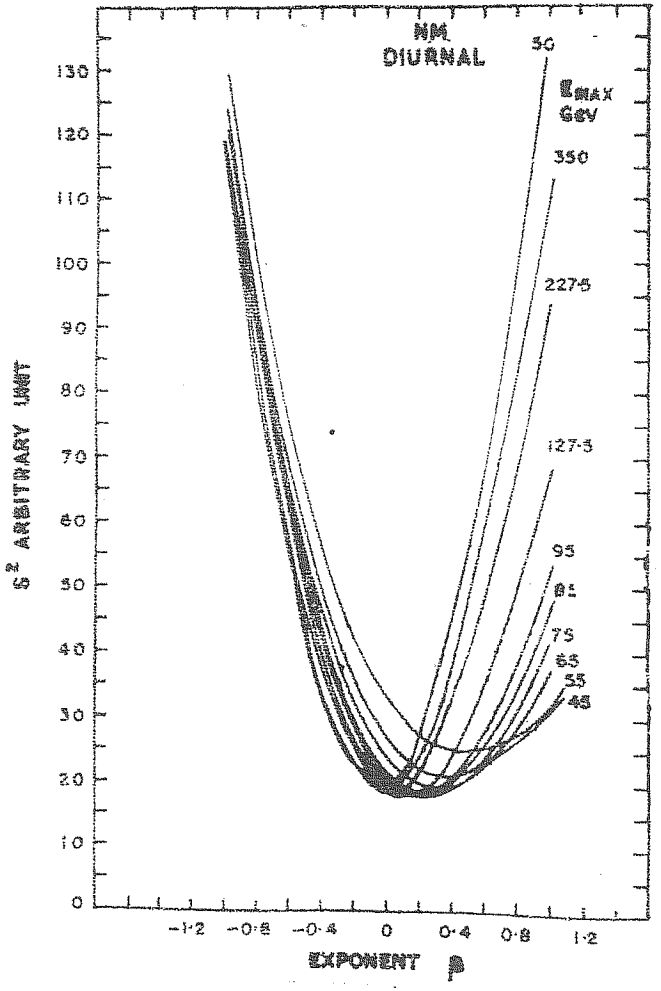

(a)

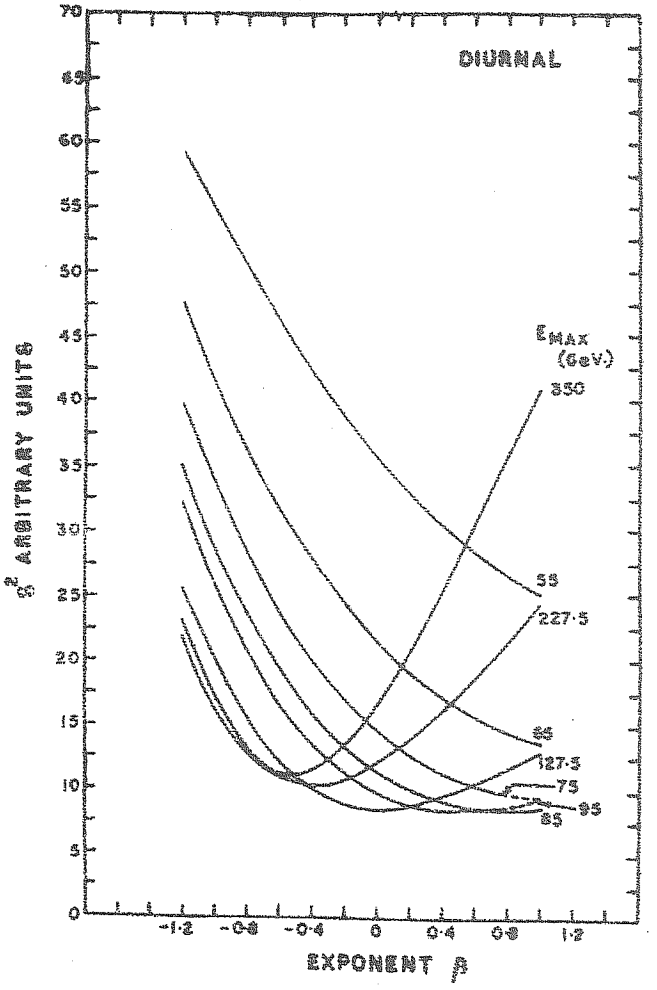

(b)

Fig.4.11 Variance 'S^2' in the diurnal anisotropy is shown as a function of the exponent 'β' of the energy spectrum of variation for various values of the upper limiting energy E_{max}. The diurnal anisotropy is calculated using data from
(a) neutron monitors and (b) meson telescopes (W-E, W-N and W-S) at Ahmedabad.

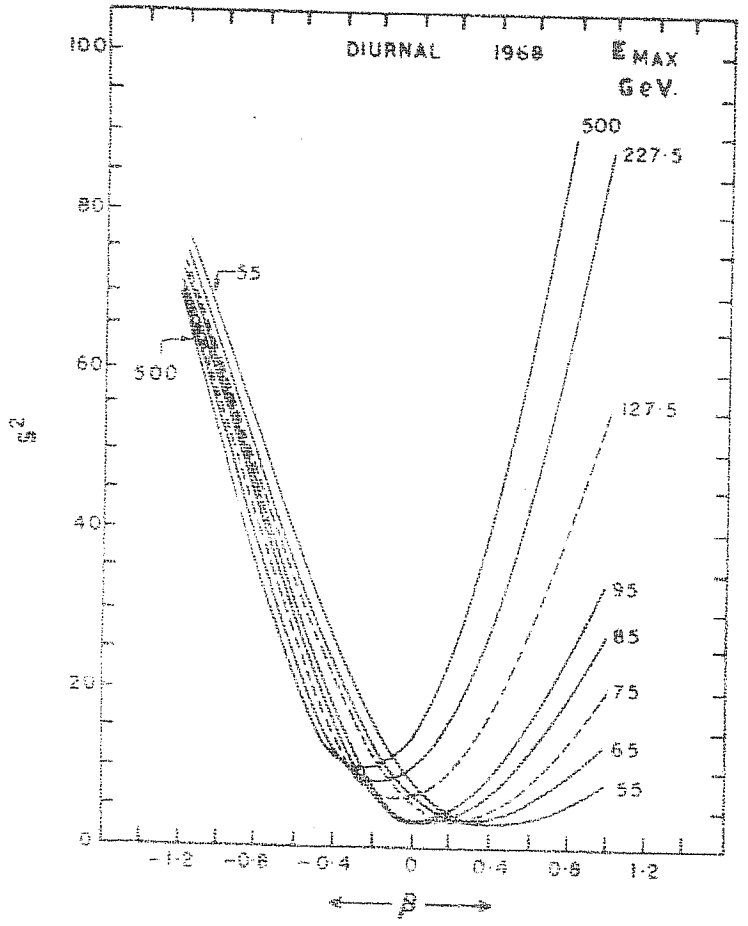

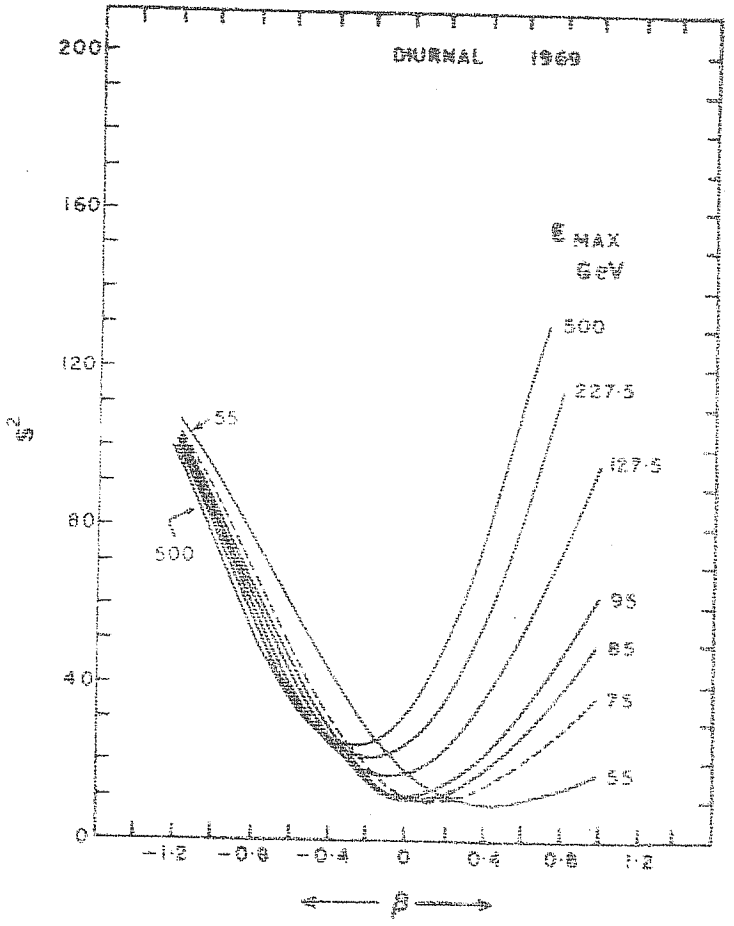

Fig.4.12 Variance δ^2 in the diurnal anisotropy calculated using data from a number of neutron monitors and Ahmedabad meson telescopes (difference-telescopes) is shown as a function of $1/\beta$ for various values of E_{max}.

above for 1968 and 1969 is consistent with the values reported by Ahluwalia and Ericksen (1969) and Agrawal et.al.(1971). The observed amplitudes and time of maximum of the yearly average diurnal anisotropy for these years have also been computed using both neutron and meson monitor observations and are given in Table 4.05.

Table 4.05

Diurnal Anisotropy

Neutron + Meson telescopes at Ahmedabad

Year	E_{max} GeV	β	r_1^* %	ϕ_1^*
1968	85 ± 10	0 ± 0.2	0.42 ± 0.014	272 ± 2°
1969	85 ± 10	0 ± 0.2	0.44 ± 0.011	273 ± 2°

The amplitude of the diurnal anisotropy is $\sim$ 0.43% and the time of maximum of the anisotropy is along 1800 hours. The coupling constants used for neutron monitors are those from IQSY manual and the variational coefficients are normalised upto 500 GeV. As shown by Subramanian (1971), if normalisation of variational coefficient are done upto ∞ and adequate correction for the changes in primary energy spectrum are considered the above value will correspond to the theoretical corotational amplitude.

From the preceeding discussion it is evident that for a better determination of many of the anisotropy characteristics it is essential to have both neutron and meson data. The

diurnal anisotropy seems to exhibit a very high degree of variability on a day-to-day basis in phase, amplitude and in the spectral characteristics. On an yearly average basis, however, the diurnal anisotropy is observed to be energy independent and exhibit a time of maximum corresponding to 1800 hour direction in space, consistent with the concept of cosmic ray current undergoing corotation. During the period 1968-1969 the values of E_{max} the maximum energy upto which particles seem to exhibit rigid corotation was found to be 85 $\pm$ 10 GeV.

4.4 Average semi-diurnal anisotropy

4.4.1 Characteristics of the average semi-diurnal anisotropy

Following equation 4.02 we may represent the spectrum of the semi-diurnal component as a power law type

$$\text{i.e. } \frac{\delta D(E)}{D(E)} = a E^{\beta} \quad \text{for } E < E_{max}$$

$$= 0 \quad \text{for } E > E_{max} \qquad \ldots\ldots\ldots 4.03$$

where 'a' is the amplitude of the anisotropy at GeV energy. β is the exponent and E_{max} is the upper limiting energy above which limit, particles do not experience semi-diurnal modulation.

Following the procedure as discussed in section 4.2 the variance 'S^2' in the harmonic components of the semi-diurnal anisotropy has been determined for different assumed values of the exponent 'β' and upper limiting energy E_{max}, using the values of average semi-diurnal variation as observed by number of neutron monitors and Ahmedabad meson monitors separately.

Figures (4.13 a) and (4.13 b) show the plot of 'S^2' values as a function of 'β' for nine different values of E_{max}. It is seen from the figure that even with the meson data alone, both 'β' and E_{max} corresponding to minimal variance can be unambiguously identified i.e. even after considering the error in 'S^2_{min}' it is possible to define these spectral parameters accurately by using meson data alone. The variance obtained using neutron data is large and hence with such data alone determination of 'β' and E_{max} is difficult. This is due to the lower energy of response of these monitors and the positive spectral exponent of the semi-diurnal anisotropy.

For better statistics, however, we have utilised both neutron and meson data together to derive the characteristics of the semi-diurnal anisotropy. The results obtained are presented in Table 4.06.

Table 4.06

Semi-diurnal Anisotropy

Year	E_{max} GeV.	β	a_2%	t_2 hours.
1968	227.5	1.0 ± 0.2	0.0029 ± 0.0002	3.2 ± 0.13
1969	227.5	1.0 ± 0.2	0.0020 ± 0.0002	3.2 ± 0.19

4.4.2 Semi-diurnal anisotropy using (W-E) data

It has been shown in Chapter III that the geomagnetic bending-difference between East and West telescope is $\sim$6 hours and the ratio of the expected relative, semi-diurnal amplitudes of East/West is $\sim$ 1.1 for a positive spectrum ($\beta > 0$) with E_{max} greater than 100 GeV. Further it has also been shown that the

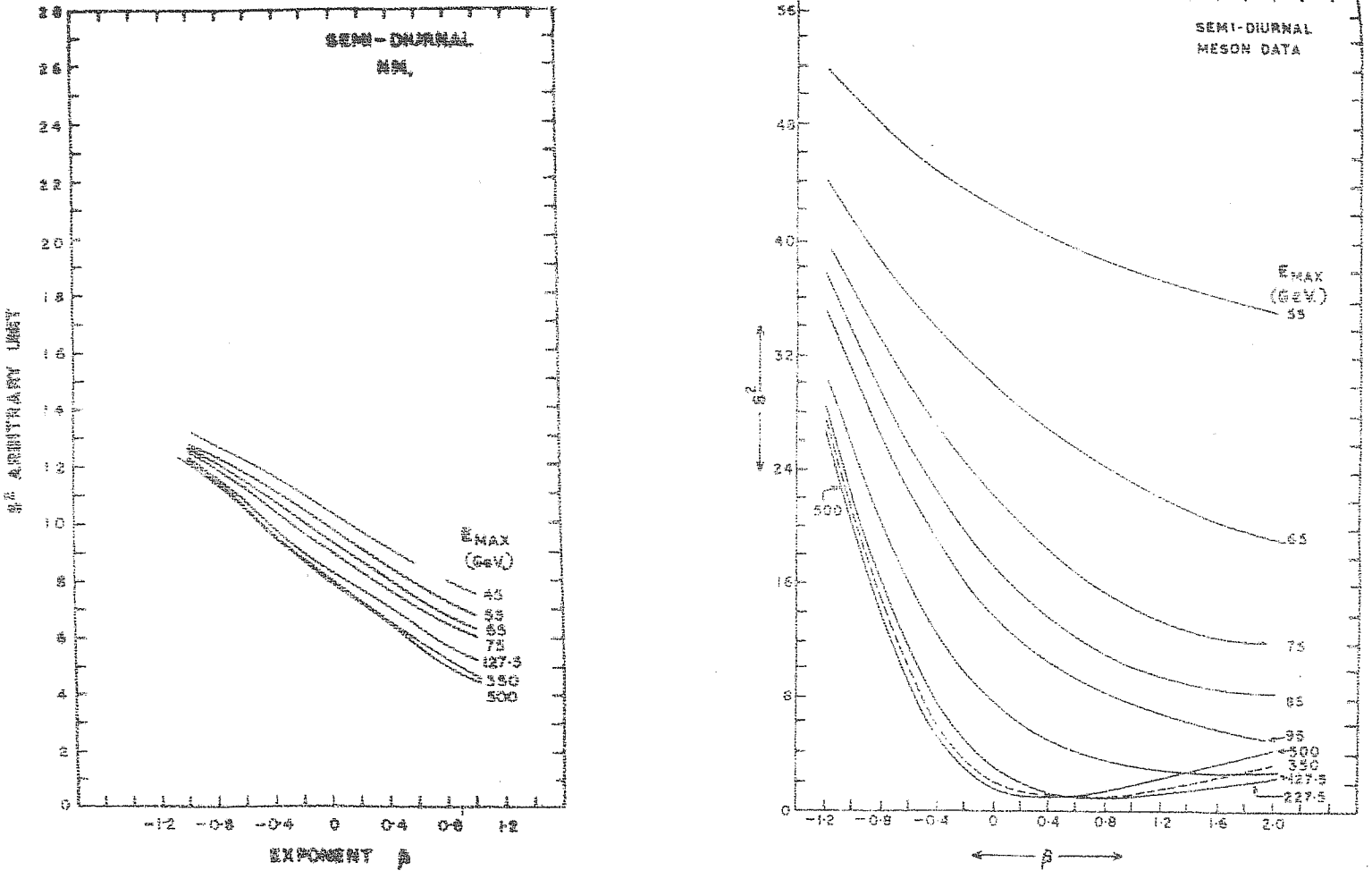

Fig.4.13 Variance S^2 in the semi-diurnal anisotropy is shown as a function of the exponent 'β' for various values of the upper limiting energy E_{max}. The semi-diurnal anisotropy is calculated using data from only (a) neutron monitors and (b) meson telescopes (W-E, W-N and W-S) at Ahmedabad.

semi-diurnal component of difference-telescope (W-E) will be $\left\{1 + \left(\frac{\alpha 2W}{\alpha 2E}\right)\right\}$ times the value of the semi-diurnal component observed by East pointing telescope. In other words the semi-diurnal component exhibited by (W-E) data will be approximately twice the semi-diurnal component observed by an East or West pointing telescope. This feature allows us to study the semi-diurnal anisotropy with (W-E) data alone. In figure 4.14 the semi-diurnal anisotropy derived from the observed (W-E) data alone has been plotted, where the anisotropy is computed assuming $\beta = 1.0$ and $E_{max} = 250$ GeV.

It is seen from the figure that the amplitude of the semi-diurnal anisotropy shows a gradual reduction in magnitude from 1968 to 1970. The direction of the average semi-diurnal anisotropy, however, remains practically constant and is along the 0300 hour direction which is perpendicular to the average interplanetary magnetic field vector.

The most significant feature of the semi-diurnal component is its time of maximum which is along the 0300 hour direction. Figure 4.15 shows the histogram of occurrence of the semi-diurnal time of maximum in space on a day-to-day basis for a period of about 6 months during June to December 1968 obtained from the (W-E) difference-telescope. The period has been specifically selected because of the availability of concurrent inter-planetary magnetic field data. In the same figure, the histogram of occurrence of the direction of the interplanetary magnetic

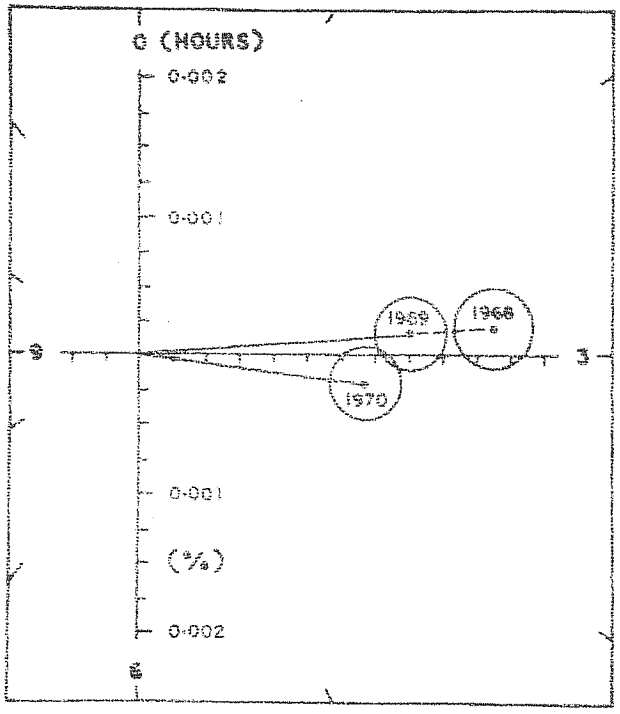

Fig.4.14 Semi-diurnal anisotropy in space derived using data from only W-E telescope and assuming an exponent 'β' equal to +1 and an upper limiting energy E_{max} as 250 GeV. The amplitude of the anisotropy at 1 GeV. primary energy is plotted.

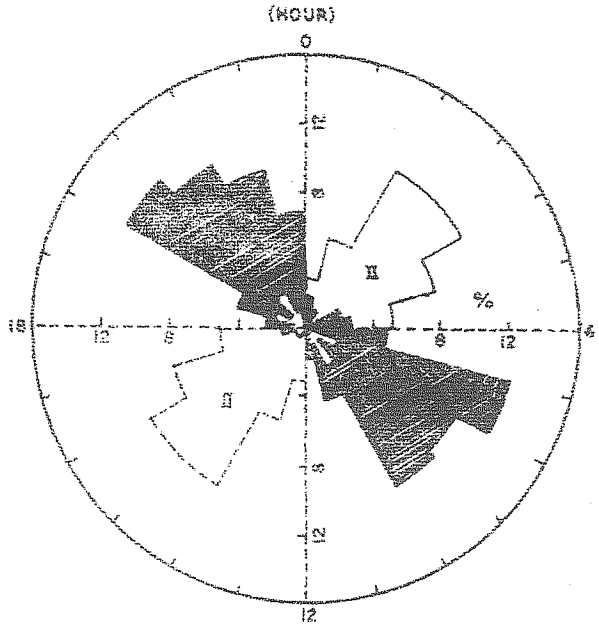

Fig.4.15 Polar histogram of the time of maximum of the semi-diurnal anisotropy and the interplanetary magnetic field direction during 1968. Shaded plot shows the histogram of the interplanetary magnetic field direction. The other plot shows the histogram of the time of maximum of the semi-diurnal anisotropy in space derived from (W-E) telescope data at Ahmedabad. Dotted histogram is the reflection of the semi-diurnal phase considering the second cycle of the semi-diurnal component.

field is also shown which clearly indicates that the field is aligned along the 0900 or 2100 hour direction and thus the semi-diurnal anisotropy is perpendicular to the interplanetary magnetic field direction.

Summarising the previous discussion we conclue that the semi-diurnal anisotropy of cosmic radiation can be represented by a power low spectrum as

$$\frac{\delta D(E)}{D(E)} = a_2 \; E^{\beta} \cos^2\lambda \quad \text{for} \quad E < E_{max}$$

The value of the relevant parameters β, E_{max} 'a_2' and 'ϕ_2' for 1968 and 1969 are given in table 4.06. The semi-diurnal time of maximum both on an average and on a day-to-day basis is mainly aligned along the 0300 hour direction and is in general perpendicular to the mean direction of the interplanetary magnetic field vector.

4.5 Study of the anisotropies resulting from cosmic ray density gradients and the interplanetary magnetic field direction

As shown in Chapter I (1.5.2 equation 1.28) expression for the streaming of cosmic ray particles in the interplanetary space contains four terms, viz. that due to radial convection, diffusion along and perpendicular to the interplanetary magnetic field line and the streaming resulting from the cosmic ray density gradients and the direction of the interplanetary magnetic field. The fourth term due to density gradient is

dependent on ipmf.direction and is represented by

$$S = \frac{-v^2}{3\omega}\left(\frac{\partial \vec{U}}{\partial r} \times \frac{\vec{B}}{B}\right) = -\frac{\rho v}{3}\left(\frac{\partial \vec{U}}{\partial r} \times \frac{\vec{B}}{B}\right) \qquad \therefore v = \omega\rho$$

The anisotropy is given by $\xi = \frac{3S}{vU} = -\frac{\rho}{U}\left(\frac{\partial \vec{U}}{\partial r} \times \frac{\vec{B}}{B}\right)$ 4.04

$$\frac{1}{U}\ \frac{\partial U}{\partial r} = \text{Gradient}$$

This anisotropy vector reverses its direction with the reversal of the interplanetary magnetic field direction or with the reversal of the cosmic ray density gradient. The anisotropy is perpendicular to the interplanetary magnetic field and the cosmic ray density gradient. The vector equation 4.04 can be written as

$$\xi = \begin{vmatrix} i & j & k \\ G_x & G_y & G_z \\ B_x & B_y & B_z \end{vmatrix} = -\rho \left[i(G_y B_z - G_z B_y) - j(G_x B_z - G_z B_x) + k (G_x B_y - G_y B_x) \right] \qquad .....4.05$$

Where G_x and G_y are the radial and azimuthal cosmic ray density gradients respectively. G_z is the cosmic ray density gradient perpendicular to the ecliptic plane. The interplanetary magnetic field is mainly lying in the ecliptic plane and therefore B_z is very small (~ 0). Hence only four terms remain in equation 4.05. For one solar rotation period, the azimuthal gradient (i.e. G_y) can be considered as zero. The interplanetary magnetic field direction to a first degree of approximation, is

equally oriented towards and away from the sun and therefore the anisotropy due to the perpendicular gradient (i.e. G_z) is also expected to be zero or negligible when time averaged anisotropies over periods of 27 day or longer period are considered. Thus the diurnal anisotropy vector averaged over sufficiently long period is expected to be virtually along 1800 hour direction, consistent with the corotational mechanism.

On a day-to-day basis, however the variability in the cosmic ray density gradients and in the interplanetary magnetic field characteristics will cause additional anisotropies, with the result the net anisotropy on a day-to-day basis will exhibit considerable departure from the corotational anisotropy. If days are grouped according to the interplanetary magnetic field direction (i.e. towards or away from the sun) the anisotropy due to the cosmic ray density gradient and the ipmf.direction being in the opposite direction for the two groups, the resultant anisotropy which is a sum of the corotation and gradient related anisotropy should be different for the two groups. Thus a comparison of the observed anisotropy for these two groups should in principle be useful for studying the ipmf. related anisotropy. The anisotropy not related to the gradient and the ipmf.direction will contribute equally in both the groups.

Cosmic ray particles from above and below the ecliptic plane, can spiral round the sector field lines to enter the ecliptic plane. If the direction of the sector field is away

from the sun and if there is a deficiency of cosmic ray particles above the ecpliptic then the north-south density gradient would lead to a diurnal component from 15 hour direction and the amplitude of the resultant diurnal component will increase. When the sector field reverses the direction the anisotropy will also reverse its direction and the amplitude of the resultant diurnal component will decrease.

In addition, there will be an anisotropy perpendicular to the ecliptic plane, because of the radial heliocentric cosmic ray density gradient (Swinson, 1969) and the azimuthal component of the interplanetary magnetic field (i.e.B_y). This perpendicular anisotropy also changes its direction with the reversal of the magnetic field direction. In solar time, the perpendicular anisotropy will average out to zero.

Attempts to isolate magnetic field related anisotropies by considering the observed interplanetary magnetic field directions have been made by several workers, (Swinson, 1969, 1970, 1971; Hashim and Bercovitch, 1971 and Hatton and Barker, 1971), by using data from a number of neutron and meson monitors. In this section we present the results obtained for the years 1968 and 1969 with data from six neutron monitors and Ahmedabad meson monitors. From these results we show that the magnetic field related anisotropy exhibits entirely different characteristics during 1969 as compared to the earlier years indicating that the interplanetary conditions radically changed during this period.

4.5.1 Study of the ipmf.related anisotropy by using the actual measured interplanetary magnetic field direction data during 1968

Since the detailed interplanetary magnetic field data from Explorer 33 was available to us only for about 95 days during the period May to December 1968, we first derive the field related anisotropy characteristics for this period. We also obtain a rough estimate of the North-South cosmic ray density gradient by attributing the observed anisotropy to the N-S gradient. To improve the statistical accuracy, we extended the study of anisotropy characteristics to the entire period covering 1968 and 1969, using the data on interplanetary magnetic field sector polarity given by Wilcox and Colburn (1970, 1972).

For the preliminary analysis the ipmf. data for 95 days were grouped according to the interplanetary magnetic field direction. Out of these, on approximately 22 days ipmf.direction had a value $135^{\circ} \pm 15^{\circ}$ (positive) and for about equal number of days it had a value $315^{\circ} \pm 15^{\circ}$ (negative). Such a rigid classification was made to ensure that the results would clearly show the field related anisotropy characteristics without any contamination from other effects (Bercovitch, 1971). The average diurnal variation for these two groups was determined for a number of neutron monitors and Ahmedabad meson monitors (difference-telescope) separately. The values of diurnal variation observed at the instrument for each monitor during periods of

positive and negative magnetic field directions are given in table 4.07 and are also plotted in Fig.4.16. Since the values of

Table 4.07

1968

Average diurnal variation during ipmf.direction

$135^{\circ} \pm 15^{\circ}$ and $315^{\circ} \pm 15^{\circ}$

	$r_1\%$	ϕ_1(deg.)	$r_1\%$	ϕ_1(deg.)
Sulphur Mt.	0.461 ± 0.055	258	0.347 ± 0.055	264
Deep River	0.426 ± 0.050	238	0.289 ± 0.052	241
Kiel	0.407 ± 0.055	223	0.225 ± 0.055	233
Lindau	0.422 ± 0.053	217	0.241 ± 0.053	236
Pic du Midi	0.412 ± 0.053	196	0.270 ± 0.053	208
Chacaltaya	0.362 ± 0.045	201	0.219 ± 0.045	230
W-S	0.130 ± 0.055	276	0.053 ± 0.052	360
W-N	0.200 ± 0.054	286	0.100 ± 0.054	343
W-E	0.220 ± 0.054	289	0.161 ± 0.054	337

the semi-diurnal component do not show any significant differences, we have not considered the semi-diurnal component in the analysis. It is clear from both the table (4.07) and the figure (4.16) that the amplitude of the diurnal variation at all stations during positive ipmf. direction is larger than the corresponding values obtained for the negative ipmf. direction. Similarly the time of maximum for the positive ipmf. direction is found to be earlier than for that during negative

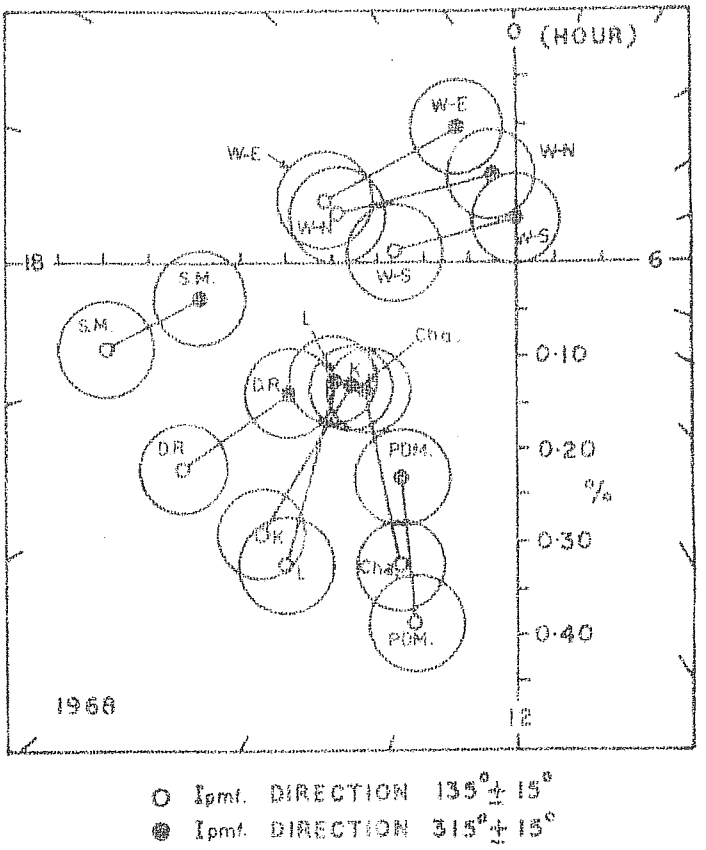

Fig.4.16 Harmonic dials showing the average diurnal variation during days when the interplanetary magnetic field direction was $135^{\circ} \pm 15^{\circ}$ and when it was $315^{\circ} \pm 15^{\circ}$. The data are from the Deep River (D.R.), Chacaltaya (Cha.), Pic du Midi (PDM), Kiel(K), Lindau(L), Sulpher Mt.(S.M.) and difference-telescopes (W-E, W-N and W-S) at Ahmedabad for the period 1968.

ipmf.direction. The vector differences between the positive and negative field average diurnal variation for all stations have also been computed.

Assuming equal contribution of the corotational anisotropy in both positive and negative ipmf.group days, the above vector differences will show twice the amplitude of an anisotropy resulting from the ipmf.direction and the cosmic ray density gradient. The vector difference thus computed has been utilised to derive the spectral characteristics of the magnetic field related anisotropy. The results obtained by using both neutron and meson monitor data are given in Table 4.08.

Table 4.08

$\vec{r}_1$ %	$\vec{\phi}_1$	β	E_{max} GeV.
0.0236 ± 0.005	16.6 hrs.	+ 0.6 ± 0.2	85

The results are in substantial agreement with the results reported by Hashim and Bercovitch (1971).

4.5.2. Study of the ipmf.related anisotropy during 1968 and 1969 using sector polarity data

Both for improving the statistics and also to investigate the field related anisotropy as a function of the solar activity, we have extended the analysis for the entire period during 1968 and 1969. Study of such anisotropies from 1965 to

1968 has been reported by various workers. Even though the actual value of the interplanetary magnetic field direction for this period could not be obtained, the total ipmf.sector information for this period given by Wilcox and Colburn (1970, 1972) has been used for grouping the data. The average diurnal variation for each of the neutron and Ahmedabad meson monitors for the two groups of days one having a dominant positive polarity and the other having a negative polarity, have been computed for 1968 and 1969 separately. In order to ensure that the analysis is restricted to days having unambiguously positive and negative polarity of the magnetic field and to avoid any contribution from mixed polarity (a) days occurring only within the larger sectors (>5 days duration) have been used (b) days immediately before and after a sector boundary crossing have been excluded and and (c) days on which the cosmic ray intensity showed large disturbances such as Forbush decrease days have been omitted (decrease $>3\%$ at high latitude N.M.). Enhanced diurnal variation days ($r_1 > 0.95\%$ for a station like Deep River) also have been omitted. This selection criteria limited the number of available days to 120 in 1968 and 180 in 1969.

The average diurnal variation characteristics for both groups of days obtained for each of the meson and neutron monitors are given in table 4.09. Since the number of days in the positive and in the negative sector are approximately the same during different seasons of the year, we can assume that

Table 4.09

Average diurnal variation in positive and negative sector of the interplanetary magnetic field.

	Positive sector		Negative sector	
	r_1(%)	φ_1(deg.)	r_1(%)	φ_1(deg.)
		1968		
Sulphur Mt.	0.338 ± 0.041	255	0.282 ± 0.031	246
Deep-River	0.340 ± 0.040	234	0.248 ± 0.031	232
Kiel	0.306 ± 0.038	221	0.261 ± 0.032	216
Lindau	0.345 ± 0.038	212	0.247 ± 0.030	218
Pic du Midi	0.374 ± 0.042	189	0.260 ± 0.033	191
Chacaltaya	0.305 ± 0.034	197	0.178 ± 0.028	223
W-S	0.112 ± 0.034	303	0.081 ± 0.032	325
W-N	0.201 ± 0.034	283	0.106 ± 0.031	312
W-E	0.209 ± 0.033	277	0.121 ± 0.032	316
		1969		
Sulphur Mt.	0.291 ± 0.031	252	0.332 ± 0.024	258
Deep-River	0.258 ± 0.033	232	0.284 ± 0.025	238
Kiel	0.278 ± 0.031	226	0.312 ± 0.025	228
Lindau	0.273 ± 0.032	218	0.306 ± 0.025	227
Pic du Midi	0.306 ± 0.033	191	0.322 ± 0.027	202
Chacaltaya	0.232 ± 0.024	210	0.220 ± 0.018	218
W-S	0.053 ± 0.034	360	0.084 ± 0.027	320
W-N	0.063 ± 0.033	325	0.144 ± 0.025	293
W-E	0.072 ± 0.033	335	0.136 ± 0.025	302

the temperature effect will contribute more or less equally to the positive and negative sector group. Hence a vector difference of diurnal component between positive and negative sector group obtained from even Ahmedabad meson monitors will be free from the temperature effect.

The observed diurnal variation for positive and negative polarity days obtained for each of the neutron and meson monitors are plotted separately for the years 1968 and 1969 in figure 4.17 a & b. For the year 1968, it is clear from the figure that the diurnal amplitude is larger in magnitude and generally has an earlier time of maximum for positive polarity days. This result is consistent with the conclusions derived from lesser sample of days on which the actual ipmf. data is available, as discussed in 4.5.1. However, in 1969, the results are entirely different. The diurnal amplitude for positive polarity days is less than the observed amplitude for negative polarity days.

In order to quantitatively determine the characteristic of the ipmf.related anisotropy (due to cosmic ray density gradients) contributing during positive and negative polarity days, the observed values have been subjected to spectral analysis after computing the vector differences between average amplitudes in positive and negative polarity days for each monitor. Before proceeding with a rigourous examination of these results, we may compare the average diurnal anisotropy in space for positive and negative days, obtained from all the

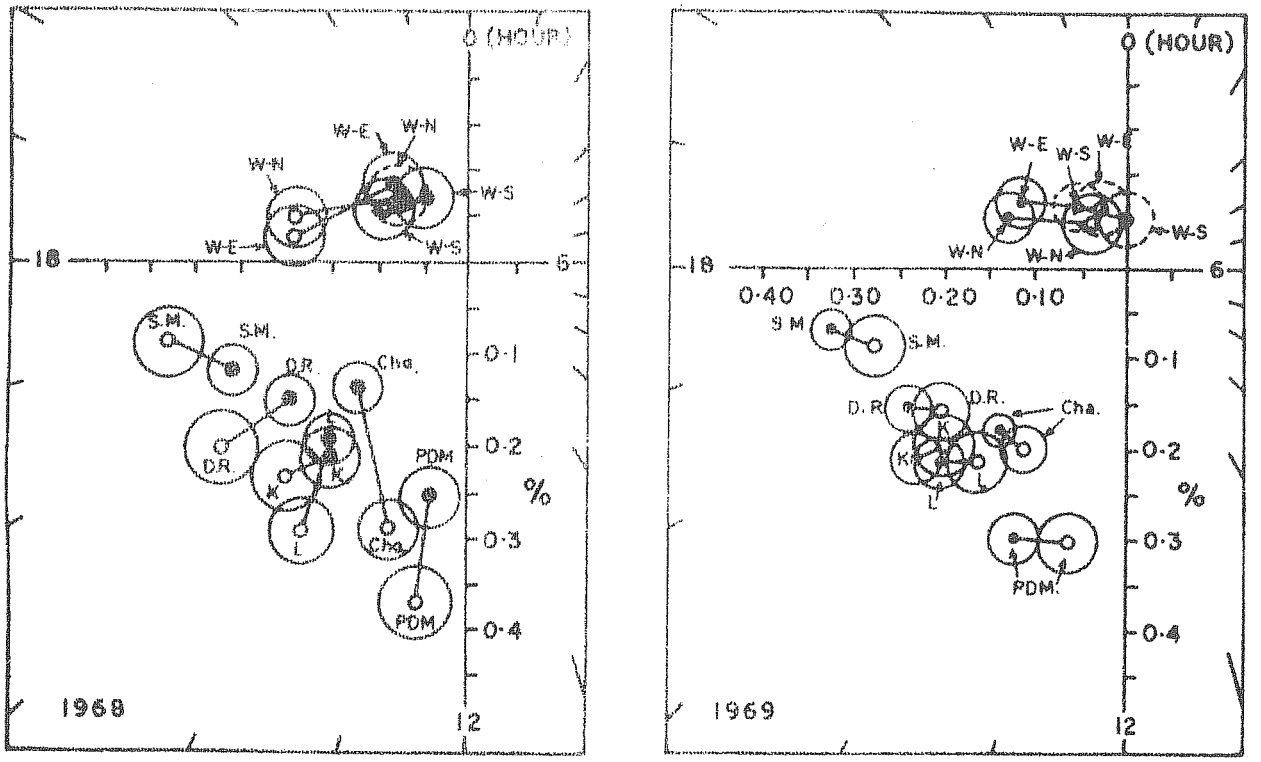

(a) (b)

Fig.4.17 Harmonic dials showing the average diurnal variations observed by neutron monitors and meson telescopes (W-E, W-N and W-S) at Ahmedabad for positive sector (shown by open dots) and for negative sector (shown by dark dots) of the interplanetary magnetic field during (a) 1968 and (b) 1969.

available data of both neutron and meson monitors for the years 1968 and 1969. The average anisotropy vectors have been derived assuming an energy independent variational spectrum ($\beta = 0$) with E_{max} at about 95 GeV. Figure (4.18) shows the average diurnal anisotropy vector in space for positive and negative polarity days separately during 1968 and 1969. The dotted line shows the difference vector which is twice the anisotropy vector due to cosmic ray density gradient and the ipmf.direction.

Since the average anisotropy vector during positive and negative polarity days is determined using spectral exponent $\beta = 0$ these results are not rigourous, because this method tacitly assumes $\beta = 0$ also for the ipmf.related anisotropy. However, these results will serve to show the clear change in the field related anisotropy observed in 1969. The figure clearly indicates that the amplitude of the field related anisotropy in 1969 is less than that during 1968 and its phase is practically opposite to that of 1968.

For a more rigourous determination of the spectral characteristics of the field related anisotropy the vector-differences observed at each of the station have been computed and subjected to spectrum analysis. The results obtained for the best fit values discribing the spectral characteristics of the field related anisotropy namely its amplitude, phase, spectral exponent and E_{max} are given in table 4.10. The variance 'S^2' in the space values, determined for different assumed values

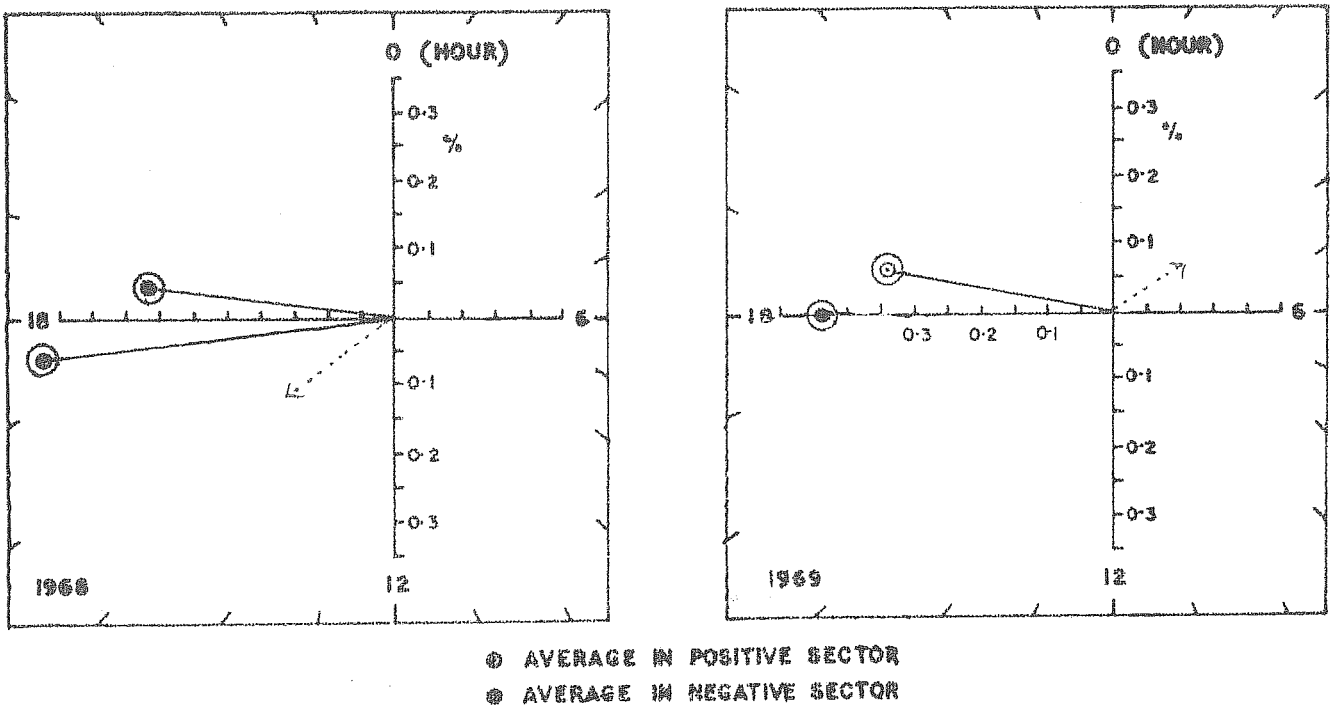

Fig.4.18 Assuming the exponent of the energy spectrum $\beta = 0$ and $E_{max} = 95$ GeV the observed diurnal variations for all the stations presented in Fig.4.17 are extrapolated to space and their mean value in each sector for 1968 and 1969 is shown.

of the exponent 'β' and E_{max} for 1968 are shown in Figure 4.19.

Table 4.10

Year	E_{max} GeV	β	r_1^* %	ϕ_1^* (hours)
1968	65	1.0	0.0047 ± 0.0007	16.30
1969	65	1.0	0.0017 ± 0.0005	5.6

The mean, field related, anisotropy vector during 1968 and 1969 obtained as a best fit to the observed values are plotted in Figure (4.20). The results clearly indicate that the magnetic field related anisotropy is higher by a factor of about three during 1968 than in 1969. The time of maximum of the anisotropy is along 16.30 hours during 1968 whereas it is practically in the opposite direction namely along 5.6 hours during 1969. The anisotropy seems to vary as E^{β} where β is positive and the upper limiting energy E_{max} is < 75 GeV. Attributing the ipmf. related anisotropy observed in 1968 only to the north-south cosmic ray density gradient we get a value of the north-south gradient as (1.08 ± 0.16)%/A.U. and it is found to be energy independent (for $\beta = +1$, as the spectrum of the anisotropy).

The observed reversal in time of maximum during 1969 could be due to either or both of the following reasons:

1) the reversal of North-South cosmic ray density gradient

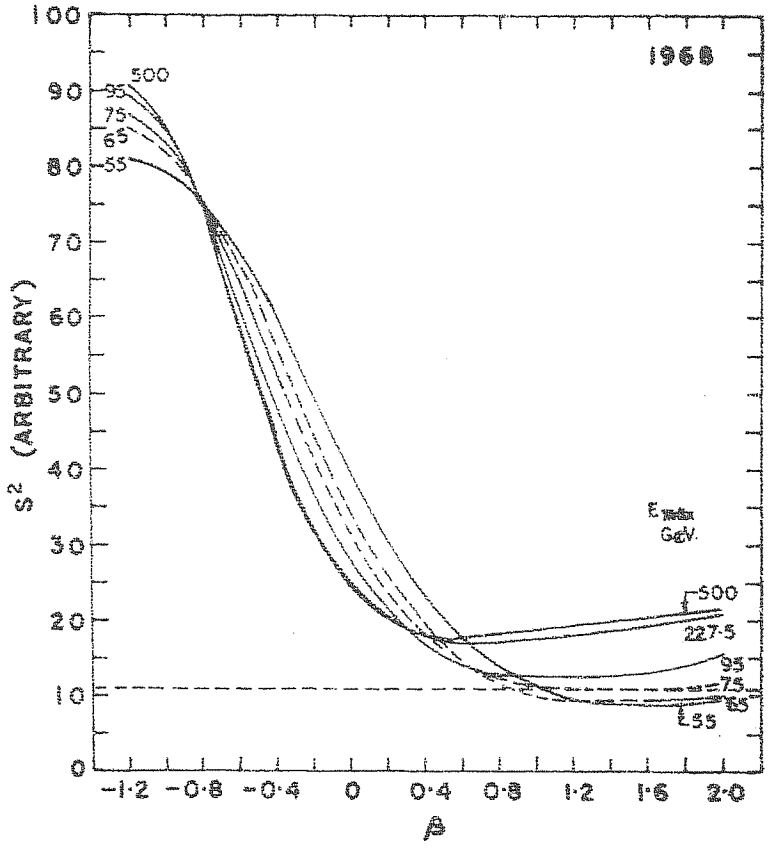

Fig.4.19 Variance 'S^2' in the 'inter-planetary magnetic field related anisotropy' as a function of 'β' for various values of E_{max} during 1968.

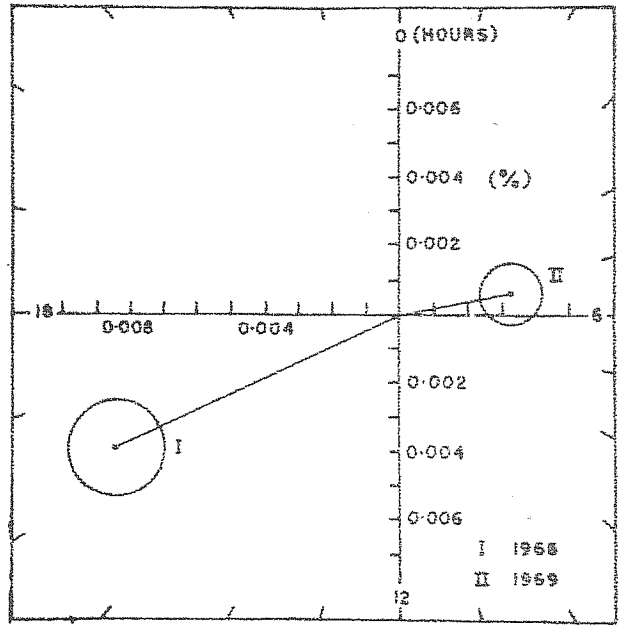

Fig.4.20 Harmonic dials showing the 'inter-planetary magnetic field related anisotropy' in space during (I) 1968 and (II) 1969.

Using the vector-differences between the average diurnal variation in positive and negative magnetic field sectors the ipmf. related anisotropy in space is obtained for the best fit values of the exponent 'β'(=+1) and the upper limiting energy E_{max}(65 GeV.). The average amplitude of the anisotropy in space (at 1 GeV.primary energy) is shown for 1968 & 1969.

(2) the effect due to the B_z component.

The observed anisotropy on any day can be represented as

$$A = A_{corot.} + A_{ipmf.} \quad \ldots\ldots\ldots\ldots 4.06$$

Where A_{corot} is the corotational anisotropy and $A_{ipmf.}$ is the anisotropy related to the interplanetary magnetic field.

The yearly average ipmf.related anisotropy (in solar time) obtained from the vector-difference of the average diurnal variations in positive sector and in the negative sector of the interplanetary magnetic field can be represented as

$$A_{ipmf.} = A_{(n-s)} + A_{(B_z)} \quad \ldots\ldots\ldots\ldots 4.07$$

where $A_{(n-s)}$ is the anisotropy due to north-south cosmic ray density gradient and $A_{(B_z)}$ is the anisotropy due to the north-south component of the interplanetary magnetic field (B_z) and the radial density gradient.

From equation 4.05 we can write

$$\left.\begin{aligned} A_{(n-s)} &= \varsigma(i\, G_z\, B_y - j\, G_z\, B_x) \text{ and} \\ A_{(B_z)} &= \varsigma(j\, G_x\, B_z) \end{aligned}\right\} \quad \ldots\ldots\ldots 4.08$$

Now, the reversal of $A_{ipmf.}$ in 1969 could therefore be due to either or both of these components (i.e. $A_{(n-s)}$ and $A_{(B_z)}$.

(1) Effect due to north-south cosmic ray density gradient

It has already been explained in section 4.5 that the existence of a north-south density gradient can contribute to

diurnal anisotropy either along 0300 hour or along 1500 hour direction depending on the polarity of the interplanetary magnetic field.

Knowing that the cosmic ray intensity and the solar activity are negatively correlated, the north-south density gradient of the cosmic ray flux can be inferred by examining the solar activity at different heliolatitudes. We have examined the coronal (λ5303) intensity and the sun-spot group, data (Waldmeier, 1971) in the latitude range -40° to 40° during 1968 and 1969. The values of λ 5303 intensity and sun-spot groups are presented in table (4.11). Examination of the table does not indicate the existence of any such reversal in λ 5303 intensity or in sun-spot groups during 1969. Nevertheless a general decrease in the magnitude of the north-south asymmetry in 1969 compared to the asymmetry in 1968 has been established (Pathak, 1972) which indicates that the north-south density gradient must have decreased in 1969 as compared to its value in 1968.

The intensity of 9.1 cm. flux from 0 to 10° heliolatitude, (Stanford Solar Radio Emission Spectro-heliograms solar geophysical data 1969) also does not show a reversal in the north-south asymmetry in 1969. The data shows a decrease in north-south asymmetry during later months of 1969, in reasonable agreement with λ5303 intensity and sun-spot group observations.

Therefore we conclude that even though $A_{(n-s)}$ has probably decreased from 1968 to 1969, it has not changed its

Table 4.11

Sun-spot group yearly data *

	South Heliolatitude (degree)								North Heliolatitude (degree)							
Year	35-40	30-35	25-30	20-25	15-20	10-15	5-10	0-5	0-5	5-10	10-15	15-20	20-25	25-30	30-35	35-40
1968	2	15	38	46	68	79	31	11	14	49	89	89	53	24	12	1
1969	1	7	13	25	62	75	39	11	22	73	95	76	38	13	2	3

λ5303 Intensity (arbitrary Unit)

	South Heliolatitude (degree)								North Heliolatitude (degree)							
Year	40	35	30	25	20	15	10	5	0	5	10	15	20	25	30	35	40
1968	4.67	5.38	6.10	6.73	7.06	6.90	5.94	5.14	4.99	5.72	6.92	7.71	7.82	7.27	6.27	5.28	4.48
1969	3.80	4.31	4.85	5.63	6.27	6.59	6.20	5.63	5.60	6.21	6.92	7.18	7.04	6.27	5.38	4.71	4.23

* Data from Astronomische Mitteilungen der Eidgenossischen Sternwarte Zurich - No. 288 and No. 296 (M. Waldmeier) (1971)

sign and consequently the reversal of $A_{ipmf.}$ in 1969 cannot be attributed to a reversal in the north-south cosmic ray density gradient. Therefore $A_{(B_z)}$ can be considered to be the cause of the reversal of the ipmf.related anisotropy ($A_{ipmf.}$) in 1969. In the following section we attempt to investigate whether the reversal could be due to the B_z component of the interplanetary magnetic field.

(2) Effect due to north-south (B_z) component of the interplanetary magnetic field.

With limited available data from Explorer-33 during June to December 1968, the average value of B_z is found to be + 0.04γ (northward) for days in the positive sector of the interplanetary magnetic field. The average B_z is found to be -0.4γ (i.e.southward) for days in the negative sector. The change in B_z from positive to negative sector i.e. δB_z is -0.44γ. If the B_z component is positive in positive sector and is negative in negative sector, the radial gradient will produce an anisotropy, whose time of maximum will be along the 1800 hour direction in the positive sector and along the 0600 hour direction in the negative sector. In other words, this anisotropy will add to the corotational anisotropy during positive polarity (sector) days and will subtract from the corotational value during negative polarity (sector) days. In this case the vector-difference between the average diurnal anisotropy in the poisitive sector and that in the negative sector will be $A_{(B_z)}$ and it will have a time of maximum along 1800 hour direction.

Knowing the radial density gradient we can calculate $A_{(B_z)}$ during 1968 for $\int B_z = -0.44\gamma$. Bercovitch (1971) has reported a radial gradient of 1.6%/A.U. at 20 GeV.energy during 1967-1968. Assuming a radial gradient with a rigidity spectra given by $\frac{\nabla N}{N} = \frac{32}{P}$ %/A.U. and assuming a 5γ interplanetary magnetic field(B) the anisotropy '$A_{(B_z)}$' in space, during 1968 will be calculated as follows.

$$A_{(B_z)} = \rho \times \frac{32}{P} \times \frac{0.44}{5} \quad \%$$

For a 5γ magnetic field the gyroradius ρ will be $\frac{P}{225}$ A.U. where P is the rigidity of the particle.

Therefore

$$A_{(B_z)} = \frac{P}{225} \times \frac{0.44}{5} \times \frac{32}{P} \simeq 0.013\%$$

The exponent of the energy spectrum of this anisotropy will be zero. This would give rise to a diurnal variation having an amplitude of $\sim 0.006\%$ at (W-E) telescope at Ahmedabad. This is negligible compared to the observed value of 0.089%. Therefore the major contribution to '$A_{ipmf.}$' during 1968, must be due to the $A_{(n-s)}$ component arising due to the north-south cosmic ray density gradient.

There are reasons to expect that the $A_{(B_z)}$ will be higher in 1969. The depression of the mean intensity in 1969 was more than that in 1968. This would indicate an increase in the value of the radial density gradient in 1969, as compared to that in 1968, if the extent of the modulating region and the rigidity spectrum remain the same. Considering the value of the inter-

planetary magnetic field in 1969 to be the same as in 1968, we can expect an increase in the amplitude of $A_{(B_z)}$ in 1969 due to an increase in the radial density gradient.

As discussed earlier, the comparison of solar activity data during 1968 and 1969 suggests a corresponding decrease in the north-south cosmic ray density gradient in 1969 than that in 1968. Therefore the anisotropy '$A_{(n-s)}$' due to the north-south density gradient will decrease during 1969.

If B_z is negative in positive sector and positive in negative sector, the observed reversal in '$A_{ipmf.}$' during 1969 can be well understood. However, this hypothesis needs actual veritication with the interplanetary magnetic field data. If this is proved it will be clear that the study of ipmf.related diurnal anisotropy will be effectively useful for studying the north-south component (B_z) of the interplanetary magnetic field.

4.5.3 Interplanetary magnetic field related sidereal diurnal anisotropy

Swinson (1969) has shown that the azimuthal component of the interplanetary magnetic field (B_y) and the radial density gradient can produce a sidereal anisotropy which can be seen by comparing the average diurnal variation in positive and in the negative polarity days when arranged according to the sidereal time. The entire data of 1969 has been divided into three monthly groups and the average magnitudes of daily variation for positive and negative polarity (sector) days have been determined

separately for each of these groups. The vector-difference between the average diurnal variations in positive sector and in the negative sector have been obtained for each three monthly period. The vector-difference thus obtained was plotted on a sidereal and antisidereal summation-dial. The resulting sidereal and antisidereal vectors obtained for all the monitors during 1969 are given in Table 4.12.

It is seen from the table that the amplitudes of the sidereal and antisidereal vectors obtained for neutron monitors are not statistically significant. Both are of low amplitude and comparable with each other. On the other hand the sidereal vectors obtained for meson monitor data besides being quite significant is $\sim$2 to 4 times the antisidereal vectors. Further the phase observed by E. W, N, S and Vertical telescopes in sidereal time show a phase difference between each other, which is consistent with the expected geomagnetic bending difference between them.

The sidereal variation observed by meson data have been subjected to spectrum analysis and the best fit parameters obtained are given in table (4.13). Using the α_j and γ_j for 'E_{max} and 'β' ' as obtained in table (4.13) the sidereal vectors observed by meson monitors are converted to space. Figure (4.21) shows (a) the plot of the sidereal vectors as observed by each of the monitors and also (b) the sidereal vectors in space after correcting for geomagnetic bending and the width of the cones of acceptance. The mean value of the sidereal anisotropy observed by various monitors is also shown in the same figure

Table 4.11

Interplanetary magnetic field related diurnal variation

Neutron Monitor

	Sidereal vector		Antisidereal vector	
	r_1%	ϕ_1(deg.)	r_1%	ϕ_1(deg.)
Sulphur Mt.	0.036 ± 0.038	268	0.039 ± 0.038	229
Deep River	0.009 ± 0.040	23	0.017 ± 0.040	190
Kiel	0.046 ± 0.039	239	0.051 ± 0.039	181
Lindau	0.046 ± 0.041	244	0.054 ± 0.041	159
Pic du Midi	0.037 ± 0.040	259	0.069 ± 0.041	168
Chacaltaya	0.026 ± 0.028	102	0.045 ± 0.028	104
	Meson Telescopes at Ahmedabad			
Vertical	0.086 ± 0.020	56	0.040 ± 0.020	115
West	0.095 ± 0.028	99	0.033 ± 0.029	191
South	0.109 ± 0.026	54	0.029 ± 0.026	63
North	0.115 ± 0.026	38	0.036 ± 0.026	15
East	0.106 ± 0.027	9	0.024 ± 0.027	279

Table 4.13

Ipmf.related sidereal diurnal anisotropy

r_1^* %	ϕ_1^*	β	E_{max} GeV.
0.0098 ± 0.0012	6.9 hrs.	1.0	85

with a dotted line. It is seen that the sidereal anisotropy has an amplitude of $\frac{0.0098\%}{2}$/GeV. and has a time of maximum along 6.9 hour direction.

For comparison, the sidereal variation observed by Swinson (1969, 1971) using the underground monitors at Bolivia and Embudo are also shown in figure (4.22). The sidereal vectors plotted in the figure (4.22) have not been corrected for the geomagnetic bending and the width of the cones of acceptance. Due to the unavailability of the correction factor to correct the observed amplitude for the width of the cones of acceptance, the actual magnitudes of the vectors, cannot be compared with our data. Inspite of the large mean standard deviation error in the Embudo and Bolivia data, the phases of the difference vectors for different telescopes seem to be quite consistent.

The time of maximum of the sidereal anisotropy vectors can be approximately computed from the above data. When the sidereal anisotropy vectors, in space, are derived from the above data it is found that the time of maximum of these vectors are along 0700 to 0900 hours direction and thus the results presented by us are quite consistent with Swinson's (1969, 1971) result.

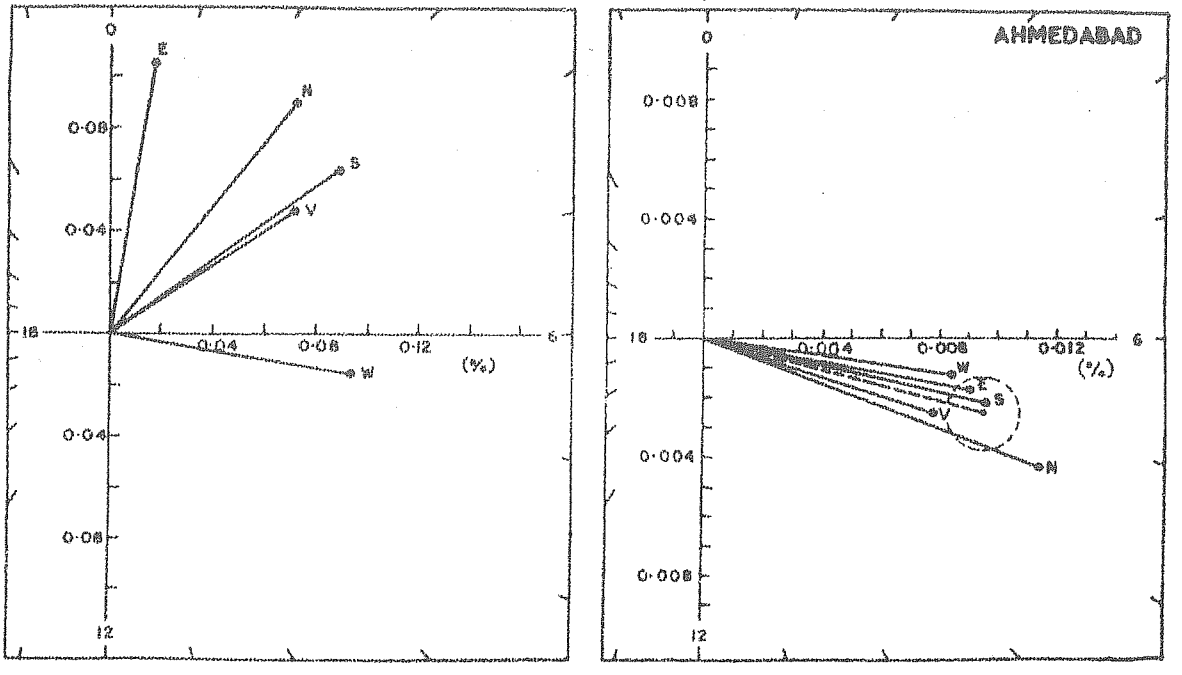

Fig.4.21 The interplanetary magnetic field related sidereal diurnal variation observed at Ahmedabad meson monitors during the year 1969 is plotted in sidereal harmonic dial.
(a) Vector differences between the diurnal variations in positive and negative polarity of the interplanetary magnetic field for East, West, North, South and Vertical telescopes at Ahmedabad are shown.
(b) The vectors shown in (a) are plotted after correcting for the width of the cones of acceptance and geomagnetic deflections corresponding to the best fit values of the exponent 'β' (+1) and E_{max}(85 GeV). The dashed line shows the mean.

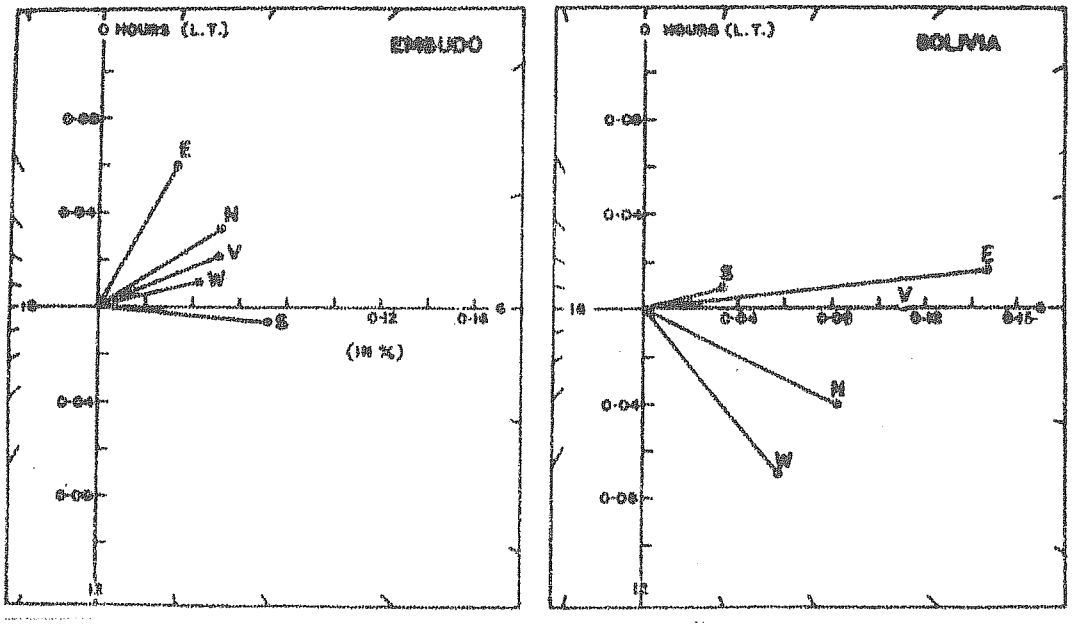

Fig.4.22 Interplanetary magnetic field related sidereal diurnal variations observed at Bolivia and Embudo underground meson monitors (East, West, North, South and Vertical telescopes) during January 1967 to May 1968 and May 1965 to October 1968 respectively. The basic data is from Swinson (1971).

CHAPTER V

SUMMARY OF THE RESULTS AND THE CONCLUSIONS

The variational coefficients for East, West, North, South and Vertical (meson) telescopes at Ahmedabad have been computed for different values of 'β' and E_{max}. To overcome the difficulties in the correction of meson intensity due to atmospheric temperature variation data of difference-telescopes have been extensively used by the author. Atleast, to a first degree of approximation the difference-telescope data is assumed to be free from the atmospheric temperature variations. In order to relate the secondary variations observed by difference-telescopes, with the primary anisotropy, the variational coefficients for difference telescopes at Ahmedabad have also been calculated.

Daily variations observed by difference-telescopes(meson) at Ahmedabad during 1968 to 1970 are presented. Data from a number of super neutron monitors, for the year 1968 and 1969 are also presented and meson observations are compared with the neutron observations.

Spectrum analysis of the daily variations both on a day-to-day basis and on an yearly average basis have been done. An attempt is made to study the anisotropies related to the interplanetary magnetic field directions and the cosmic ray density gradients for the years 1968 and 1969. Following are the main conclusions drawn from the above studies:

1) The diurnal variations observed by the various difference-telescopes at Ahmedabad during 1968 to 1970 are consistent with the corotational anisotropy with E_{max} being 80 to 100 GeV.

2) Spectral exponent 'β' for diurnal as well as for semi-diurnal anisotropy fluctuate considerably on a day-to-day basis. However the average value of 'β' is zero for the diurnal anisotropy and 'β' is +1 for the semi-diurnal anisotropy.

3) The average diurnal anisotropy is energy independent and it is along 1800 hour direction. The appropriate value of E_{max} applicable during this period is 85 ± 10 GeV. Diurnal anisotropy does not exhibit any significant change from 1968 to 1970.

4) The average semi-diurnal anisotropy is E^{+1} dependent and the value of E_{max} applicable for the semi-diurnal anisotropy is ≥ 125 GeV. Amplitude of the semi-diurnal anisotropy seems to show a gradual decrease from 1968 to 1970. The time of maximum of the semi-diurnal anisotropy is along $\sim$ 0300 hours direction and is perpendicular to the interplanetary magnetic field vector.

5) Significant differences are obtained in the average behaviour of diurnal anisotropies during days on which the interplanetary magnetic field is towards the sun (negative) and days on which it is away from the sun (positive). In 1968, the amplitude of the anisotropy, had a larger amplitude during positive polarity days than that during the negative polarity days. The time of maximum of the anisotropy was earlier for

positive polarity days and it was later during negative polarity days. Approximately opposite results are obtained during 1969. The vector difference between the diurnal variations observed in positive and negative polarity days have been used to study the anisotropy related to the interplanetary magnetic field direction.

6) The interplanetary magnetic field related anisotropies resulting due to the cosmic ray density gradients and the ipmf. direction has a positive exponent of the energy spectrum of variation.

7) The ipmf.related gradient anisotropy in 1968 shows an amplitude of~(0.004 ± 0.000) E^{+1}. The time of maximum is at 16.3 hours. The results are in substantial agreement with the results reported by other workers. The ipmf. related anisotropy in 1969, however, shows a drastic change from that observed in 1968. The time of maximum observed in 1969 is 5.7 hours with its amplitude being about one third of that in 1968.

8) The upper limit of the energy E_{max} applicable for the ipmf. related anisotropy is about 55-85 GeV which is lower than the value of E_{max} obtained for the corotational anisotropy.

9) The reversal in interplanetary magnetic field related anisotropy can possibly be explained as due to the reversal in the polarity of B_z during positive and negative sector of the interplanetary magnetic field in 1969 as compared to that in

1968. The hypothesis however requires confirmation from actual observations.

10) Sidereal anisotropy vector resulting from the azimuthal component of the interplanetary magnetic field and the radial cosmic ray density gradient has a positive spectral exponent and an E_{max} = 85 GeV. The amplitude of the anisotropy in space is $(0.0049 \pm 0.0006)\ E^{+1}$ and time of maximum is in ~0700 hour direction. The results about sidereal anisotropy are in agreement with the results presented by Swinson (1971) with Chacaltaya and Bolivia underground meson data.

11) We conclude that the diurnal anisotropy can satisfactorily be explained by equation 1.28 (Chapter I, Gleeson's equation) on a day-to-day basis as well as on an average basis. This gives us a method by which the cosmic ray density gradients can be estimated by using measured anisotropy and the interplanetary magnetic field.

.. .. ..

REFERENCES

Ables, J.G., McCracken, K.G. and Rao, U.R.	1966	Proc.Int.Conf.Cosmic Rays (London) 1, 208.
Agrawal, S.P., Ananth, A.G. and Rao, U.R.	1971	Proc.Int.Conf.Cosmic Rays (Hobart) 2, 646.
Ahluwalia, H.S. and Dessler, A.J.	1962	Planet.Space Sci., 9, 195.
Ahluwalia, H.S. and Ericksen, J.H.	1969	Acta Physica Hung- 29, Suppl. 2,139.
Ahluwalia, H.S. and McCracken, K.G.	1965	Proc.Int.Conf.Cosmic Rays (London) 1, 568.
Akimov, Yu.K.	1965	Scintillation Counters in High Energy Physics, Academic Press, N.Y.
Alfven, H.	1950	Cosmical Electrodynamics, Oxford Press, (London).
Alpher, R.A.	1950	J.Geophys.Res., 55, 437.
Axford, W.I.	1965	Planet.Space Sci., 13, 115.
Axford, W.I.	1968	Space Sci.,Rev. 8, 331.
Bachelet, F. and Conforto, A.M.	1956	Nuovo Cimento, 4, 1479.
Bachelet, F., Balata, P., Dyring, E. and Iucci, N.	1964	Nuovo Cimento, 31,1126
Bachelet, F., Balata, P., Dyring, E. and Iucci, N.	1965 a	Nuovo Cimento, 35, 23.
Bachelet, F., Balata, P. and Iucci, N.	1965 b	Nuovo Cimento,40, 250.
Bame, S.J., Asbridge, J.R., Hundhausen, A.J. and Strong, I.B.	1967	Trans. Amer. Geophys. Union, 68, 190.

Bartley, W.C., Bukata, R.P., McCracken, K.G. and Rao U.R.	1966	J.Geophys.Res., 71, 3297.
Bercovitch, M.	1963	J.Geophys.Res., 68, 4366.
Bercovitch, M.	1968	Proc.Int.Conf.Cosmic Rays (Calgary) A, 269.
Bercovitch, M.	1971	Proc.12th Int.Conf.Cosmic Rays (Hobart) 2, 579.
Biermann, L.	1951	Z.Astrophys. 29, 274.
Biermann, L.	1957	Observatory 77, 109.
Birks, J.B.	1953	Scintillation Counters, McGrawhill Co., N.Y.
Bonetti, A., Bridge, H.S., Lazarus, A.J., Lyon, E.F., Rossi, B. and Scherb,F.	1963 a	Space Res., 3, 540
Bonetti, A., Bridge, H.S., Lazarus, A.J., Rossi, B. and Scherb, F.	1963 b	J.Geophys.Res., 68, 4017.
Brunberg, E.A.	1958	Ark. for Physik, 14, 195.
Brunberg, E.A. and Dattner, A.	1953	Tellus 5, 135 & 269.
Buck, W.L., and Swank, R.K.	1953	Nucleonics, 11, 11, 48.
Carmichael, H., Bercovitch, M., Steljes, J.F. and Magidin, M.	1965	Proc.Int.Conf.Cosmic Rays (London), 1, 553.
Carmichael, H., Bercovitch, M. and Steljes, J.F.	1967	Tellus, 19, 143

Carmichael, H., Bercovitch, M., Shea, M.A., Magidin, M. and Peterson, R.W.	1968	Can.J.Phys., 1, S1006.
Clark, G.W., Scherb, F. and Smith, W.B.	1957	Rev.Sci Instr., 28, 474.
Coleman, P.J.Jr.	1966	J.Geophys.Res., 71, 5509.
Coleman, P.J.Jr., Smith, E.J., Davis, L.Jr. and Jones, D.E.	1966 a	Space Res., 6, 907.
Coleman, P.J.Jr., Davis, L.Jr., Smith, E.J. and Jones, D.E.	1966 b	J.Geophys.Res., 71, 2831.
Compton, A.H. and Getting, I.A.	1935	Phy.Rev., 47, 817.
Crowden, J.B. and Marsden, P.L.	1962	J.Phys.Soc., Japan, 17, 484.
Curran, S.C.	1953	Luminescence and the Scintillation Counter,
Daniel, R.R. and Stephens, S.A.	1966	Proc.Ind. Aca.Sci., A, 63, 276.
Davis, L.Jr., Smith, E.J., Coleman, P.J.Jr and Sonett, C.P.	1966	Interplanetary magnetic measurements in The Solar Wind, 35, Pergamon Press, New York.
Deshpande, R.Y. and Bhide, G.K.	1961	A.E.E.T.(India)/T.P./2.
Dessler, A.J.	1967	Rev.Geophys., 5, 1.
Dhanju, M.S. and Sarabhai, V.	1967	Phys.Rev.Letters, 19, 252.
Dorman, L.I.	1957	Cosmic Ray Variations, State Publishing House, Moscow.
Dorman, L.I.	1963	Prog.in Elementary Particle and Cosmic Ray Physics, Vol.VII, North-Holland Publishing Co., Amsterdam.

Dorman, L.I.	1969	Ann.IQSY, 4, 217.
Dorman, L.I. and Feinberg, E.L.	1955	Memoria del V Congreso Internacional de Radiacion Cosmica(Guanajuato), 393.
Dorman, L.I. and Fischer, S.	1965	Proc.Int.Conf.Cosmic Rays (London), 1, 239.
Duggal, S.P. and Pomerantz, M.A.	1966	Trans.AGU. 47, 157.
Duggal, S.P., Forbush, S.E. and Pomerantz, M.A.	1967	Nature, 214, 154.
Duggal, S.P., Forbush, S.E. and Pomerantz, M.A.	1970 a	J.Geophys.Res., 75, 1150.
Duggal, S.P., Forbush, S.E. and Pomerantz, M.A.	1970 b	Acta.Phys.Hung.29, Suppl. 2, 55.
Elliot, H. and Dolbear, D.W.N.	1951	J.Atmo.Terr.Phys.1, 205.
Elliot, H. and Rothwell, P.	1956	Phil.Mag., 1, 699.
Faller, A.M. and Marsden, P.L.	1966	Proc.Int.Conf.Cosmic Rays (London), 1, 231.
Finch, H.P. and Leaton, B.R.	1957	Monthly Notices, Roy.Astron. Soc.Geophys.Suppl., 1, 314.
Firor, J.W.	1954	Phys.Rev., 94, 1017.
Fisher, J.	1955	Nucleonics, 13, 5, 52.
Fisk, L.A. and Axford, W.I.	1968	J.Geophys.Res. 73, 4396.
Fisk, L.A. and Axford, W.I.	1969	J.Geophys.Res. 74, 4973.
Fisk, L.A. and Axford, W.I.	1970	Solar Phys. 12, 304.
Fonger, W.H.	1953	Phys.Rev., 91, 351.

Forbush, S.E. and Venkatesan, D.	1960	J.Geophys.Res.65, 2213.
Forbush, S.E.	1966	Handbuch der Physik, 49, 1, 159.
Forbush, S.E.	1967	J.Geophys.Res. 72, 4937.
Forbush, S.E.	1969	J.Geophys.Res. 74, 3451.
Forman, M.A.	1970	Planet.Space Sci. 18, 25.
Forman, M.A. and Gleeson, L.J.	1970	Preprint, Monash Univ.
Fujii, Z., Fujimoto, K., Ueno, H., Kondo, I. and Nagashima, K.	1970	Acta. Phys.Hung., 29, Suppl. 2, 83.
Gall, R.	1968	J.Geophys.Res., 73, 4400.
Gall, R., and Lifshitz, J.	1958	Proc.IUPAP, Cosmic Ray Conf. Mexico , 66.
Gall, R., Jimenez, J. and Camacho, L.	1968	J.Geophys.Res., 73, 1593.
Gall, R., Jimenez, J. and Orozco, A.	1969	J.Geophys.Res., 74, 3529.
Gleeson, L.J.	1969	Planet.Space Sci., 17, 31.
Gleeson, L.J.	1971	Astrophys.Space Sci., 10, 471.
Gleeson, L.J. and Axford, W.I.	1967	Astrophys. J.149, L.115.
Gleeson, L.J. and Axford, W.I.	1968 a	Can.J.Phys., 46, 937.
Gleeson, L.J. and Axford, W.I.	1968 b	Astrophys. J.151, 1011.
Gleeson, L.J. and Axford, W.I.	1968 c	Astrophys.Space Sci., 9, 431.
Gosling, J.T., Hansen, R.T. and Bame, S.J.	1971	J.Geophys.Res., 76, 1811.

Griffiths, W.K., Hatton, C.J., Ryder, P. and Harman, C.V.	1966	J.Geophys.Res., 71, 1895.
Gringauz, K.I.	1961	Space Res., 2, 539.
Gringauz, K.I., Bezrukikh, V.V., Ozerov, V.D. and Rybchinsky, R.E.	1960	Soviet Phy., Doklady, 5, 361.
Gringauz, K.I., Kurt, V.G., Moroz, V.I. and Shklovskii, I.S.	1962	Planet.Space Sci., 2, 21.
Hashim, A. and Bercovitch, M.	1971	Proc.12th Int.Conf.Cosmic Rays, (Hobart), 2, 596.
Hashim, A. and Thambyahpillai, T.	1969	Planet.Space Sci., 17, 1879.
Hashim, A., Thambyahpillai, T., Thomson, D.M. and Mathews, T.	1968	Can.J.Phys. 46, S 801.
Hashim, A., Bercovitch, M. and Steljes, J.F.	1972	Solar Physics., 22, 220.
Hatton, C.J. and Barker, M.C.	1971	Proc.12th Int.Conf.Cosmic Rays (Hobart), 2, 603.
Holzer, T.E. and Axford, W.I.	1970	Ann.Rev.Astron.Astrophys. 8, 31.
Holzer, R.E., McLeod, M G and Smith, E.J.	1966	J.Geophys.Res., 71, 1481.
Hundhausen, A.J.	1968	Space Sci. Rev., 8, 690.
Hundhausen, A.J.	1970	Rev.Geophys.Space Phys. 8, 729.
Hundhausen, A.J., Asbridge, J.R., Bame S.J. and Strong, I.B.	1967	J.Geophys.Res., 72, 1979.
Jacklyn, R.M. and Humble, J.E.	1965	Aust.J.Phys., 18, 451.

Jacklyn, R.M., Duggal, S.P. and Pomerantz, M.A.	1969	Nature, 223, 601.
Jacklyn, R.M., Duggal, S.P. and Pomerantz, M.A.	1970	Acta Phys.Hung.29, Suppl.2, 47.
Jokipii, J.R.	1967	Astrophys.J. 149, 405.
Jokipii, J.R.	1971	Rev.Geophys.Space Phys.9, 27.
Jokipii, J.R. and Parker, E.N.	1967	Planet.Space Sci., 15, 1375.
Jokipii, J.R. and Parker, E.N.	1968	Phys.Rev.Letters 21, 44.
Jokipii, J.R. and Parker, E.N.	1969	Astrophys.J. 155, 777.
Jokipii, J.R. and Parker, E.N.	1970	Astrophys.J. 160, 735.
Jokipii, J.R. and Coleman, P.J.Jr.	1968	J.Geophys.Res., 73, 5495.
Jory, P.	1956	Phys.Rev., 102, 1167.
Kane, R.P.	1962	J.Phys.Soc.Japan, 17, 468.
Kane, R.P. and Rao, U.R.	1958	Proc.Ind.Acad.Sci., 57, 30.
Koski, W.S.	1951	Phys.Rev., 82, 230.
Krimsky, G.F.	1964	Geomagn.and Aeronomy, 4, 763.
Krimsky, G.F., Krivoshapkin, P.A. and Skripin, G.V.	1966	Proc.Int.Conf.Cosmic Rays, (London) 1, 503.
Lemaitre, G. and Vallarta, M.S.	1936 a	Phys. Rev. 49, 719.
Lemaitre, G. and Vallarta, M.S.	1936 b	Phys. Rev. 50, 493.
Lietti, B. and Quenby, J.J.	1968	Can.J.Phys., 46, S942.
Lindgren, S. and Lindholm, F.	1961	Tellus, 13, 280.

Lindgren, S.T.	1970	Acta Phys.Hung. 29, Suppl.2,401.
Lust, R.	1967	The Properties of Interplanetary Space in Solar Terrestrial Physics edi.by King and Newman, p.1, Academic, New York.
Lust, R., Schluter, A. and Kallerbach, K.	1955	Nachr.Acad.Wiss.Gottingen, Math-Phys. K.L. 11 a, 8, 128.
Mead, G.D.	1964	J.Geophys.Res., 69, 1181.
Maeda, K.	1960	J.Atm.Terr.Phys. 19, 184.
Maeda, K. and Wada, M.	1964	J.Sci.Res.Inst.Tokyo, 48, 71.
Makino, T. and Kondo, I.	1965	Proc.Int.Conf.Cosmic Rays (London), 1, 564.
Malmfors, K.G.	1945	Arkiv Math.Astron.Fysik, 32 A, 473.
Malmfors, K.G.	1949	Tellus, 1, 55.
Mathews, P.M.	1959	Can.J.Phys. 37, 85.
Mathews, T., Venkatesan, D. and Wilson, B.G.	1969	J.Geophys. Res. 74, 1218.
Mathews, T., Quenby, J.J. and Sear, J.	1971	Nature, 229, 246.
McCracken, K.G.	1962	J.Geophys.Res., 67, 447.
McCracken, K.G. and Johns, D.H.	1959	Nuovo, Cim. 13, 96.
McCracken, K.G. and Ness, N.F.	1966	J.Geophys.Res., 71, 3315.
McCracken, K.G. and Rao, U.R.	1965	Proc.Int.Conf.Cosmic Rays (London), 1, 213.
McCracken, K.G. and Rao, U.R.	1966	Planet.Space Sci., 14, 649.
McCracken, K.G. and Rao, U.R.	1970	Space Sci.Rev., 11, 155.
McCracken, K.G., Rao, U.R. & Ness, N.F.	1968	J.Geophys. Res., 73, 4159.

McCracken, K.G., Rao, U.R. and Shea, M.A.	1962	Tech.Rept.77, Mass.Inst. Tech., 1962.
McCracken, K.G., Rao, U.R. and Bukata, R.P.	1967	J. Geophys.Res., 72, 4293.
McCracken, K.G., Rao, U.R., Bukata, R.P. and Keath, E.	1971	Solar Phys., 18, 100.
McCracken, K.G., Rao, U.R., Fowler, B.C., Shea, M.A. and Smart, D.F.	1965	IQSY Instr.Manual No.10 (IQSY Committee), London.
Michel, F.C.	1967	J.Geophys.Res. 72, 1917.
Mori, S.	1968 a	Nuovo Cimento 58 B, 1.
Mori, S.	1968 b	Nuovo Cimento 58 B, 58.
Morrison, P.	1956	Phys.Rev., 101, 1397.
Mott, W.E. and Sutton, R.B.	1958	Scintillation and Cerenkov Counters, 45, 86, Handbook der Physik Springer Verlag, Berlin.
Nagashima, K.	1953	J.Geomag.Geoelec., 5, 141.
Nagashima, K., Duggal, S.P. and Pomerantz, M.A.	1966	Planet.Space Sci., 14, 177.
Neher, H.V.	1952	Progress in Cosmic Ray Physics Vol.I, Interscience Publishers, p.245.
Ness, N.F.	1967	Amer.Rev.Astron.Astrophys., 6, 79.
Ness, N.F. and Wilcox, J.M.	1964	Phys.Rev.Letters, 13, 461.
Ness, N.F. and Wilcox, J.M.	1966	Astrophys.J. 143, 23.
Neugebauer, M. and Snyder, C.W.	1962	Science, 138, 1095.
Ng, C.K. and Gleeson, L.J.	1971	Solar Phys., 20, 166.

Nagashima, K., Fujimoto, K., Fujii, Z., Ueno, H., and Kondo, I.	1971	Nagoya University Report D.P.N.U. 9 Part IV.
Newell, H.E.	1948	Rev.Sci.Instr., 19, 384.
Newell, H.E. and Pressly, E.C.	1950	Rev.Sci.Instr., 21, 918
Ostman, B. and Awadalla, E.	1970	Preprint, Cosmic Ray Group Inst.of Physics, Uppsala.
Pai, G.L., Bridge, H.S., Lyon, E.F. and Egidi, A.	1967	Trans.Amer.Geophys.Union, 48, 176.
Pal, Y. and Peters, B.	1963	Proc.Int.Conf.Cosmic Rays, Jaipur.
Parker, E.N.	1958	Astrophys. J., 128, 664.
Parker, E.N.	1958 a	Phys.Rev., 110, 1445.
Parker, E.N.	1964	Planet.Space Sci., 12, 735.
Parker, E.N.	1965	Planet.Space Sci., 13, 9.
Parker, E.N.	1965 a	Space Sci., Rev., 4, 666.
Parker, E.N.	1966	Proc.Int.Conf.Cosmic Rays, (London), 1, 26.
Parker, E.N.	1966 a	Planet.Space Sci., 14, 371.
Parker, E.N.	1967	Solar Terr.Phy.Edited by King J.W. and Newman, W.S., Academic Press, New York.
Parker, E.N.	1967 a	Planet.Space Sci., 15, 1723.
Parker, E.N.	1969	Space Sci. Rev., 9, 325.
Parsons, N.R.	1957	Rev.Sci.Instr., 28, 265.
Patel, D., Sarabhai, V. and Subramanian, G.	1968	Planet.Space Sci., 16, 1131.
Pathak, P.N.	1972	Solar Physics. (in Press).

Peacock, D.S., Dutta, J.C. and Thambyahpillai, T.	1968	Can.J.Phys., 46, S788.
Pomerantz, M.A. and Duggal, S.P.	1971	Space Sci.Rev., 12, 75.
Quenby, J.J.	1967	Handbuch der Physik, 46,2,310.
Quenby, J.J. and Lietti, B.	1968	Planet Space Sci., 16, 1209.
Quenby, J.J. and Webber, W.	1959	Phil.Mag., 4, 90.
Quenby, J.J. and Wenk, G.J.	1962	Phil.Mag., 7, 1457.
Rao, U.R.	1972	Space Sci.Rev., 12, 719.
Rao, U.R. and Sarabhai, V.	1961	Proc.Roy.Soc., A 263, 101.
Rao, U.R. and Sarabhai, V.	1964	Planet.Space Sci., 12, 1055.
Rao, U.R. and Agrawal, S.P.	1970	J.Geophys.Res., 75, 2391.
Rao, U.R., McCracken, K.G. and Venkatesan, D.	1963	J.Geophys.Res., 68, 345.
Rao, U.R., Ananth, A.G. and Agrawal, S.P.	1972	Planet.Space Sci. (under publication)
Razdan, H. and Bemalkhedkar, M.M.	1971	Proc.12th Int.Conf.Cosmic Rays, (Hobart), 2, 697.
Ryder, P. and Hatton, C.J.	1968	Can.J.Phys., 46, S 999.
Sandstrom, A.E.	1965	Cosmic Ray Physics, North-Holland Publishing Co., Amsterdam P.201.
Sandstrom, A.E., Dyring, E. and Lindgren, S.	1962	J.Phys.Soc., Japan, Suppl.A II, 17, 471.

Sandstrom, A.E., Dyring, E., Larfors, O., Lindgren, S., Sporre, B. and Ostman, B.	1968	Scientific Note No.6, Uppsala Univ., Sweden.
Sarabhai, V. and Kane, R.P.	1953	Phys.Rev., 90, 204.
Sarabhai, V., and Subramanian, G.	1965	Proc.Int.Conf.Cosmic Rays, (London), 1, 204.
Sarabhai, V. and Subramanian, G.	1966	Astrophys. J., 145, 206.
Sarabhai, V., Desai, U.D. and Venkatesan, D.	1954	Phys.Rev., 96, 469.
Sarabhai, V., Pai, G.L. and Wada, M.	1965	Nature, 206, 703.
Sari, J.W. and Ness, N.F.	1969	Solar Phys. 8, 155.
Schatten, K.H.	1971	Rev.Geophys.and Space Phys., 9, 773.
Schluter, A.Z.	1951	Naturforsch 6a, 613.
Schorr, M.G. and Torney, F.L.	1950	Phys.Rev., 80, 474.
Sekido, Y. and Yoshida, S.	1950	Rep.Ionosph.Res., Japan, 4, 37.
Severney, A., Wilcox, J.M., Scherrer, P.H. and Colburn, D.S.	1970	Solar Phys., 15, 3.
Shea, M.A., Smart, D.F. and McCracken, K.G.	1965	J.Geophys. Res., 70, 4117.
Shklovsky, I.S., Moroz, V.I. and Kurt, V.G.	1961	Soviet Astron. AJ. 4, 871.
Simpson, J.A., Fonger, W.H., and Treiman, S.B.	1953	Phys.Rev., 90, 934.

Sisco, G.L., Davis, L.Jr., Coleman, P.J.Jr., Smith, E.J. and Jones, D.E.	1968	J.Geophys. Res., 73, 61.
Skadron, G.	1967	Tech.Report No.678, Univ. of Maryland.
Snyder, C.W., Neugebauer, M. and Rao, U.R.	1963	J.Geophys.Res., 68, 6361.
Steinmaurer, R. and Gheri, H.	1955	Naturwissenschaften, 42, 294.
Stern, D.	1964	Planet.Space Sci., 12, 973.
Stormer, G.	1936	Astrophys.Norvey 2, No.1.
Strong, I.B., Asbridge, J.R., Barne, S.J. and Hundhausen, A.J.	1967	Zodiacal light and the Interplanetary medium, NASA SP-150 (edited by J.Weinberg).
Subramanian, G.	1964	Ph.D.thesis, Gujarat Univ.
Subramanian, G.	1971 a	J.Geophys.Res., 76, 1093.
Subramanian, G.	1971 b	Can.J.Phys., 49, 34.
Subramanian, G. and Sarabhai, V.	1965	Proc.9th Symp.on Cosmic Rays, Ele.Particle Phys. and Astrophysics, Bombay, 217.
Subramanian, G. and Sarabhai, V.	1967	Astrophys. J., 149, 417.
Swinson, D.B.	1969	J.Geophys.Res., 74, 5591.
Swinson, D.B.	1970	Acta Phys.Hung.29, Suppl.1, 501.
Swinson, D.B.	1971 a	Proc.12th Int.Conf.Cosmic Rays, (Hobart), 2, 588.
Swinson, D.B.	1971 b	J.Geophys.Res., 76, 4217.
Tanskanen, P.J.	1968	Can.J.Phys., 46, S819.
Thambyahpillai, T. and Elliot, H.	1953	Nature, 171, 918.
Treiman, S.B.	1952	Phys.Rev., 86, 917.

Venkatesan, D. and Mathews, T.	1968	Can.J.Phys., 46, S794.
Wada, M.	1961	Sci.Papers Inst.Phys.Chem.Res., Tokyo, 55, 7.
Wada, M. and Kudo, S.	1968	Can.J.Phys., 46, S934.
Waldmeier, M.	1971	Astr.Mitte.der Eidge.Stern. Zurich, No.288, 296.
Webber, W.R.	1968	Proc.Int.Conf.Cosmic Rays, (Calgary), A, 148.
Webber, W.R.	1969	Leningrad Symp. 188.
Wilcox, J.M.	1968	Space Sci., Rev. 8, 258.
Wilcox, J.M. and Ness, N.F.	1965	J.Geophys.Res., 70, 5793.
Wilcox, J.M. and Ness, N.F.	1967	Solar Phys. 1, 437.
Wilcox, J.M. and Colburn, D.S.	1969	J.Geophys. Res., 74, 2388.
Wilcox, J.M. and Colburn, D.S.	1970	J.Geophys. Res., 75, 6366.
Wilcox, J.M. and Colburn, D.S.	1972	J.Geophys. Res., 77, 751.
Williams, D.J. and Mead, G.D.	1965	J.Geophys. Res., 70, 3017.
Wouters, L.F.	1955	UCRL Report No.4516.
Yoshida, S.	1955	Proc.Int.Conf.Cosmic Rays, Guanajuato, 358.

.. ..